A STUDY ON FLOW THROUGH POROUS MEDIUM

THESIS FOR THE DEGREE OF PH.D.

MICHIGAN STATE UNIVERSITY
HON - HSIEH SU

1968

This is to certify that the

thesis entitled

"A STUDY ON FLOW THROUGH POROUS MEDIUM"

presented by

Hon-Hsieh Su

has been accepted towards fulfillment
of the requirements for

Ph. D. degree in Civil Engineering

K. K. Wen

Major professor

Date March 13, 1968

ABSTRACT

A STUDY ON FLOW THROUGH POROUS MEDIUM

by Hon-Hsieh Su

The present investigation is a probabilistic study of the porous medium and the mechanism of fluid flow in the pore system. If the porous medium is such that its pores have different orientation with respect to certain direction and the hydraulic gradient is the sole cause for the fluid particle to move in the pores, then the tortuous paths of the pores will result in a dispersion of fluid flow in a porous medium.

A canal network model of a porous medium was assumed in this study. An orientation factor was used to represent the preferred orientation of the pore canals. For given canal distributions, it was possible to calculate the degree of dispersion at a given time. A theoretical analysis of dispersion was made based on the assumption that a fluid particle would travel in a pore canal network system by following the probability distribution function for the choice of direction. A functional relationship was derived for the dispersion that includes the longitudinal distance of fluid particle movement, the length of the unit canal, and the orientation factor of the porous medium. It was also shown that the orientation factor of the porous medium could be related to the ratio of permeability coefficients measured in two perpendicular directions in the porous medium.

A laboratory experiment was set up to investigate the dispersion phenomenon. The laboratory analysis showed that the dispersion phenomenon in a porous medium is a macroscopically measurable

quantity. The factors affecting the quantity of dispersion were found to be the length of the pore canals, the distance of travel by the fluid particles, and the orientation of the pore canals. It was also found that the packing characteristics such as porosity, packing uniformity which were not considered in the present theoretical analysis also affect the dispersion. The experimental results showed that the functional relationships as derived theoretically appeared to be qualitatively correct.

Therefore, it is in principle possible to predict the dispersion from a knowledge of the characteristics of the porous medium. From the results of this study, it can be stated that the assumption of the canal network model and a corresponding probabilistic calculation appear to help in explaining the dispersion phenomenon of the fluid flow through porous medium.

A STUDY ON FLOW THROUGH POROUS MEDIUM

By

Yon-Hsieh Su

A THESIS

Submitted to
Michigan State University
in partial fulfillment of the requirements
for the degree of

DOCTOR OF PHILOSOPHY

Department of Civil Engineering

1968

ACKNOWLEDGEMENT

The writer wishes to express his indebtedness to all of his committee members for their valuable assistance and guidance during his course work and the development of this thesis. Sincere appreciation is due to Doctor T. H. Wu who had given his constant and valuable suggestions and instructions during the preparation of this thesis and to Doctor K. J. Arnold for his critical review of this thesis. The writer also wishes to express his appreciation to Doctors C. E. Cutts, R. K. Wen and O. E. Andersland for their review of the manuscript.

TABLE OF CONTENTS

LIST OF FIGURES

LIST OF TABLES

LIST OF APPENDICES

CHAPTER 1

INTRODUCTION

Many studies on the flow of fluids through porous materials have been undertaken. Darcy's law is valid for most cases when an average rate of flow through a porous medium is considered. Many investigations have been made to study the coefficient of permeability in Darcy's equation. Most of these attempts were based on the so-called capillary model. This is the simplest model of a porous medium and consists of a bundle of parallel capillaries with uniform cross sections. This model plus Poiseuille's viscous flow equation leads directly to Darcy's equation. Unfortunately, the permeabilities derived from this type of model are not entirely satisfactory when used to describe the phenomenon of flow through porous materials.

It is apparent that difficulties with the capillary model arise because the capillaries are all parallel and that they have identical cross sectional area and length. The model is far from reality and therefore it is unreasonable to expect a consistent functional relationship among several measurable properties.

The shortcomings of the capillary model led some investigators to an entirely different approach based on the statistical treatment of the porous medium. Dispersion phenomenon was used to study the movement of fluids in the porous medium and investigations have been reported in the past ten years. Most of these are theoretical studies.

The present investigation is a probabilistic analysis of fluid flow through porous medium. A porous medium in this investigation

is assumed to consist of a network of pore canals linked together. A fluid particle is assumed to follow a probability function in choosing a flow path while travelling from one position to another in the porous medium. Different paths have different lengths between two positions and also require different travel times. If, during continuous flow, a fluid is replaced abruptly by another miscible fluid so that they occupy two distinct phases at the beginning, the difference in flow paths causes a mixing of the two fluids. This mixing is the phenomenon of dispersion. A theoretical analysis of dispersion based on these assumptions was made and a functional relationship was derived for the dispersion in porous media.

A laboratory experiment was set up to investigate the dispersion phenomenon. The experimental results showed that the dispersion is a function of the medium properties. The characteristics of dispersion as observed in the experiments are in general agreement with the theoretical predictions. The theoretical relationship between the standard deviation of dispersion and the distance was found to be correct.

It is hoped that a study of this nature would lead to a better understanding of the basic aspects of the fluid flow through porous materials.

CHAPTER 2

LITERATURE REVIEW

The well known Darcy's law (1856), an empirical expression of the flow of fluids through porous materials based on measurements of the flow of water through sands and sandstones, may be written as

$$v = k \frac{\Delta p}{\Delta z} \quad \ldots\ldots\ldots\ldots\ldots\ldots \quad (1)$$

where v is the velocity of flow, Δp is the pressure head difference between two points in the porous medium, and Δz is the distance between them. The coefficient of permeability k as defined in the above equation is the rate of flow of fluids across a unit cross sectional area of the porous medium under a unit pressure gradient.

Refinements to Darcy's equation were made by many investigators such as Blake (2), Kozeny (9), and Carman (3) in attempts to generalize the equation for flow through porous materials. While keeping the fundamental form of Eq. (1) unchanged, these studies tried to relate the permeability coefficient to the physical and geometrical characteristics of the porous medium. A widely known equation is the Kozeny-Carman equation

$$k = \frac{1}{k_1 \mu S_o^2} \frac{\epsilon^3}{(1 - \epsilon)^2} \quad \ldots\ldots\ldots\ldots \quad (2)$$

where μ is the viscosity of the fluid in the porous medium, ϵ is the porosity, S_o is the specific surface area, k_1 is a constant expressed as

$$k_1 = k_o \left(\frac{L_e}{L_1}\right)^2 \quad \ldots\ldots\ldots\ldots\ldots \quad (3)$$

in which L_e is the actual path of the fluid flow and L_1 is the distance between the two sections of porous medium under consideration. k_o is a constant representing the shape effect of the pores in the medium.

In the above treatment, the porous medium is represented by a bundle of parallel capillaries, and the laws of viscous flow are applied to flow in the capillaries. Relationships between the various macroscopically measurable quantities are deduced from this model. Experimental evidence shows that the theory applies with considerable accuracy to porous media composed of nearly spherical particles of relatively large size. However, it is unsuccessful in describing the flow characteristics of clays, which are composed of fine, plate-shaped particles.

Two groups of factors have been brought out to explain the failure of the Kozeny-Carman equation. The first is the forces at the liquid-solid interface. This includes the assumption of high viscosity close to the particle surface or the presence of immobile films of adsorbed fluids at the particle surface, Terzaghi (19) and Zunker (20). Other investigations were reported by Bastwo and Bowden (1), Elton (7), and Michaels and Lin (12). The second is the change in the packing characteristics of the material. This includes the orientation of the particles and pore size distribution. Michell (13) and Lambe (10) studied the effect of the particle orientation and Olsen (14) studied the effect of changing pore size distributions. The experimental evidence shows that changes in the packing characteristics affect the nature of fluid flow in fine-grained soils and the relationship between the property of the porous medium and the fluid flow remains indefinite.

Other investigators tried the statistical approach. In 1950, Childs and Collis-George (4) proposed a theory wherein flow was determined by the pore radii and by the probability of continuity of pores of different radii. Spherical particles were assumed. Marshall (11) in 1958 and Quirk (15) in 1959 proposed alternatives to Childs and Collis-George's method. Scheidegger (17), (18) in 1954 derived the differential equations of motion of fluid through a porous medium from probability theory. An average ensemble represents all parts of the porous medium under the so-called "hypothesis of disorder". The geometrical conditions for the motion of a particle prevailing at a spot in a porous medium are assumed to be entirely uncorrelated with those at any other spot of that material. The movement of fluid particles in such a medium is then considered as steps with respect to time or distance. Then, by virtue of the Central Limit Theorem, the probability of a specific particle being at x at time t is a Gaussian distribution

$$p(x,t) = (4\pi Dt)^{-3/2} \exp\left(-\frac{(x-\bar{x})^2}{4Dt}\right) \quad (4)$$

where $\bar{x}$ is the average distance and D is called the factor of dispersion. However, Scheidegger's differential equation for fluid motion in a porous medium is too complicated for practical application. Experimental results by Day (5) confirm the existence of the dispersion phenomenon in porous materials but are not extensive enough to verify Scheidegger's theory. Scheidegger's statistical treatment does not define the microscopical mechanism of the fluid movement in the pores. Therefore, his result contains a numerical constant describing the granular properties of the porous medium which can only be

determined by experiment. According to Scheidegger, the dispersion constant should have equal magnitude in both longitudinal and transversal dispersion. However, Day's experimental result indicates that there is a marked difference of about 6 to 8 times in longitudinal and transversal dispersion.

De Josselin de Jong (6) in 1958 also derived an expression to describe the fluid movement in a porous medium from probability considerations. The pore system of a packed material is represented by a network of unit canals continuous throughout the medium. The probability of a fluid particle moving in this network to travel a certain distance within a certain time was calculated. Molecular diffusion is not considered. The computation gives explicit values for the coefficients of the longitudinal and transversal dispersions as follows:

$$\sigma_x = u \left(\frac{3Z_o}{L} \left(\lambda + \frac{3}{4} - \log r \right) \right)^{1/2} \quad \ldots\ldots\ldots (5)$$

$$\sigma_z = \frac{L}{3} \left(\frac{3Z_o}{L} \left(\lambda + \frac{3}{4} - \log r \right) \right)^{1/2} \quad \ldots\ldots\ldots (6)$$

In these expressions σ_x and σ_z are the standard deviations in transversal and longitudinal dispersion respectively; u is the residence time for elementary canal in principal flow direction; Z_o is the average distance travelled along the longitudinal direction; L is the length of the unit canal; log r is Euler's constant and is equal to 0.577 approximately; and λ is a function of distance Z_o. De Josselin de Jong also performed one experiment and measured the dispersion in sand. The measured longitudinal dispersion co-

efficient increases with the distance and the relationship between the standard deviation and the square root of distance is linear as indicated by Eq. (6). However, De Josselin de Jong's computations are rather complicated and apply only to a porous medium with completely random pore orientation.

Saffman (16) in 1959 also applied statistics to the dispersion in a porous medium. Saffman considered three conditions: (a) molecular diffusion is very large compared to velocity of flow, (b) molecular diffusion is very small compared to velocity of flow, (c) intermediate case in which the fluid is completely mixed across each channel but not along the channel. Case (c) is analogous to De Josselin de Jong's model. Saffman obtained solutions for all three cases. He arrived at the following expressions for the standard deviation of the longitudinal dispersion of a fluid particle

in a porous medium after time T

$$\sigma_z = (TVLS^2)^{1/2} \quad \ldots\ldots\ldots\ldots\ldots\ldots \quad (7)$$

where the quantity S^2 is represented by the following equations. For idealized fluid particles where $t_o = t_1 = \infty$, or fluid particles very close to idealized conditions

$$S^2 = \frac{1}{48} \left(\log \frac{54VT}{L}\right)^2 \quad \ldots\ldots\ldots\ldots \quad (8)$$

if $\dfrac{4Vt_o/L}{n^{-1/2} \log n^{1/2}} \gg 1.$

For the fluid particles with conditions of $Vt_1/L \ll 1$, $Vt_o/L \gg 1$

$$S^2 = \frac{1}{3} \log \frac{3Vt_o}{L} - \frac{1}{12} \quad \ldots\ldots\ldots\ldots \quad (9)$$

$$\text{if } \frac{Vt_o/L}{\bar{n}^{1/2}(\log \frac{3Vt_o}{L})^{1/2}} \ll 1.$$

$$S^2 = \frac{1}{6} \log \frac{27VT}{2L} \quad \ldots\ldots\ldots\ldots\ldots\ldots \quad (10)$$

$$\text{if } \frac{3Vt_o/L}{\bar{n}^{1/2}(\log \bar{n}^{1/2})^{1/2}} \gg 1.$$

Therefore, the standard deviation increases linearly with the logarithm of distance. In the above equations, V is the average velocity of the fluid flow, T is the duration of time, L is the length of the unit pore canal, $\bar{n}$ is the average number of displacements, t_o is the estimate of the time for appreciable diffusion along the pore and t_1 is the estimate of time for appreciable diffusion across the pore.

Thus two essentially different approaches have been employed to study the flow of fluids through a porous medium; namely, investigation of the factors affecting the permeability coefficients in the classical Darcy's law based on the capillary model and the statistical approach based on the canal network model. The capillary model has proved itself to be an adequate model for permeability of certain types of porous materials but it does not apply to dispersion. The statistical approach has been applied to fluid flow through porous materials only in the last ten years and is not yet completely developed. However, statistics have been used to describe diffusion problems successfully and the recent application of statistics as described in the preceding paragraphs gives a consistent explanation of the

dispersion phenomenon. Therefore it appears that the statistical approach is a tool that deserves more attention in the study of the flow through porous materials.

CHAPTER 3

THEORETICAL ANALYSIS

1. Dispersion Phenomenon.

Dispersion is a phenomenon observed in a porous medium as a mixing of two miscible fluids when a fluid flowing in a porous medium is abruptly replaced at its bottom by another completely miscible fluid. This phenomenon is also called a "miscible displacement" and is different from the molecular diffusion. The microstructure of the porous medium results in a tortuous path for a fluid particle travelling through the pores. This tortuosity of the flow path causes the individual fluid particles travelling in the pores to arrive at different places after a given time interval. The relationship between this dispersion and the structure of the porous medium is a basic characteristic of the flow through a porous medium.

2. Canal Network Model.

In order to study the mechanism of fluid flow in the porous medium, a canal network model is constructed for the pore canals. The following assumptions are made regarding this model.

(1) The pores between grains of the porous medium can be represented by a system of unit canals joined together to form a network as illustrated schematically in Figure 3-1.

(2) The unit canals in the model of the porous medium have a length and an average cross sectional area that are representative of the average size of the pores that form the canals.

(3) The grains in the porous medium are assumed to be rigid.

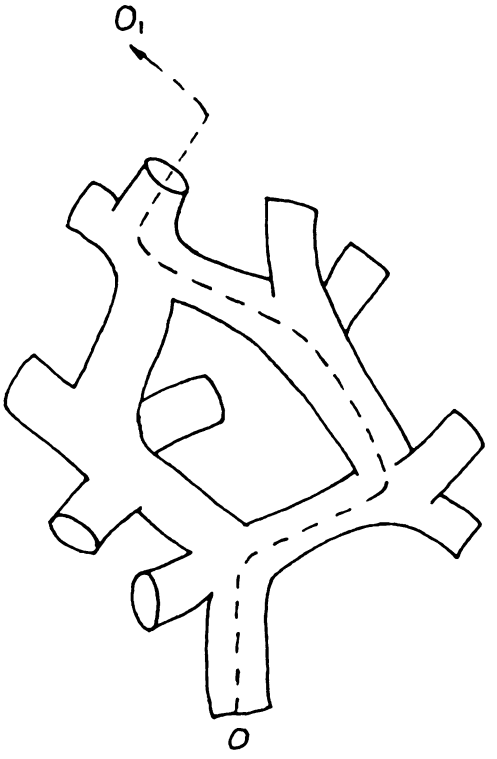

Figure 3-1. The schematic sketch of a canal network system in a porous medium and a random path chosen by a fluid particle.

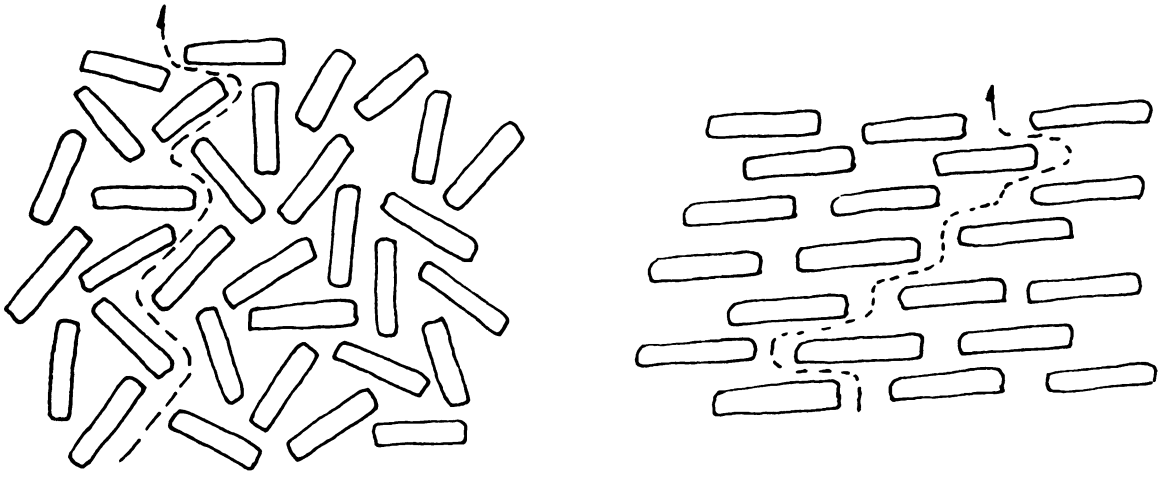

Completely random

Completely oriented

Figure 3-2. The schematic sketch of grain particle arrangements in a porous medium for two extreme cases.

(4) The external forces on the fluid in the porous medium are homogeneous and time independent. The gravitational force is neglected.

(5) The pressure gradient in each canal is proportional to the cosine of the angle between the direction of the canal and the principal direction of the gradient.

(6) Any part in the porous medium is macroscopically identical with other parts in the same sample. This implies that a fluid particle travelling in the porous medium finds exactly the same probability function for displacement at any point in the medium.

3. Pore Geometry.

Since a porous medium is constituted by packing of the grain particles, the shape, size and direction of the individual canal in the medium depend upon those of its adjacent grain particles. The directions of the canals in a porous medium which is made up of uniform spherical particles are approximately randomly oriented. For a porous medium consisting of plate-shaped particles, anisotropy is dependent on its packing characteristics and the canals usually show some preferred orientation. In Figure 3-2, schematic sketches of these two extreme conditions are shown for plate shaped particles.

A mathematical expression for the distribution of the canal direction is required. For a randomly oriented porous medium (Figure 3-3), let the direction of canal be represented by the fraction of surface area on a hemisphere. Then the probability for a fluid particle to find a direction defined by dA which is contained between θ, ϕ and $\theta + d\theta$, $\phi + d\phi$ may be represented as

$$p = \frac{r^2 \sin\theta \, d\theta \, d\phi}{2\pi r^2}$$

$$= \frac{1}{2\pi} \sin\theta \, d\theta \, d\phi \quad \ldots\ldots\ldots\ldots\ldots\ldots \quad (11)$$

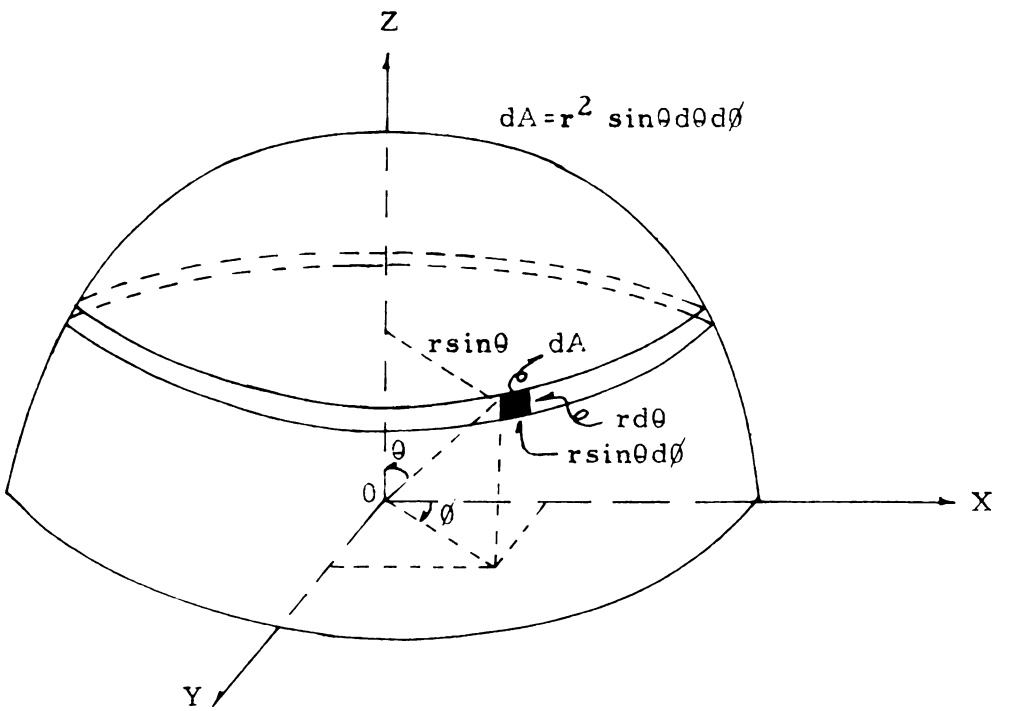

Figure 3-3. The distribution of pore canals as represented by the fraction of surface area over a hemisphere.

An anisotropic porous medium is one in which particles show preferred orientations. It is assumed here that the distribution of canal direction for the general anisotropic case has the following form

$$p = \frac{a}{2\pi} \sin^n\theta \, d\theta \, d\phi \quad \ldots\ldots\ldots\ldots\ldots\ldots \quad (12)$$

in which n is a positive number (equal to or greater than unity) that characterizes the particle orientation. a is a normalization constant which can be expressed by the following equation. (See Appendix I, section 1, for derivation).

$$a = \frac{n(n-2)(n-4)\ldots\ldots}{(n-1)(n-3)\ldots\ldots}\left(\frac{2}{\pi}\right)^b \quad \ldots\ldots\ldots\ldots \quad (13)$$

where b = 1 for n even and b = 0 for n odd. It is seen that when n is equal to unity, Eq. (12) represents the case for a randomly oriented porous medium and when n approaches infinity, Eq. (12) represents a case where all the canals are lined up at θ equals 90 degrees, a completely oriented porous medium.

4. Probability Distribution Function of Fluid Flow.

A fluid particle travelling in a porous medium will have to make a choice of direction whenever it arrives at a junction of canals. This choice of direction not only depends on the pore canal distribution as discussed in the preceding section but also depends on the direction of the individual canals. The discharge of each individual canal is proportional to the cosine of θ by virtue of assumption (5) in section 2. Therefore, those canals making angles perpendicular to the gradient will have no discharge at all. This means that the probability of a fluid particle entering such a canal is zero even though there may exist a large portion of canals in that particular direction. The probability of a fluid particle to take up the direction defined by an area dA which is contained between θ, ∅ and θ + dθ, ∅ + d∅ is assumed to be equal to the proportion of the discharge in that direction to the total discharge (all canals in all directions). The discharge of a canal with angle θ_j is

$$q_j = q_o \cos\theta_j \quad . \quad . \quad . \quad . \quad . \quad . \quad . \quad . \quad . \quad . \quad . \quad . \quad . \quad . \quad . \quad (14)$$

where q_o is the maximum possible discharge of a canal and is equal to the discharge of that canal with θ_j equal to zero.

Therefore, the discharge toward the direction dA can be defined as, by combining Eq. (14) and Eq. (12),

$$q_{\theta\phi} = \frac{aq_o}{2\pi} \sin^n\theta \cos\theta \, d\theta \, d\phi \quad . \quad . \quad . \quad . \quad . \quad . \quad . \quad . \quad . \quad (15)$$

Let Q be the overall average discharge for all directions, then,

$$Q = \int_0^{2\pi} d\phi \int_0^{\frac{1}{2}\pi} \frac{aq_o}{2\pi} \sin^n\theta \cos\theta d\theta = \frac{aq_o}{n+1} \quad . \quad . \quad . \quad . \quad . \quad (16)$$

Let $g_{\theta\phi}$ denote the fraction of the discharge in the direction defined by dA which is contained between θ, ϕ and $\theta + d\theta$, $\phi + d\phi$.

$$g_{\theta\phi} = \frac{q_{\theta\phi}}{Q} = \frac{n+1}{2\pi} \sin^n\theta \cos\theta \, d\theta \, d\phi \quad . \quad . \quad . \quad . \quad . \quad (17)$$

Eq. (17) is the probability distribution function for the choice of direction based on discharge and geometric distributions of the pore canals. Probability distribution functions for various orientation factors are computed from Eq. (17) and are shown in Figure 3-4.

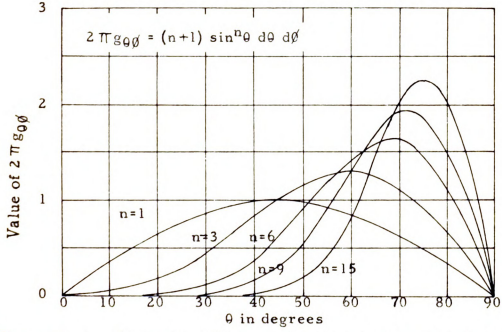

Figure 3-4. The probability distribution curves of the choice of directions at a junction in a porous medium.

5. Longitudinal Displacement of Fluid Particle After N Consecutive Steps.

The process of the fluid particle movement in the porous medium is considered as a series of consecutive steps of displacement in the unit canal network. Here a step of displacement is defined as the journey through a unit canal. The distance of this displacement in the gradient direction is called the longitudinal displacement and is equal to

$$z_j = L \cos\theta_j \quad . \quad . \quad . \quad . \quad . \quad . \quad . \quad . \quad . \quad . \quad . \quad . \quad . \quad . \quad . \quad (18)$$

Now, after N consecutive steps the total longitudinal displacement is

$$Z = L \sum_{j=1}^{N} \cos\theta_j \quad . \quad . \quad . \quad . \quad . \quad . \quad . \quad . \quad . \quad . \quad . \quad . \quad . \quad . \quad (19)$$

in which Z is a function of the choice of direction at every step of displacement and therefore is dependent on the probability distribution of θ and $\emptyset$.

If the probability distribution of θ and $\emptyset$ is that given by Eq. (17), then the average displacement of each step in the longitudinal direction may be evaluated as follows. Let E(z) be the average longitudinal displacement for each step in a unit canal, then

$$E(z) = \int_g L \cos\theta \, g_{\theta\emptyset} \quad . \quad . \quad . \quad . \quad . \quad . \quad . \quad . \quad . \quad . \quad . \quad . \quad . \quad . \quad (20)$$

Substitute Eq. (17) into Eq. (20) and integrate, it is obtained that

$$E(z) = \frac{L(n+1)\,(n-1)\,.\,.}{(n+2)\,n\,(n-2)\,.\,.} \left(\frac{\pi}{2}\right)^b \quad . \quad . \quad . \quad . \quad . \quad . \quad . \quad (21)$$

The variance of z is evaluated as (see Appendix I, section 2)

$$\mathrm{Var}(z) = \sigma_z^2 = \frac{2L^2}{n+3} - \left(\frac{L(n+1)(n-1)\cdots}{(n+2)n(n-2)\cdots}\left(\frac{\pi}{2}\right)^b\right)^2 \quad . \quad . \quad . \quad . \quad (22)$$

The average displacement of a fluid particle in the longitudinal direction after N consecutive steps is

$$E(Z) = NE(z). \quad . \quad . \quad . \quad . \quad . \quad . \quad . \quad . \quad . \quad . \quad . \quad . \quad . \quad (23)$$

and the variance of Z is the sum of the variances of the N steps

$$\mathrm{Var}(Z_N) = N\,\mathrm{Var}(z) = N\sigma_z^2 \quad . \quad . \quad . \quad . \quad . \quad . \quad . \quad . \quad . \quad . \quad (24)$$

From Eq. (21) through Eq. (24) it can be seen that the average displacement and the standard deviation of each step not only depend on the length of the unit canal but also depend on the canal orientation factor n.

According to probability calculus, after N repeated trials the distribution approaches the Gaussian distribution provided N is sufficiently large. Therefore, the probability for a fluid particle to arrive at a distance between Z and Z+dZ along the gradient direction after N steps is

$$p(Z_N) = \frac{1}{(2\pi N\sigma_z^2)^{1/2}} \exp\left(-\frac{(Z-E(Z))^2}{2N\sigma_z^2}\right) . \quad . \quad . \quad . \quad . \quad (25)$$

where σ_z is the standard deviation of each step as expressed by Eq. (22) and Z is the longitudinal displacement travelled by the fluid particle after N repeated steps as represented by Eq. (19). E(Z) is the average longitudinal displacement after N steps as represented by Eq. (21) and Eq. (23).

6. The Mechanism of Fluid Flow in a Porous Medium.

Considering now the mechanism of fluid flow in a porous medium. Let t_o denote the shortest time possible for a fluid particle to pass through a unit canal of length L. Then by virtue of the preceding assumptions made with regard to the canal network model,

$$t_j = t_o \sec\theta_j \quad . \quad . \quad . \quad . \quad . \quad . \quad . \quad . \quad . \quad . \quad . \quad . \quad . \quad . \quad . \quad (26)$$

where t_j is the time required for a fluid particle to pass through a canal making angle θ_j with the gradient direction. If N canals are taken, then the total time required T_N will be

$$T_N = t_o \sum_{j=1}^{N} \sec\theta_j \quad . \quad . \quad . \quad . \quad . \quad . \quad . \quad . \quad . \quad . \quad . \quad . \quad . \quad (27)$$

Therefore, the distribution function represented by Eq. (25) in the preceding section involves an unknown distribution of time which is dependent on the path taken by an individual particle. Two fluid particles may pass through the same number of canals arriving at different longitudinal distances and spending different times. Also, two fluid particles may pass through different number of canals by taking different paths and arriving at different longitudinal distances for the same amount of time. Furthermore, two fluid particles may pass through different paths in arriving at a given longitudinal distance but the time spent and the number of canals traversed are different.

If, in a given porous medium, a large number of fluid particles are introduced and the journey of each individual fluid particle is followed closely. Then, for a given longitudinal distance Z_o, the

number of unit canals traversed by individual particles to arrive at Z_o may be averaged as $\bar{N}_{Z_o}$, and the time required for each individual particle to arrive at this longitudinal distance may be averaged as $\bar{T}_{Z_o}$. Letting L, the length of the unit canal and t_o, the minimum time required for a fluid particle to pass through a unit canal be equal to unity, the following two equations may be written from Eqs. (19) and (27).

$$Z_o = \bar{N}_{Z_o} \langle \overline{\cos\theta} \rangle_{Z_o} \quad \ldots\ldots\ldots\ldots\ldots \quad (28)$$

$$\bar{T}_{Z_o} = \bar{N}_{Z_o} \langle \overline{\sec\theta} \rangle_{Z_o} \quad \ldots\ldots\ldots\ldots\ldots \quad (29)$$

where $\langle \overline{\cos\theta} \rangle_{Z_o}$ is the average longitudinal distance of each step and is a representative value of the orientation of the given porous medium which is defined by $Z_o/\bar{N}_{Z_o}$ and $\langle \overline{\sec\theta} \rangle_{Z_o}$ is the average time required for one step of journey for the given porous medium.

In Eqs. (28) and (29), $\bar{N}_{Z_o}$ is the average number of canals and $\bar{T}_{Z_o}$ is the average time required for a given Z_o. If an individual fluid particle travelling an arbitrary path is considered, then the number of canals travelled N_{Z_o}, and the time required T_{Z_o} are random variables depending on the path taken. This is illustrated in Figure 3-5 as case (c). The following two equations may be written to describe these random variables:

$$Z_o = N_{Z_o} \langle \cos\theta \rangle_{Z_o} \quad \ldots\ldots\ldots\ldots\ldots \quad (30)$$

$$T_{Z_o} = N_{Z_o} \langle \sec\theta \rangle_{Z_o} \quad \ldots\ldots\ldots\ldots\ldots \quad (31)$$

Now, if the average number of canals in the above case is considered as fixed, then for this fixed $\bar{N}_{Z_o}$, the average distance travelled by the fluid particles and the average time required to complete this fixed number of steps may be expressed as

$$\bar{Z}_{\bar{N}} = \bar{N}_{Z_o} \langle \overline{\cos\theta} \rangle_{\bar{N}} \quad . \quad . \quad . \quad . \quad . \quad . \quad . \quad . \quad . \quad . \quad . \quad . \quad (32)$$

$$\bar{T}_{\bar{N}} = \bar{N}_{Z_o} \langle \overline{\sec\theta} \rangle_{\bar{N}} \quad . \quad . \quad . \quad . \quad . \quad . \quad . \quad . \quad . \quad . \quad . \quad . \quad (33)$$

and similarly the individual fluid particles in an arbitrary path may have distributions of longitudinal distance $Z_{\bar{N}}$ and $T_{\bar{N}}$ as follows:

$$Z_{\bar{N}} = \bar{N}_{Z_o} \langle \cos\theta \rangle_{\bar{N}} \quad . \quad . \quad . \quad . \quad . \quad . \quad . \quad . \quad . \quad . \quad . \quad . \quad (34)$$

$$T_{\bar{N}} = \bar{N}_{Z_o} \langle \sec\theta \rangle_{\bar{N}} \quad . \quad . \quad . \quad . \quad . \quad . \quad . \quad . \quad . \quad . \quad . \quad . \quad (35)$$

This is the case illustrated in Figure 3-5 as case (b), and it can be seen that this is exactly the case investigated in the preceding section and expressed in Eq. (25). The conditional probability distribution for the longitudinal displacement $Z_{\bar{N}}$ may now be rewritten in the following form

$$p(Z_{\bar{N}}) = \frac{1}{(2\pi \bar{N}_{Z_o} \sigma_z^2)^{1/2}} \exp\left(- \frac{(Z_{\bar{N}} - \bar{Z}_{\bar{N}})^2}{2 \bar{N}_{Z_o} \sigma_z^2} \right) \quad . \quad . \quad . \quad (25a)$$

The above expression is the distribution function of longitudinal distances travelled after a fixed number of canals $\bar{N}$ and is obtainable by knowing exactly the pore canal distribution. However, a measurement of such a distribution in a laboratory is practically impossible.

Another type of distribution may be investigated. If the average

time $\bar{T}_{Z_o}$ in Eq. (29) is fixed, then there exists a distribution in the longitudinal displacement for this fixed time and there also exists a distribution of the number of canals taken by an individual fluid particle. This is the case of (a) in Figure 3-5 and may be expressed in the following equations:

$$\bar{Z}_{\bar{T}} = \bar{N}_{\bar{T}} \langle \overline{\cos\theta} \rangle_{\bar{T}} \quad \ldots\ldots\ldots\ldots\ldots\ldots \quad (36)$$

$$\bar{T}_{Z_o} = \bar{N}_{\bar{T}} \langle \overline{\sec\theta} \rangle_{\bar{T}} \quad \ldots\ldots\ldots\ldots\ldots\ldots \quad (37)$$

For the individual particle in an arbitrary path, the random variables may be expressed in the forms

$$Z_{\bar{T}} = N_{\bar{T}} \langle \cos\theta \rangle_{\bar{T}} \quad \ldots\ldots\ldots\ldots\ldots\ldots \quad (38)$$

$$\bar{T}_{Z_o} = N_{\bar{T}} \langle \sec\theta \rangle_{\bar{T}} \quad \ldots\ldots\ldots\ldots\ldots\ldots \quad (39)$$

The distribution of longitudinal displacement for fixed time as expressed in Eq. (38) may be measured in the laboratory although difficult. It is difficult to measure the quantity of fluid particles at different positions at the same time.

In summary, for any path chosen in a porous medium, the progress of a fluid particle can be described in the following three cases (see Figure 3-5).

(a) For a fixed time of $\bar{T}_{Z_o}$, the number of canals and the distance are variables dependent on the paths.

(b) For a fixed number of canals $\bar{N}_{Z_o}$, the time spent and the distance travelled are variables depending on paths.

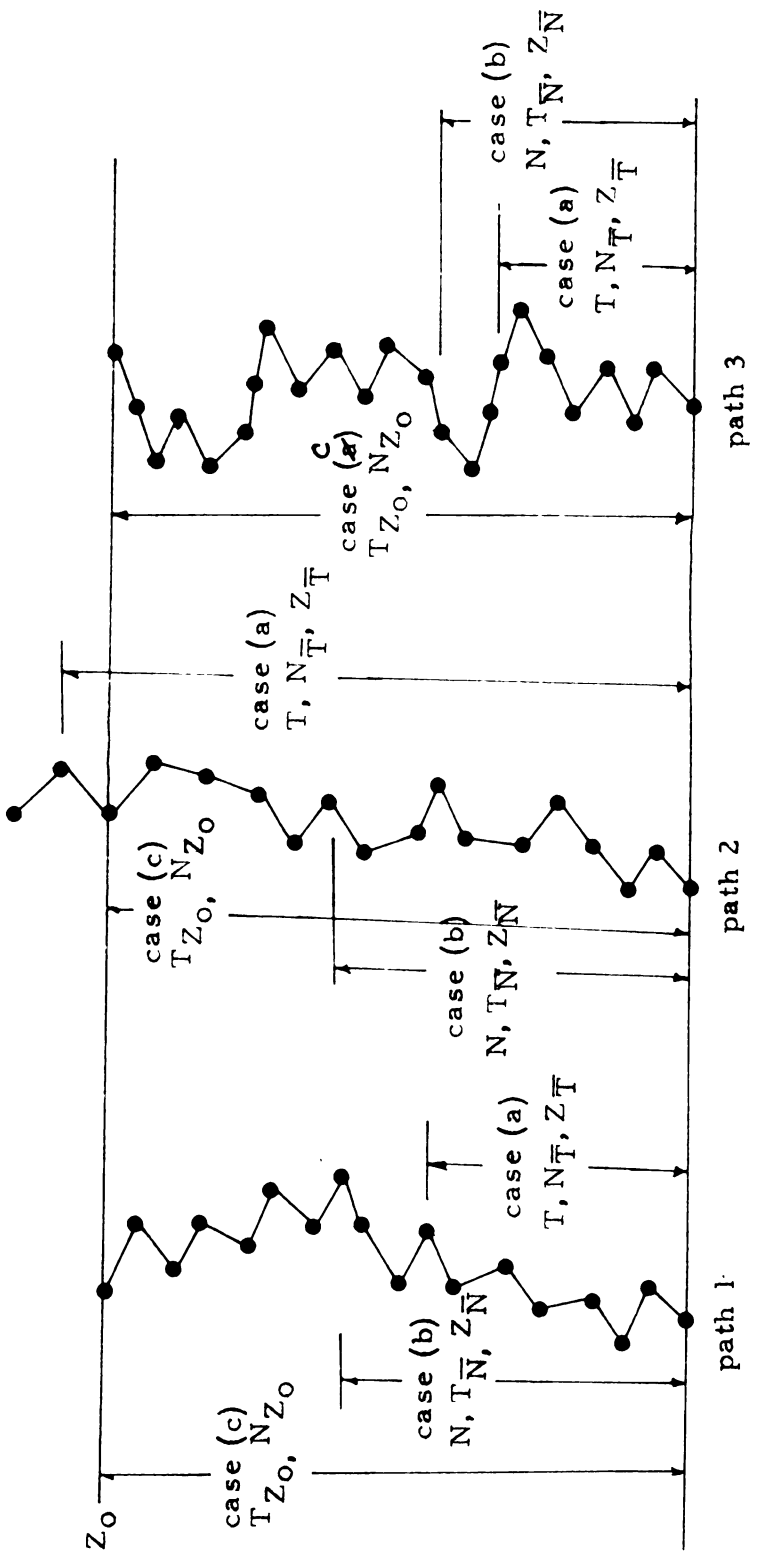

Figure 3-5. The schematic diagram for the relationship between the fixed values of Z_o, $\bar{T}$, $\bar{N}$ and the random variables in paths of a porous medium.

(c) For a given distance Z_o, the time spent and the number of canals traversed are variables depending on paths.

The relationship between the random variables in the above three cases may be evaluated as follows:

From Eqs. (32) and (38)

$$\frac{\bar{Z}_{\bar{N}}}{Z_{\bar{T}}} = \frac{\bar{N}_{Z_o} \langle \overline{\cos\theta} \rangle_{\bar{N}}}{N_{\bar{T}} \langle \cos\theta \rangle_{\bar{T}}} \quad \ldots\ldots\ldots\ldots \quad (40)$$

and from Eqs. (33) and (39)

$$\frac{\bar{T}_{\bar{N}}}{\bar{T}_{Z_o}} = \frac{\bar{N}_{Z_o} \langle \overline{\sec\theta} \rangle_{\bar{N}}}{N_{\bar{T}} \langle \sec\theta \rangle_{\bar{T}}} \quad \ldots\ldots\ldots\ldots \quad (41)$$

Therefore, by combining Eqs.(40) and (41)

$$\frac{\bar{Z}_{\bar{N}}}{Z_{\bar{T}}} = \left(\frac{\bar{N}_{Z_o}}{N_{\bar{T}}}\right)^2 \left[\frac{\langle \overline{\sec\theta} \rangle_{\bar{N}} \langle \overline{\cos\theta} \rangle_{\bar{N}}}{\langle \cos\theta \rangle_{\bar{T}} \langle \sec\theta \rangle_{\bar{T}}} \cdot \frac{\bar{T}_{Z_o}}{\bar{T}_{\bar{N}}} \right] \quad \ldots\ldots \quad (42)$$

By comparing Eqs. (38) and (34)

$$\frac{Z_{\bar{T}}}{Z_{\bar{N}}} = \frac{N_{\bar{T}} \langle \cos\theta \rangle_{\bar{T}}}{\bar{N}_{Z_o} \langle \cos\theta \rangle_{\bar{N}}} \quad \ldots\ldots\ldots\ldots \quad (43)$$

Therefore,

$$\frac{\bar{N}_{Z_o}}{N_{\bar{T}}} = \frac{Z_{\bar{N}} \langle \cos\theta \rangle_{\bar{T}}}{Z_{\bar{T}} \langle \cos\theta \rangle_{\bar{N}}} \quad \ldots\ldots\ldots\ldots \quad (44)$$

Substitution of Eq. (44) into Eq. (42) will result in

$$Z_{\bar{T}} = \frac{Z_{\bar{N}}^2}{\bar{Z}_{\bar{N}}} \left[\frac{\langle \overline{\sec\theta} \rangle_{\bar{N}} \langle \overline{\cos\theta} \rangle_{\bar{N}} \langle \cos\theta \rangle_{\bar{T}}}{\langle \sec\theta \rangle_{\bar{T}} \langle \cos\theta \rangle_{\bar{N}}^2} \cdot \frac{\bar{T}_{Z_o}}{\bar{T}_{\bar{N}}} \right] \quad . \quad . \quad . \quad . \quad (45)$$

This is the relationship between the longitudinal displacement for a fixed time $\bar{T}$ and the distribution of longitudinal displacement for a fixed number of canals $\bar{N}$. Under the assumption that for each individual path $Z_{\bar{T}}$ and $Z_{\bar{N}}$ do not differ much, the distribution Z_T may be derived using Eq. (45). In Eq. (45) the expression inside the brackets may be analyzed as follows. The ratio of $\bar{T}_{Z_o}$ to $\bar{T}_{\bar{N}}$ may be considered as approximately unity in a porous medium of large dimension compared to the length of the individual canals. Also $\langle \cos\theta \rangle_{\bar{T}}$ and $\langle \cos\theta \rangle_{\bar{N}}$ for an individual path can also be considered approximately equal by assuming that for a given path the average orientation is not changed greatly by the addition of a relatively small number of unit canals. However, the values of $\langle \cos\theta \rangle_{\bar{T}}$ times $\langle \sec\theta \rangle_{\bar{T}}$ and $\langle \overline{\cos\theta} \rangle_{\bar{N}}$ times $\langle \overline{\sec\theta} \rangle_{\bar{N}}$ are not necessarily equal or approximately equal to unity depending on the particular porous medium and the individual path. It is a function of the path including the number of canals and the canal orientations. In order to simplify the analysis, these two quantities, $\langle \cos\theta \rangle_{\bar{T}} \langle \sec\theta \rangle_{\bar{T}}$ and $\langle \overline{\cos\theta} \rangle_{\bar{N}} \langle \overline{\sec\theta} \rangle_{\bar{N}}$, may be assumed to be equal to unity. The probable error involved in this assumption is investigated and presented in Appendix II.

Now, if we compare Eqs. (30) and (38)

$$\frac{Z_o}{Z_{\bar{T}}} = \frac{N_{Z_o} \langle \cos\theta \rangle_{Z_o}}{N_{\bar{T}} \langle \cos\theta \rangle_{\bar{T}}} \quad . \quad . \quad . \quad . \quad . \quad . \quad . \quad . \quad . \quad . \quad . \quad . \quad (46)$$

and from Eqs. (39) and (31)

$$\frac{\bar{T}_{Z_o}}{T_{Z_o}} = \frac{N_{\bar{T}} \langle \sec\theta \rangle \bar{T}}{N_{Z_o} \langle \sec\theta \rangle Z_o} \quad \ldots\ldots\ldots\ldots\ldots\ldots \quad (47)$$

Therefore, from Eqs. (46) and (47)

$$T_{Z_o} = \frac{Z_o \bar{T} Z_o}{Z_{\bar{T}}} \left[\frac{\langle \cos\theta \rangle_{\bar{T}} \langle \sec\theta \rangle_{Z_o}}{\langle \cos\theta \rangle_{Z_o} \langle \sec\theta \rangle_{\bar{T}}} \right] \quad \ldots\ldots\ldots \quad (48)$$

where T_{Z_o} is the distribution in time required to arrive at a given longitudinal distance Z_o as represented by case (c) in Figure 3-5. T_{Z_o} is a measurable quantity and the laboratory set-up for this measurement is usually more convenient because many time readings can be taken at one location whereas there is a serious limitation on the number of locations that can be measured at a given time. The quantity inside the brackets of Eq. (48) may be considered as approximately equal to unity if it is assumed that for a fluid particle travelling in a given path the average orientation will not change appreciably from one stage to another. This is a reasonable assumption considering that the range of the dispersion in the porous medium is usually small compared to the overall size of the medium.

Approximations other than that obtained by replacing the bracket of Eq. (48) by unity are possible, for example, by substitution of Eqs. (32) and (34) into Eq. (45), Eq. (45) may be rewritten in the following manner:

$$Z_{\bar{T}} = \frac{Z_{\bar{N}}^2}{\bar{Z}_{\bar{N}}} \left[\frac{\bar{Z}_{\bar{N}} \langle \overline{\sec\theta} \rangle_{\bar{N}} \langle \cos\theta \rangle_{\bar{T}} \quad \bar{T}_{Z_o}}{Z_{\bar{N}} \langle \sec\theta \rangle_{\bar{T}} \langle \cos\theta \rangle_{\bar{N}} \quad \bar{T}_{\bar{N}}} \right]$$

or

$$Z_{\overline{T}} = Z_{\overline{N}} \left[\frac{\langle \overline{\sec\theta} \rangle_{\overline{N}} \langle \cos\theta \rangle_{\overline{T}} \quad \overline{T}_{Z_o}}{\langle \sec\theta \rangle_{\overline{T}} \langle \cos\theta \rangle_{\overline{N}} \quad \overline{T}_{\overline{N}}} \right] . \quad . \quad . \quad . \quad . \quad . \quad (49)$$

Therefore, the distribution of longitudinal displacement for fixed $\overline{T}$ is now expressed as proportional to the distribution of longitudinal displacement for fixed $\overline{N}$. Based on the foregoing discussions, the quantities in the bracket of Eq. (49) may be considered as approximately equal to unity except the ratio of $\langle \overline{\sec\theta} \rangle_{\overline{N}}$ to $\langle \sec\theta \rangle_{\overline{T}}$. This ratio may be larger or smaller than unity dependent on their average orientations because they represent two different paths in a porous medium.

The following additional assumptions are necessary with regard to Eqs. (45), (48) and (49) in order to simplify the relationships between random variables.

(1) In a given path the average orientation of the path is approximately the same at different stages. This implies that if $\langle \cos\theta \rangle_{\overline{N}}$ is obtained for a fixed $\overline{N}$ steps, then, provided the fluid particle continue this path until a fixed time $\overline{T}$, the new $\langle \cos\theta \rangle_{\overline{T}}$ will still be approximately equal to $\langle \cos\theta \rangle_{\overline{N}}$. Therefore, the quantity

$$\left[\frac{\langle \cos\theta \rangle_{\overline{T}} \langle \sec\theta \rangle_{Z_o}}{\langle \cos\theta \rangle_{Z_o} \langle \sec\theta \rangle_{\overline{T}}} \right]$$

in Eq. (48) will be approximately equal to unity.

(2) The ratio $\overline{T}_{Z_o} / \overline{T}_{\overline{N}}$ is assumed to be approximately equal to unity. Since $\overline{N}$ is the average number of steps required to arrive at a given longitudinal distance Z_o, therefore, the average time required for particles to complete a longitu-

dinal distance of Z_o should be approximately equal to the average time required for completion of $\bar{N}$ steps.

(3) In a given path if an average $\langle\cos\theta\rangle$ is obtained, then there exists an average $\langle\sec\theta\rangle$ such that $\langle\cos\theta\rangle = 1/\langle\sec\theta\rangle$. This assumption will inevitably produce an error whose magnitude depends on individual paths. An investigation of the magnitude of error for this assumption is presented in Appendix II.

(4) The ratio of $\langle\overline{\sec\theta}\rangle_{\bar{N}}$ to $\langle\sec\theta\rangle_{\bar{T}}$ in Eq. (49) is assumed to be approximately equal to unity. The possible error involved in this assumption is investigated and presented in Appendix II.

Based on the above assumptions, we may replace Eq. (45) by

$$Z_{\bar{T}} = \frac{Z_{\bar{N}}^2}{\bar{Z}_{\bar{N}}} \qquad \ldots\ldots\ldots\ldots\ldots\ldots \quad (50)$$

and Eq. (49) may be replaced by

$$Z_{\bar{T}} = Z_{\bar{N}} \qquad \ldots\ldots\ldots\ldots\ldots\ldots \quad (51)$$

Also, Eq. (48) may be replaced by

$$Z_{\bar{T}} = \frac{Z_o \; {}_{\bar{T}}Z_o}{{}_{\bar{T}}Z_o} \qquad \ldots\ldots\ldots\ldots\ldots\ldots \quad (52)$$

Eq. (52) is to be used to obtain the distribution of the longitudinal displacement for a fixed $\bar{T}$ from the measured distribution of time for a given distance Z_o. Eqs. (50) and (51) are to be used to obtain the theoretical distribution of the longitudinal displacement from the known distribution of longitudinal displacement for a fixed number of steps $\bar{N}$ as expressed by Eq. (25a).

7. The Longitudinal Dispersion of Fluid Flow in a Porous Medium.

During the displacement of one miscible fluid by another, the break through curve obtained from Eqs. (50) or (51) gives the particle concentration at the mixing front. The degree of dispersion is measured by the standard deviation. It is necessary to derive the expressions for the expected mean and standard deviation for the distribution of longitudinal displacement at a fixed time $\bar{T}_{Z_o}$.

Define μ_i' as the "i"th moment about an arbitrary point and μ_i as the "i"th moment about the mean. Then, by definition the following general equations may be written (see Kendall (8)).

$$\mu_i' = \int_{-\infty}^{\infty} (x)^i p(x)dx \quad . \quad . \quad . \quad . \quad . \quad . \quad . \quad . \quad . \quad . \quad . \quad . \quad (53)$$

$$\mu_i = \int_{-\infty}^{\infty} (x-\mu_i')^i p(x)dx \quad . \quad . \quad . \quad . \quad . \quad . \quad . \quad . \quad . \quad . \quad . \quad . \quad (54)$$

We have

$$\mu_2' = \mu_2 + \mu_1'^2 \quad . \quad . \quad . \quad . \quad . \quad . \quad . \quad . \quad . \quad . \quad . \quad . \quad . \quad (55)$$

and

$$\mu_4' = \mu_4 + 4\mu_1'\mu_3 + 6\mu_1'^2\mu_2 + 4\mu_1'^3\mu_1 + \mu_1'^4 \quad . \quad . \quad . \quad . \quad (56)$$

where μ_2 is the variance and since for the normal distribution

$$\mu_1 = \mu_3 = 0$$

and

$$\mu_4 = 3\mu_2^2$$

therefore, Eq. (56) may be written as

$$\mu_4' = 3\mu_2^2 + 6\mu_1'^2\mu_2 + \mu_1'^4 \quad . \quad . \quad . \quad . \quad . \quad . \quad . \quad . \quad . \quad . \quad (56a)$$

Now, from Eq. (50), the expected value for $Z_{\bar{T}}$ may be evaluated as

$$E(Z_{\bar{T}}) = \bar{Z}_{\bar{N}}^{-1} E(Z_{\bar{N}}^2) \quad . \quad . \quad . \quad . \quad . \quad . \quad . \quad . \quad . \quad . \quad . \quad . \quad (57)$$

and from Eq. (55), $E(Z_{\bar{N}}^2)$ may be written as

$$E(Z_{\bar{N}}^2) = \sigma_{\bar{N}}^2 + E(Z_{\bar{N}})^2 \quad . \quad . \quad . \quad . \quad . \quad . \quad . \quad . \quad . \quad . \quad . \quad . \quad (58)$$

Therefore, by substitution of Eq. (58) into Eq. (57), it is obtained that

$$E(Z_{\bar{T}}) = \bar{Z}_N^{-1} (\sigma_{\bar{N}}^2 + \bar{Z}_{\bar{N}}^2) \quad . \quad . \quad . \quad . \quad . \quad . \quad . \quad . \quad . \quad . \quad (59)$$

The variance of $Z_{\bar{T}}$ may be obtained from Eq. (55)

$$Var(Z_{\bar{T}}) = E(Z_{\bar{T}}^2) - E(Z_{\bar{T}})^2 \quad . \quad . \quad . \quad . \quad . \quad . \quad . \quad . \quad . \quad . \quad (60)$$

and from Eq. (50), since

$$E(Z_{\bar{N}}^2) = \bar{Z}_{\bar{N}}^{-2} E(Z_{\bar{N}}^4) \quad . \quad . \quad . \quad . \quad . \quad . \quad . \quad . \quad . \quad . \quad . \quad . \quad (61)$$

Also from Eq. (56a)

$$E(Z_{\bar{N}}^4) = 3\sigma_{\bar{N}}^4 + 6\bar{Z}_{\bar{N}}^2 \sigma_{\bar{N}}^2 + Z_{\bar{N}}^4 \quad . \quad . \quad . \quad . \quad . \quad . \quad . \quad (62)$$

By substitution of Eqs. (62), (61) and (59) into Eq. (60), it is obtained that

$$Var(Z_{\bar{T}}) = 2\bar{Z}_{\bar{N}}^{-2} (\sigma_{\bar{N}}^4 + 4\bar{Z}_{\bar{N}}^2 \sigma_{\bar{N}}^2) \quad . \quad . \quad . \quad . \quad . \quad . \quad . \quad (63)$$

For the case of n = 1, from Eq. (24)

$$\sigma_{\bar{N}}^2 = \frac{\bar{N} L^2}{18} \quad . \quad . \quad . \quad . \quad . \quad . \quad . \quad . \quad . \quad . \quad . \quad . \quad . \quad . \quad . \quad (64)$$

and from Eqs. (21) and (23)

$$\bar{Z}_{\bar{N}} = \frac{2}{3}\bar{N}L \quad \ldots \quad (65)$$

therefore

$$\sigma^2_{\bar{N}} = \frac{1}{12}\bar{Z}_{\bar{N}}L \quad \ldots \quad (66)$$

Substitutions of the above three equations into Eqs. (59) and (63) give the following expressions:

$$E(Z_{\bar{T}}) = \bar{Z}_{\bar{N}} + \frac{L}{12} \quad \ldots \quad (67)$$

$$Var(Z_{\bar{T}}) = \frac{L}{3}(\bar{Z}_{\bar{N}} + \frac{L}{24}) \quad \ldots \quad (68)$$

and

$$\sigma_{Z_{\bar{T}}} = \sqrt{\frac{L}{3}(\bar{Z}_{\bar{N}} + \frac{L}{24})} \quad \ldots \quad (69)$$

Eq. (59) and Eq. (63) are the general expressions for the expected mean and the variance for $Z_{\bar{T}}$. Substitutions of Eq. (21) and Eq. (22) into Eq. (59) and Eq. (63) give the expressions in terms of the orientation factor n.

$$E(Z_{\bar{T}}) = \bar{Z}_{\bar{N}} + L(\frac{2}{(n+3)C_n} - C_n) \quad \ldots \quad (70)$$

$$\sigma^2_{Z_{\bar{T}}} = 4\bar{Z}_{\bar{N}}L(\frac{2}{(n+3)C_n} - C_n) + 2L^2(\frac{2}{(n+3)C_n} - C_n)^2 \quad \ldots \quad (71)$$

where the term C_n is expressed as

$$C_n = \frac{(n+1)(n-1)\ldots}{(n+2)(n)(n-2)\ldots}(\frac{\pi}{2})^b \quad \ldots \quad (72)$$

and b = 1 for n equals even numbers and b = 0 for n equals odd numbers. Let us define a numerical constant C'_n to include all the terms that contain the orientation factor n in Eq. (70) and Eq. (71) as

$$C'_n = \frac{2}{(n+3)\,C_n} - C_n \quad \ldots\ldots\ldots\ldots\ldots \quad (73)$$

In Figure 3-6 the relationship of C'_n against n is shown. It is noted that C'_n has its maximum value at n = 4 and then decreases rather slowly as n increases.

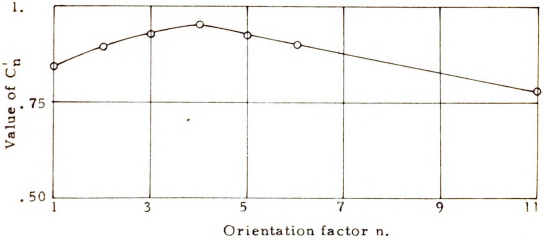

Figure 3-6. Relationship between orientation factor n and C'_n in Eq. (73).

The above analysis for the expected mean and variance for $Z_{\bar{T}}$ are based on the relationship of random variables as represented by Eq. (50). On the other hand, Eq. (51) may be used instead of Eq. (50). Since in Eq. (51) the distribution of longitudinal displacement for a fixed time is considered to be equal to the distribution of the longitudinal distance for a fixed $\bar{N}$, the expected mean and the variance for $Z_{\bar{T}}$ may be represented by Eqs. (21), (22), (23) and (24).

8. The Permeability Coefficient and Orientation Factor.

In Figure 3-1 a fluid particle enters the porous medium at point 0 and arrives at point 0_1 after travelling N unit canals. The permeability is defined as the velocity of flow for a unit pressure gradient. If the permeability of the porous medium is measured in two perpendicular directions as K_z and K_x and if $\langle\overline{\cos\theta}\rangle$ and $\langle\overline{\cos\psi}\rangle$ are used to denote the average value of the flow path through the porous medium with respect to these two gradient directions, then a relationship between canal orientation and the permeability coefficients can be established in the following manner.

If K_z and K_x are defined as the permeability coefficients along Z-direction and X-direction respectively, then the following relationships may be written:

$$K_z = Z_o / \overline{T}_{Z_o} = L \langle\overline{\cos\theta}\rangle \; / \; t_o \langle\overline{\sec\theta}\rangle \quad . \quad . \quad . \quad . \quad . \quad (74)$$

$$K_x = X_o / T_{X_o} = L \langle\overline{\cos\psi}\rangle \; / \; t_o \langle\overline{\sec\psi}\rangle \quad . \quad . \quad . \quad . \quad . \quad (75)$$

Therefore,

$$\frac{K_z}{K_x} = \frac{\langle\overline{\cos\theta}\rangle}{\langle\overline{\sec\theta}\rangle} \Big/ \frac{\langle\overline{\cos\psi}\rangle}{\langle\overline{\sec\psi}\rangle} \quad . \quad . \quad . \quad . \quad . \quad . \quad . \quad . \quad . \quad (76)$$

The quantities on the right hand side of Eq. (76) can be calculated using the equations derived in the preceding sections. Since the distribution of canal direction for the general anisotropic case was assumed to have the form represented by Eq. (12) and the theoretical probability function of the choice of canals based on discharge and geometric distribution was derived as Eq. (17) for a gradient in

Z-direction, the quantities $\langle\overline{\cos^n\theta}\rangle$ and $\langle\overline{\sec^n\theta}\rangle$ may be expressed as

$$\langle\overline{\cos^n\theta}\rangle = \int_\theta \int_\phi \beta_{\theta\phi} \cos^n\theta$$

$$= \frac{n+1}{2\pi} \int_0^{2\pi} \int_0^{\frac{1}{2}\pi} \sin^n\theta \cos^2\theta d\theta d\phi \quad . \quad . \quad . \quad . \quad (77)$$

Similarly,

$$\langle\overline{\sec^n\theta}\rangle = \frac{n+1}{2\pi} \int_0^{2\pi} \int_0^{\frac{1}{2}\pi} \sin^n\theta d\theta d\phi \quad . \quad . \quad . \quad . \quad . \quad . \quad (78)$$

The numerical values of $\langle\overline{\cos^n\theta}\rangle$ and $\langle\overline{\sec^n\theta}\rangle$ are calculated from the above two equations for various n values and plotted in Figure 3-7.

For the gradient in X-direction, similar derivations would lead to the results as follows (see Appendix I, section 3)

$$\langle\overline{\cos^n\psi}\rangle = B\frac{(n+1)(n-1)\ .\ .}{2n(n-2)\ .\ .} \int_{-\frac{1}{2}\pi}^{\frac{1}{2}\pi} \int_0^{\pi} \sin^{n+2}\theta\cos^2\phi d\theta d\phi \quad . \quad (79)$$

where B is equal to $1/\pi$ for odd numbers of n and is equal to $\frac{1}{2}$ for even numbers of n.

$$\langle\overline{\sec^n\psi}\rangle = B\frac{(n+1)(n-1)\ .\ .}{2n(n-2)\ .\ .} \int_{-\frac{1}{2}\pi}^{\frac{1}{2}\pi} \int_0^{\pi} \sin^n\theta d\theta d\phi. \quad . \quad . \quad . \quad . \quad (80)$$

The numerical values of $\langle\overline{\cos^n\theta}\rangle$, $\langle\overline{\cos^n\psi}\rangle$, $\langle\overline{\sec^n\theta}\rangle$ and $\langle\overline{\sec^n\psi}\rangle$ are calculated for various n values and are shown in Figure 3-7. It is seen that the values for $\langle\overline{\cos^n\theta}\rangle$ and $\langle\overline{\cos^n\psi}\rangle$, $\langle\overline{\sec^n\theta}\rangle$ and $\langle\overline{\sec^n\psi}\rangle$ are identical for the case of isotropical porous medium. The ratios for K_z and K_x are also calculated from Eq. (76) using these values and plotted as shown in Figure 3-8.

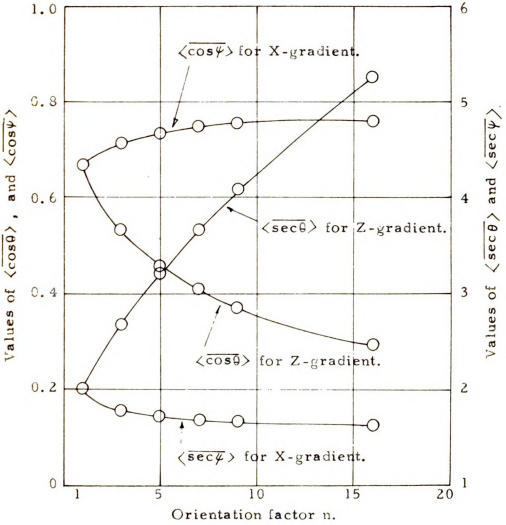

Figure 3-7. Numerical values of $\langle\overline{\cos\theta}\rangle$, $\langle\overline{\sec\theta}\rangle$, $\langle\overline{\cos\psi}\rangle$ and $\langle\overline{\sec\psi}\rangle$ for various n values.

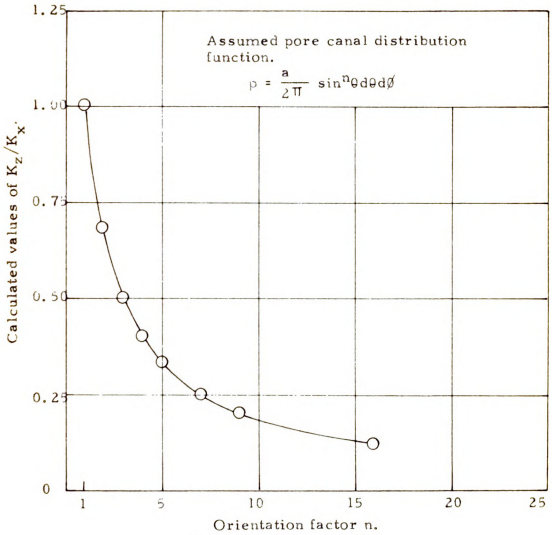

Figure 3-8. Relationship between the orientation factor n and the permeability ratio in an anisotropic porous medium calculated from Eq. (76).

CHAPTER 4

EXPERIMENTAL PROGRAMS

1. Sample Preparation.

Packings of spherical, plate shaped, and cylindrical particles were used to make the porous medium for the experiments. Ottawa sand was used to represent the spherical particles. The sieve analysis of the Ottawa sand shows that 97.7 percent of the particles have a diameter between 0.59 to 0.84 mm. Plate shaped particles were made out of plastic sheets. The plates were cut with a metal cutter carefully controlled to give uniform particle size. Besides the spherical and the plate shaped particles, cylindrically shaped particles were prepared from nylon filaments. A summary of the sample properties is given in Table 4-1.

2. Dispersion Measurements.

To measure the dispersion, a percolation apparatus as shown on Figure 4-1 was designed. The percolation cylinder was made of lucite. The cylinder was 6.35 cm. in diameter and 14 cm. in length. Pairs of electrodes were inserted at various distances from the bottom of the cylinder. The locations of the electrodes were as follows:

Position of electrodes	Distance from base
Position 1	1.25 cm.
Position 2	5.05 cm.
Position 3	8.85 cm.
Position 4	12.65 cm.

The electrodes consisted of $\frac{1}{2}$ mm. stainless steel wire and were connected to an Impedance Bridge of 1000 cycles per second. This set-up enabled the measurement of the electrical resistivity of the fluid around the electrodes.

The percolation cylinder was packed with the particles to make up the porous medium. The uniformity of the packing was controlled carefully during the process of packing. A 1.20 cm. thick layer of glass beads 6 mm. in diameter was placed underneath the percolation cylinder to serve as a filter. Between the porous medium layer and the filter a wire screen with 0.5 mm. opening was inserted.

The system was first saturated with 0.001 Normal NaCl solution. Then at the bottom of the cylinder the liquid was replaced with 0.1 Normal NaCl solution. The liquid at the bottom of the percolation cylinder was connected to a constant head supply tank of 0.1 Normal NaCl solution. Thus the liquid flow in the cylinder was upward and the flow rate was measured volumetrically at the outlet. The velocity of the flow in the porous medium was controlled by adjusting the head between the liquid surface in the supply tank and the outlet elevation of the cylinder. Different velocities were used for the same sample to obtain a range in the duration of time in order to obtain any information regarding the time effect on dispersion.

The flow velocities in the dispersion measurements were kept sufficiently small to produce laminar flow in the pore system. The actual velocities were all less than 1.0 cm/min. And since the largest size of the pore canal can be considered as to be approximately between 0.1 and 0.3 cm., the Reynold's number can be calculated as

$$R = \frac{VD\rho}{\mu} = \frac{1}{600} \text{ to } \frac{1}{200}$$

where V is the velocity, D is the size of the pore, ρ is the density of the fluid and μ is the viscosity of the fluid. A Reynold's number of unity is usually considered as the boundary between laminar and turbulent flow.

The time history of the change in NaCl concentration at each electrode position was determined by measuring the electrical resistance of the system with Impedance Bridge. From calibration test the relationship between the NaCl concentration and the electrical resistance was found to be linear in the log-log plot. Therefore, by measuring the electric resistance against time, the concentration of fluid around the electrode can be obtained by direct interpolation.

3. Permeability Measurements.

The permeability constant for the porous materials used in the dispersion measurements were determined by using a permeability apparatus shown in Figure 4-2. The apparatus was made of lucite and was designed to measure fluid flow in two perpendicular directions.

The porous materials were packed in the apparatus from the top. Preferred particle orientation was produced in the direction perpendicular to the direction of packing. After the medium was saturated with water, flow was introduced in the vertical direction and the rate of flow was measured at the outlet. The permeability coefficient was calculated by Darcy's law.

The longitudinal and transverse permeabilities K_z and K_x are defined respectively as the permeability of flow perpendicular and parallel to the direction of packing. According to the relationship derived in Chapter 3, the average orientation of the porous medium can be evaluated from the K_z and K_x data using Figure 3-8.

4. Presentation of the Experimental Data.

(1) Dispersion with respect to time.

Electric resistivity of the fluid in the percolation cylinder was measured at three electrode positions. The resistance was used to obtain the NaCl concentration of fluid at the electrode position by direct interpolation from the calibration curve. The measurements were taken at various time intervals after the 0.1 N solution was introduced. Results of these measurements are tabulated in Table V-1 through Table V-11 in the appendix. The time required for the NaCl concentration to reach 50% of 0.1 Normal NaCl concentration was taken as the average time, $\overline{T}_{Z_0}$.

(2) Dispersion with respect to distance.

As derived in Chapter 3, the break through curve with respect to distance at a given time can be calculated from the time distribution at a given distance. These break through curves are shown on Figure V-1 through Figure V-11 in Appendix V. The electrode positions were taken as the average distance of the break through curves. The standard deviations with respect to distance are also shown in the figures.

(3) Permeability coefficients.

Permeabilities were measured in the laboratory in two perpendicular directions using the procedure described in section 3. The results of the permeability determinations are listed in Table IV-1 through Table IV-5, and also shown in Figure IV-1 through Figure IV-4 in Appendix IV. A summary of these results is shown in Table 4-2. Different permeabilities are obtained for all the porous media used except the Ottawa sand.

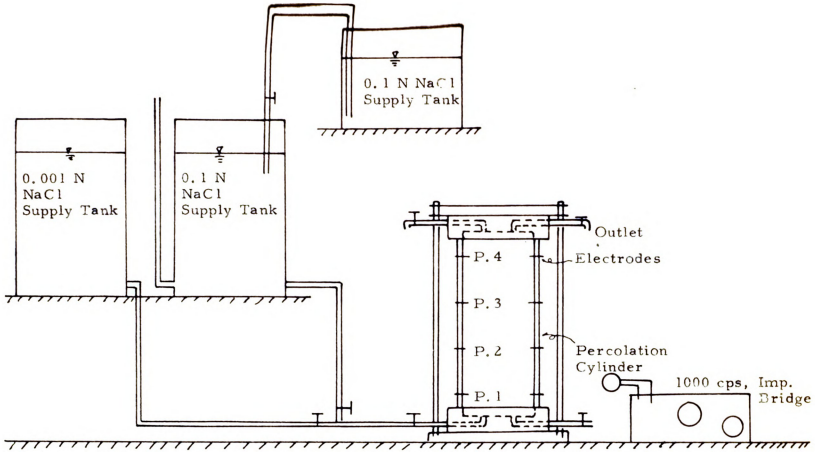

Figure 4-1. Schematic sketch of the experimental set-up for the measurements of dispersion of fluids through porous media.

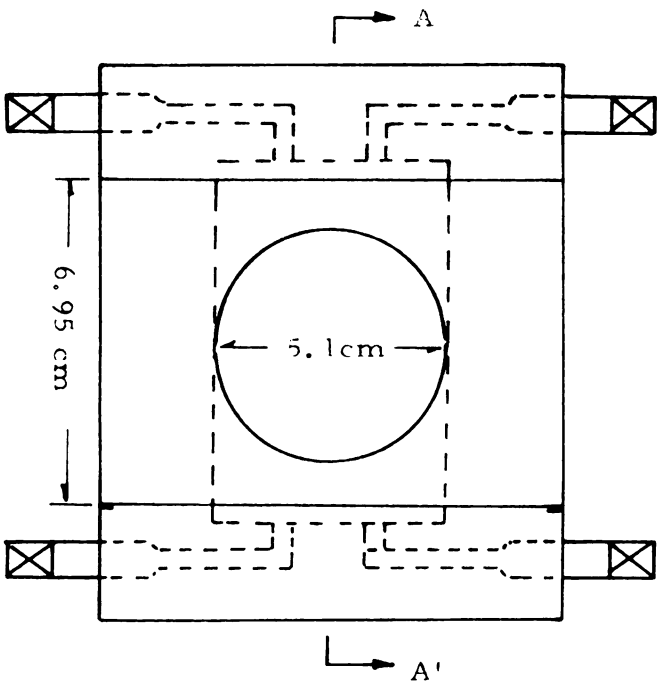

Side View

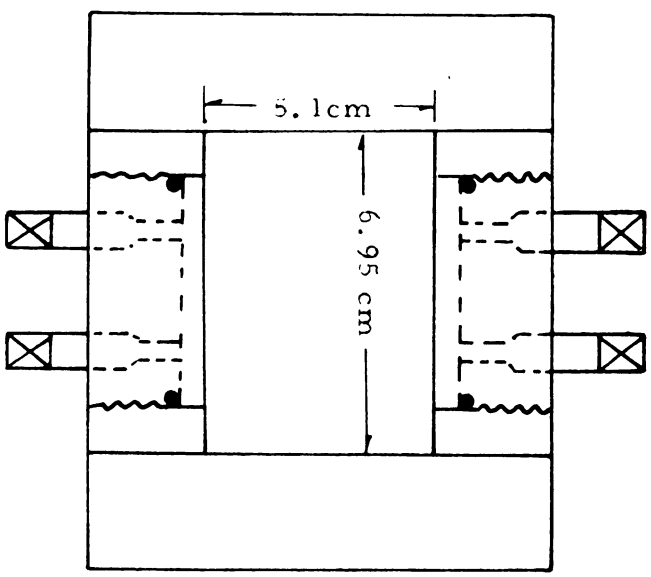

Section A-A'

Figure 4-2. Sections of permeability apparatus.

Table 4-1. Samples for dispersion measurements

Sample No.	Material	Unit Wt. gm/cm^3	Particle Dimensions	Total Wt. gms.	Particle Numbers	Porosity %
S_1	Ottawa sand	2.65	0.7 mm. dia.	771.0	5.37×10^5	34.4
S_2	"	2.65	"	763.0	5.31×10^5	35.0
P_{11}	Plastic plate	1.11	.3x. 1x. 03cm	305.5	3.05×10^5	37.9
P_{12}	"	"	"	279.0	2.79×10^5	43.3
P_{13}	"	"	"	244.0	2.44×10^5	50.4
P_{21}	"	"	.3x. 3x. 03cm	273.0	9.11×10^4	44.5
P_{22}	"	"	"	235.5	7.84×10^4	52.2
P_{31}	"	"	.3x. 1x. 06cm	300.5	1.50×10^5	38.9
P_{32}	"	"	"	272.6	1.36×10^5	44.6
P_{41}	"	"	.3x. 3x. 06cm	274.4	4.58×10^4	44.3
P_{42}	"	"	"	372.3	5.46×10^4	33.5
N_1	Nylon filament	1.041	.05[illegible]x. 5cm	234.5	5.97×10^4	49.2
N_2	"	"	"	231.5	5.90×10^4	49.8

Table 4-2. Samples for permeability measurements.

Sample test no.	Material	Particle Dimensions	Porosity %	Perm. cm/min.	Direction of flow
S	Ottawa sand	.7mm dia.	35.00	8.85	Longit. & Transv.
PP_{11}	plastics	.3×.1×.03cm	34.50	6.45	Transv.
PP_{12}	"	"	36.10	6.95	"
PP_{13}	"	"	36.80	9.60	"
PP'_{11}	"	"	34.50	8.75	Longit.
PP'_{12}	"	"	41.70	9.34	"
PP_{21}	"	.3×.3×.03cm	39.00	8.75	Transv.
PP_{22}	"	"	46.40	10.52	"
PP'_{21}	"	"	39.20	10.70	Longit.
PP'_{22}	"	"	43.10	11.22	"
PP'_{23}	"	"	43.50	11.20	"
PP_{31}	"	.3×.1×.06cm	34.00	8.04	Transv.
PP_{32}	"	"	38.60	11.00	"
PP'_{31}	"	"	29.60	8.65	Longit.
PP'_{32}	"	"	34.20	10.10	"
PP_{41}	"	.3×.3×.06cm	31.00	9.05	Transv.
PP_{42}	"	"	34.40	10.24	"
PP_{43}	"	"	35.60	10.42	"
PP'_{41}	"	"	29.60	10.42	Longit.
PP'_{42}	"	"	35.20	11.17	"
N	Nylon filaments	.05ϕ×.5cm	49.20	12.75	Transv.
N'	"	"	49.20	11.00	Longit.

CHAPTER 5

ANALYSIS OF EXPERIMENTAL RESULTS

1. The Break Through Curves.

The procedures for measuring the dispersion of fluid flow in a porous medium as described in Chapter 4 give a relationship between salt concentration of the mixing fluid front at the electrode positions and time. Figure 5-1a shows a typical curve for this concentration versus time. If there is no dispersion phenomenon taking place and the molecular diffusion is neglected, then there would be simply an abrupt change in concentration from 0.001 to 0.1 Normal at the mixing front. This is the horizontal line shown on Figure 5-1a.

Now, if $\bar{T}_{Z_o}$ is the average time, then the distance a fluid particle would have travelled at time T_{Z_o} can be calculated from Eq. (52)

$$Z_{\bar{T}} = \frac{Z_o \bar{T}_{Z_o}}{T_{Z_o}}$$

in which T_{Z_o} is the time in a curve represented by Figure 5-1a. The distance thus calculated gives the break through curves with respect to distance at a given time $\bar{T}_{Z_o}$. Figure 5-1b shows such a curve calculated from Figure 5-1a. The calculated break through curves with respect to distance are presented on Figure V-1 through Figure V-11 in Appendix V. One significant property noted in these break through curves is that the curves are asymmetric.

2. Dispersion as a Function of Distance.

Eq. (69) and Eq. (71) indicate that in a given porous medium, the standard deviation of a break through curve is a linear function

of the square root of the average distance. Table 5-1 is a summary of the standard deviations obtained in the dispersion measurements. The values of the standard deviations (Table 5-1) are obtained from Figure V-1 through Figure V-11 by taking averages of the vertical distances between 0.015 and 0.085 Normal NaCl concentrations. This assumes that the measured distribution may be approximated by a normal distribution.

Figure 5-3a through Figure 5-3f show the relationship between the average standard deviation and the average distance in square root scale. With no exception, the relationship is linear. Eq. (69) shows an existence of a finite value of the standard deviation at Z_o equals to zero. However, since the value of L is very small, it is practically insignificant.

3. The Characteristics of Pore Geometry.

Eq. (71) also shows that the standard deviation of a break through curve is a function of the orientation factor n. This orientation function is represented by Eq. (73) as C'_n and plotted against n in Figure 3-6. It can be seen from Eq. (71) and Figure 3-6 that the orientation factor n is probably the least influential factor among the variables in the right hand side of Eq. (71).

As derived in Chapter 3 the orientation factor n can be obtained from the permeability data. Table 5-2 shows the calculations and results of the orientation factor obtained using Figure 3-8 and the permeability data. The permeabilities of the porous materials were measured in two perpendicular directions as described in Chapter 4. The permeability data thus obtained permit the evaluation of the

orientation factor of the porous medium. The results are given in Table 5-2. Figure 5-4 shows the relationship between orientation and porosity. For the samples tested, the orientation factor ranges from 1.0 to 2.0 approximately.

In Figure 5-3 the slope of the line represent the ratio $\sigma_{Z=}/\sqrt{Z}_o$ which is a function of both n and L as was derived in Eq. (71). Since the values of n for the known porous materials and porosities may be obtained from Figure 5-4, the value of L can be calculated with Eq. (71). Table 5-3 shows the calculated values of L. It is seen that in general, L increases with decrease in porosity and therefore with increase in orientation factor n. For randomly oriented case (n = 1), the following comparison between the value of L and the dimensions of the grain particles constituting the porous media can be made. For Ottawa sand, the calculated value of L is 0.13 cm which is approximately twice the average diameter of the particles. For plates, the calculated L ranges from 0.12 cm to 0.37 cm which is approximately 0.5 to 1.2 times the longest side of the plates. For cylindrical particles, the value of L calculated is approximately two-thirds of the length of the particles. Since for a loose packing of uniform spherical particles, the length of the pores should not be expected to be larger than the particle diameter, the calculated L for Ottawa sand indicates that the agreement between theory and experiment is rather poor. This suggests the error introduced in the assumptions of the theoretical derivations. Although the calculated values of L for the porous materials for plates and cylinders fall in more reasonable range the same magnitude of errors may be involved in these cases also.

However, the above method of calculating the value L is based on the relationship represented by Eq. (50). If Eq. (51) instead of Eq. (50) was used to derive the standard deviation, then the standard deviation of the dispersion will be represented by Eq. (24) and the average length of pore canals L calculated will be approximately four times that calculated from Eq. (71). Therefore, the standard deviation as given by Eq. (71) seems to be in better agreement with the experimental results.

If Eq. (50) is the true representation of the distribution and if $Z_{\overline{N}}$ is normally distributed, then $Z_{\overline{T}}^{1/2}$ should also be normally distributed. Similarly $Z_{\overline{T}}$ should be normally distributed if Eq. (51) is to be the true representation of the distribution. The measured distributions for sample S_{11} are plotted on probability papers as Figure 5-2a and 5-2b. The distribution curves on these figures do not reveal any significant difference between the two assumptions made with regard to the distribution.

Different porosities were used in the dispersion measurements in order to produce a range in orientation. It is found that porosity affects both orientation and the length of canal. From Figure 5-4 it is seen that the range of porosity used produces only a range of orientation factor n from 1.0 to 2.0. This seems to indicate that the actual pore canal orientation does not follow closely the orientation of the grain particles in the porous medium. For the plate shaped particles a very dense packing should produce a particle orientation very close to a horizontal. The calculated n values from measured data (Table 5-3) do not indicate much increased n values for a dense packing. This may be due to the possibility that a dense packing of

plates may produce clusters of particles in a porous medium and fluid flow may occur largely through the continuous pores between these clusters (see Figure 5-3). Therefore, the orientation factor n is no longer controlled by the orientation of the plates. The continuous pores between the clusters will apparently reduce the value of n due to the existence of nearly vertical pores. This explanation is also supported by the observation that there is an almost consistent increase in the calculated value of L for decrease in porosity or increase in density for plate samples (Table 5-3). Since the sizes of the pores between the clusters are influenced by the size of the clusters, it may be expected that the value of L for a dense packing where clusters are likely to exist would be greater than that in a loose packing where the fluid flow takes place mainly through the pores between plates and therefore the value of L is controlled by the size of the individual plates.

4. Dispersion Coefficient.

Since the break through curve as shown in Figure 5-1b represents the distribution of the fluid particles that have travelled a longitudinal distance $Z_{\bar{T}}$ after a given time $\bar{T}$, the magnitude of the standard deviation of the break through curve is a measure of the degree of dispersion and may be designated as the 'dispersion coefficient'. It is clear from the preceding analysis that this dispersion coefficient is a function of the average distance of journey, the length of the unit canal, and the orientation factor n.

A numerical comparison is made in Appendix III for the measured dispersion coefficient in this investigation with those

which could be predicted from the present theory and the theories of De Josselin de Jong and Saffman. De Josselin de Jong's theory was derived based on the assumption that the porous medium consists of uniform spherical particles and Saffman's theory assumed a randomly oriented straight pores in a porous medium. Therefore, the equations from both theories could be applied to the experimental data of Ottawa sand samples in the present investigation where the orientation factor n is equal to unity and also could be roughly compared to the cases of loose packings of plate shaped particles.

In order to apply these theories, the length of the unit canal of pores must be evaluated. Assuming the magnitude of the molecular diffusion to be negligible, this can be done by substituting different length of L into the equations representing different theories, (Eqs. (6). (7), (69)), and compare the results with the measured dispersion coefficients. For a porous medium consisting of spherical particles, the length of the pores is not likely to be greater than the diameter of the particles even for a loose packing. Therefore, it is reasonable to assume that L lies between ½ to that of the diameter of the particles. For the Ottawa sand samples, a best agreement is obtained when L is taken as the diameter of the particles. (The value of L should be reduced if molecular diffusion is taken into account). Calculations of the dispersion coefficients from different theories are shown in Table III-2.

From this result, it can be seen that when L is taken as 0.07 cm where the De Josselin de Jong's theory agrees best with the experimental results, then the Saffman's equations would give approximately 10% to 30% higher values and the present theory would give

approximately 30% lower values compared to the De Josselin de Jong's results. The difference between De Josselin de Jong's and the present theory can readily be seen by comparison of Eqs. (7) and (69). The De Josselin de Jong's theory would approximately give a higher dispersion coefficient by a factor equal to

$$(\lambda + 3/4 - \log r)$$

which is approximately 1.4. The fact that the present theory is consistently underestimating the measured dispersion coefficient may be considered as the result of the errors involved in the assumptions made in the course of the theoretical derivation (see Appendix II).

A difference of similar magnitude is seen between these theories when applied to loose packings of plate shaped particles (Table III-2). A pore canal length of 0.1 cm is assumed for P_1 and P_3 samples and 0.3 cm for P_2 and P_4 samples. The calculated results when compared to the measured ones suggest that for plate shaped particles the lengths of the pores are likely to be smaller than the longest side of the plates constituting the porous medium.

From the preceding analyses, it can be stated that the present theory consistently underestimates the dispersion coefficient. The amount of error could be approximately 30% or even more for the case of $n = 1$. Therefore, it is probable that for the cases of n greater than 1 or for anisotropic porous media, similar magnitude of errors are existing. It is not possible to accurately predict or calculate the length of the pores for an anisotropic porous medium packed with plate shaped particles. However, by assuming that the error involved in the present theory is approximately 30%, it can be estimated that the length of the pores should be smaller than the longest

side of the plates and probably comparable to one-half the length of the longest side.

Table 5-1. The Average Standard Deviations

Sample No.	Porosity %	Electrode Position	Average σ_{Z_o} in cm.
S_1 & S_2	34.25	1	0.270
		2	0.452
		3	0.705
P_{11}	37.92	1	0.310
		2	0.747
		3	1.080
P_{12}	43.31	1	0.400
		2	0.809
		3	1.190
P_{13}	50.42	1	0.307
		2	0.625
		3	0.818
P_{21}	44.52	1	0.442
		2	1.120
		3	1.510
P_{22}	52.18	1	0.350
		2	0.843
		3	1.160
P_{31}	38.92	1	0.418
		2	0.820
		3	1.060
P_{32}	44.61	1	0.252
		2	0.540
		3	0.682
P_{41}	44.25	1	0.425
		2	0.763
		3	1. 068
P_{42}	33.46	1	0.468
		2	0.925
		3	1.338
N_1 & N_2	49.19	1	0.388
		2	0.736
		3	0.992

Table 5-2. Orientations of the porous media as calculated from the permeability data.

Porous Material	Porosity %	K_z cm/min.	K_x cm/min.	K_z/K_x	Value of n
S	35.00	8.85	8.85	1.000	1.00
P_1	32.00	5.83	8.56	0.681	2.00
	36.00	6.85	8.89	0.771	1.70
	40.00	7.88	9.20	0.857	1.45
	44.00	8.90	9.51	0.936	1.25
	47.60	9.80	9.80	1.000	1.00
P_2	36.00	8.02	10.41	0.770	1.70
	40.00	9.00	10.80	0.833	1.50
	44.00	9.98	11.30	0.883	1.35
	48.00	10.95	11.77	0.930	1.25
P_3	34.00	8.03	10.00	0.803	1.55
	36.00	9.31	10.65	0.874	1.30
	38.00	10.61	11.29	0.940	1.20
	40.00	11.87	11.91	0.997	1.05
P_4	30.00	8.74	10.48	0.834	1.50
	32.00	9.40	10.74	0.875	1.40
	34.00	10.06	11.01	0.914	1.27
	36.00	10.74	11.28	0.952	1.20
	38.00	11.42	11.55	0.989	1.10
N	49.20	11.00	12.75		

Table 5-3. Length of pore canal obtained from experimental data.

Sample No.	Porosity %	$\sigma_{Z_T}/\sqrt{Z_o}$	n	C_n' *	L, ** cm.
S	34.25	0.21	1.00	0.083	0.133
P_{11}	37.92	0.35	1.60	0.087	0.352
P_{12}	43.31	0.39	1.26	0.085	0.447
P_{13}	50.42	0.26	1.00	0.83	0.204
P_{21}	44.52	0.52	1.31	0.0855	0.791
P_{22}	52.18	0.40	1.00	0.083	0.482
P_{31}	38.92	0.35	1.11	0.845	0.362
P_{32}	44.61	0.20	1.00	0.083	0.120
P_{41}	44.25	0.35	1.00	0.083	0.369
P_{42}	33.46	0.445	1.37	0.086	0.576
N	49.19	0.33	1.00	0.083	0.328

* The values of C_n' are obtained from Figure 3-6.

** The values of L are calculated from Eq. (71) assuming that the values of n obtained from Figure 5-3 are applicable to Eq. (71), (72) and (73).

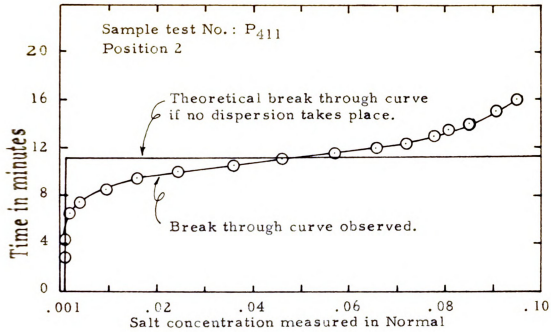

Figure 5-1a. Typical break through curve with respect to time.

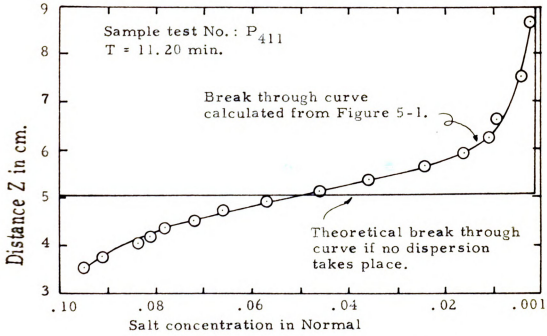

Figure 5-1b. Typical break through curve with respect to distance.

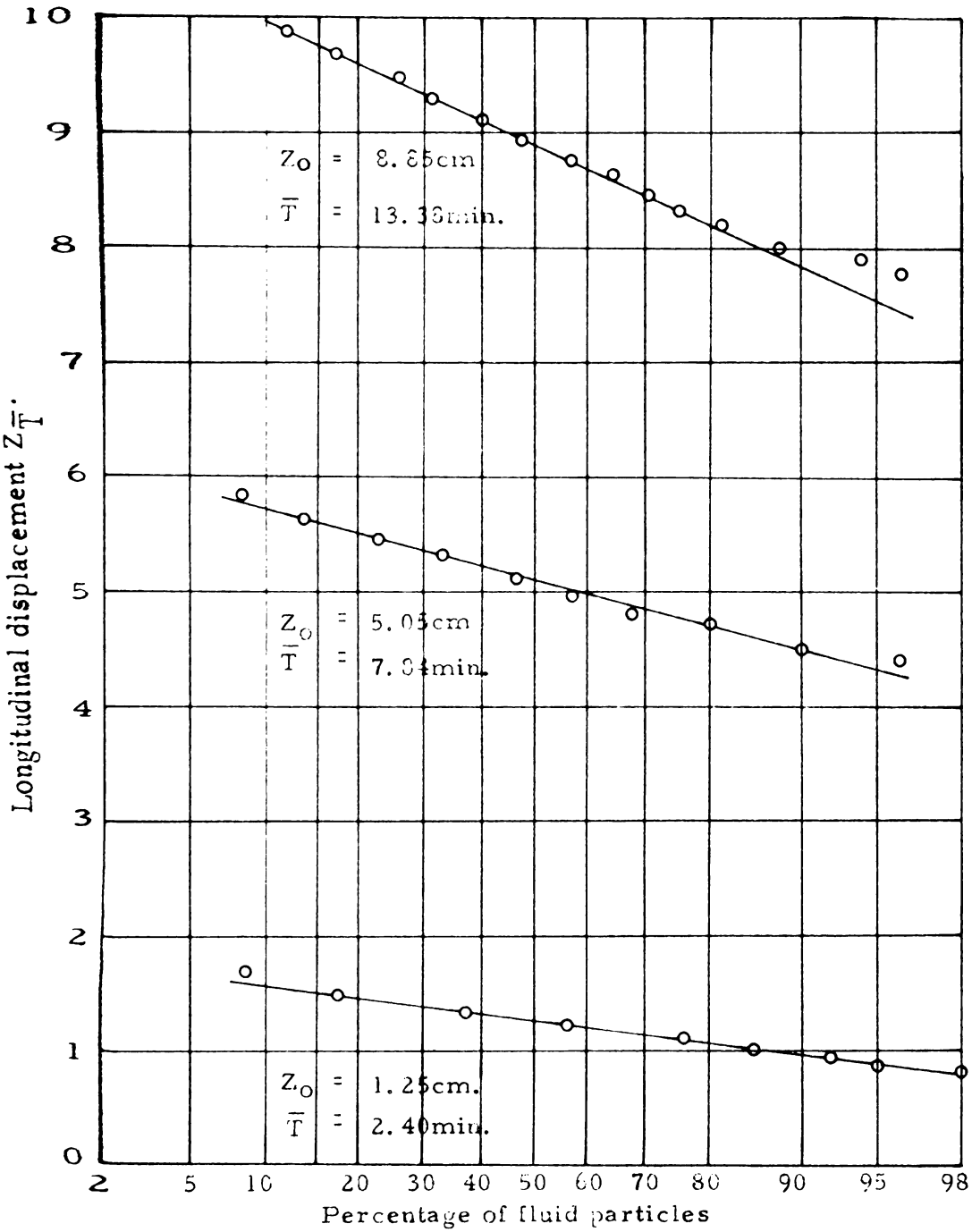

Figure 5-2a. The relationship of $Z_{\bar{T}}$ and the percentage of fluid particles that has reached the longitudinal distance of $Z_{\bar{T}}$. Sample No. S_{11}.

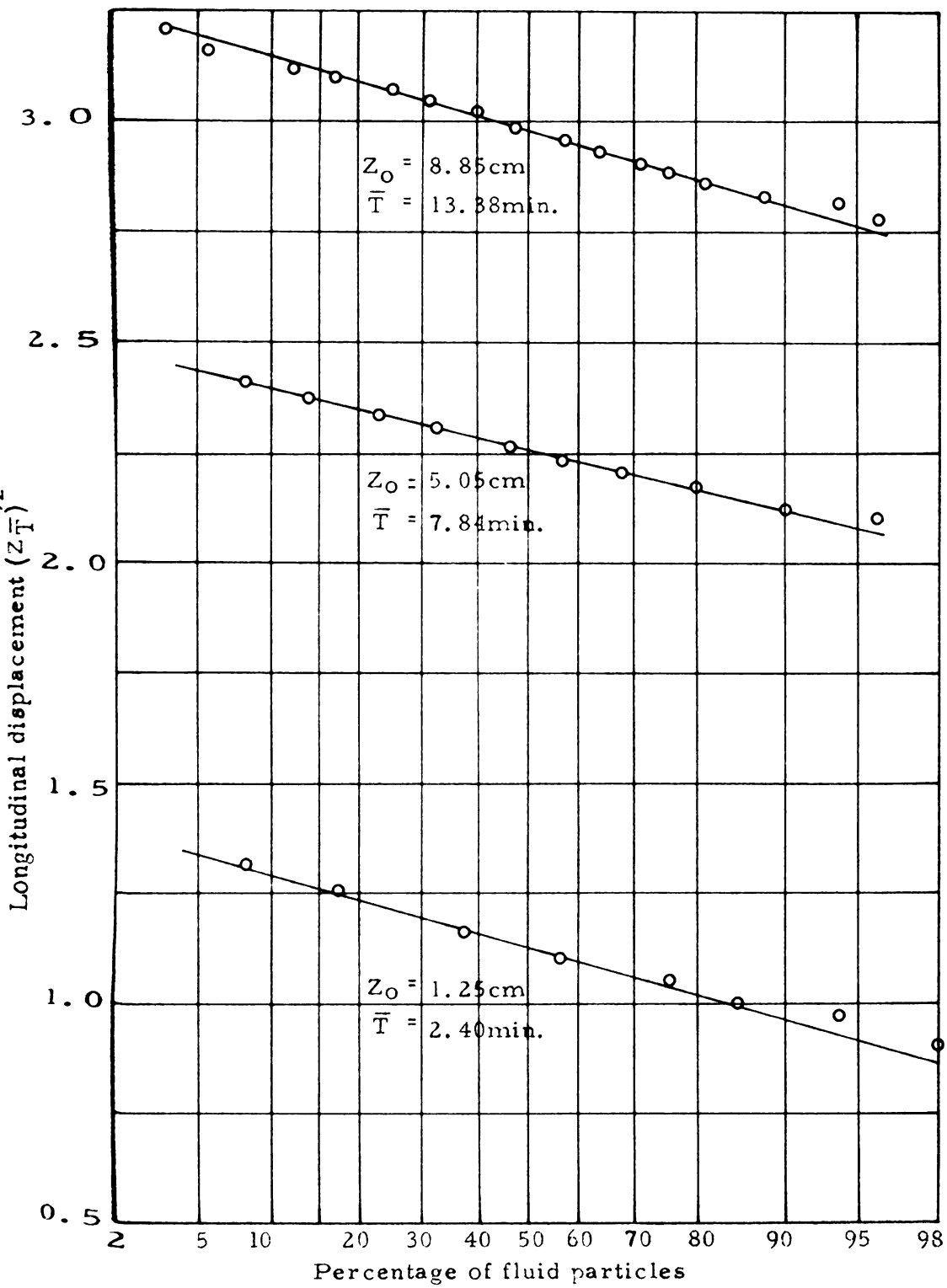

Figure 5-2b. The relationship of $(Z_{\bar{T}})^{1/2}$ and the percentage of particles that has reached the longitudinal distance of $Z_{\bar{T}}$. Sample No. S_{11}.

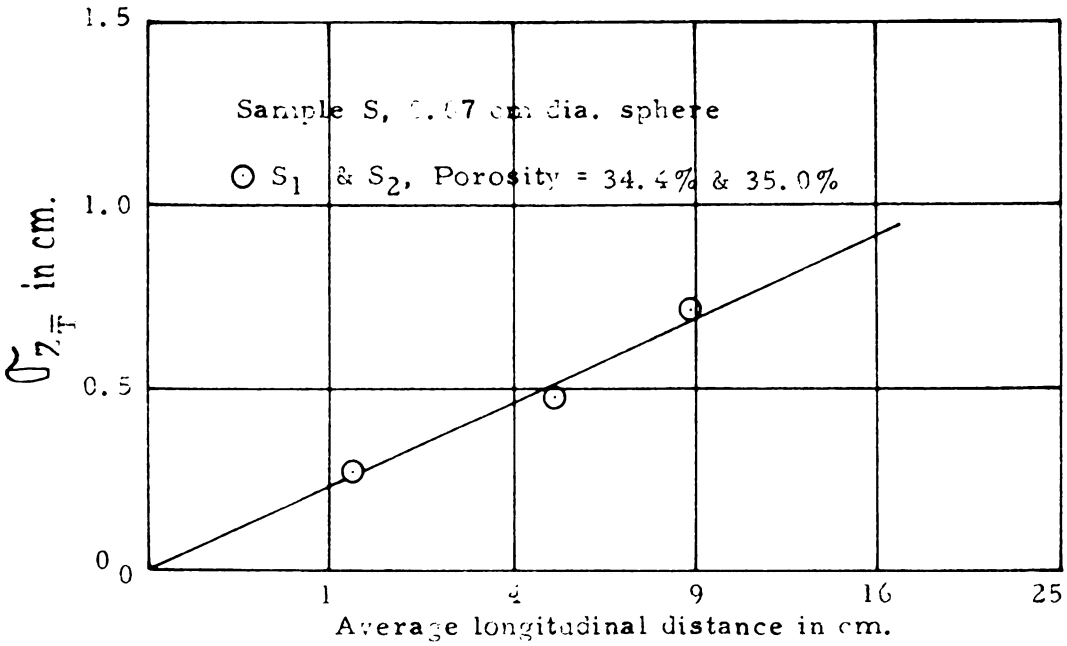

Figure 5-3a. Relation between standard deviation and the longitudinal distance, S.

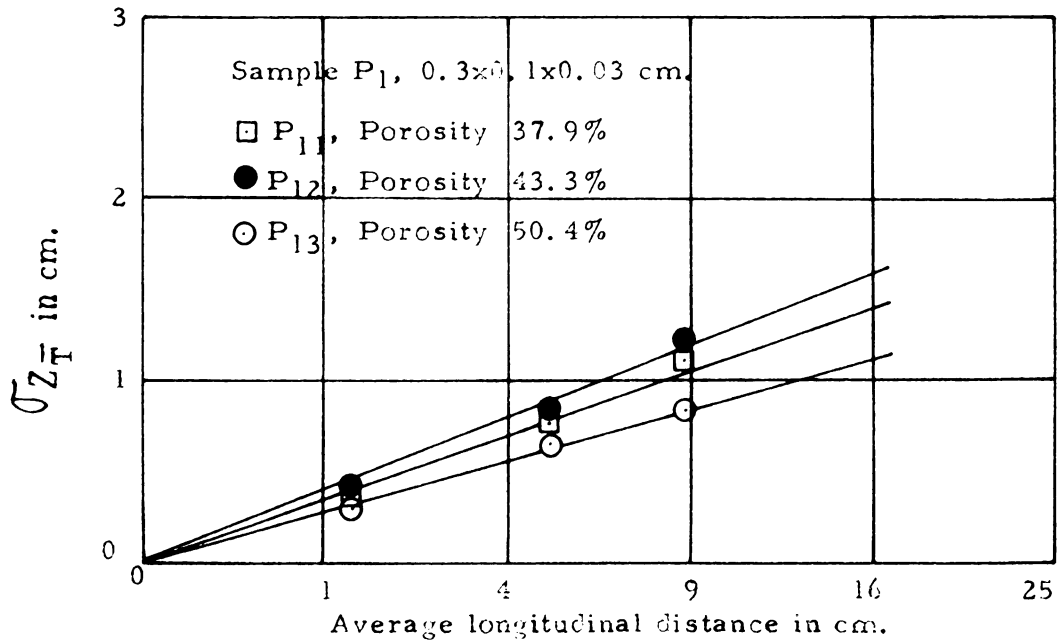

Figure 5-3b. Relation between standard deviation and the longitudinal distance, P_1.

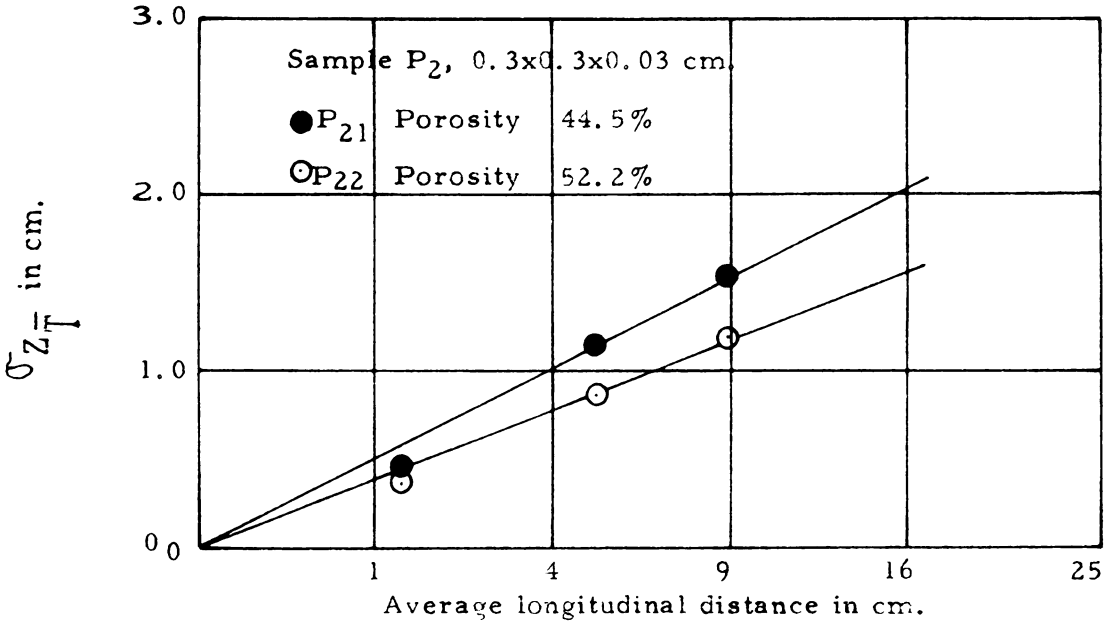

Figure 5-3c. Relation between standard deviation and the longitudinal distance, P_2.

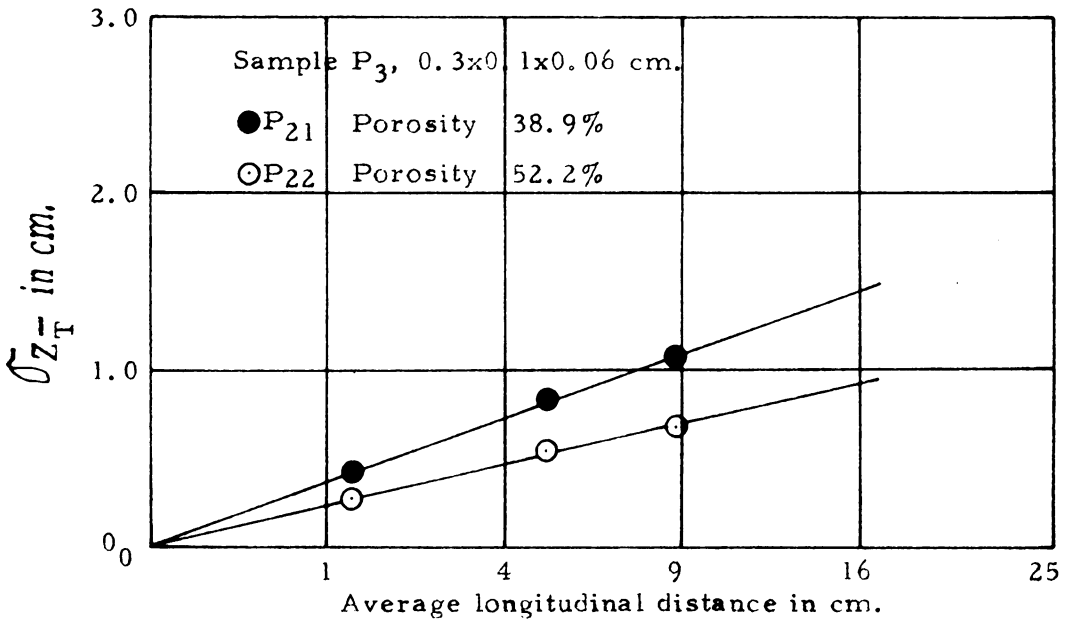

Figure 5-3d. Relation between standard deviation and longitudinal distance, P_3.

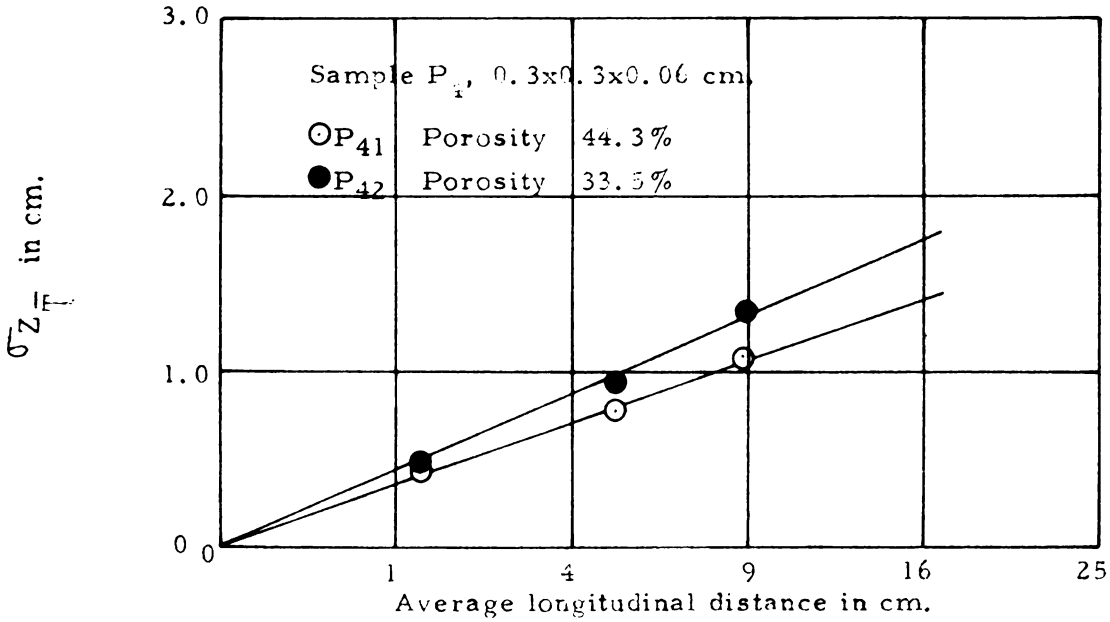

Figure 5-3e. Relation between standard deviation and longitudinal distance, P_4.

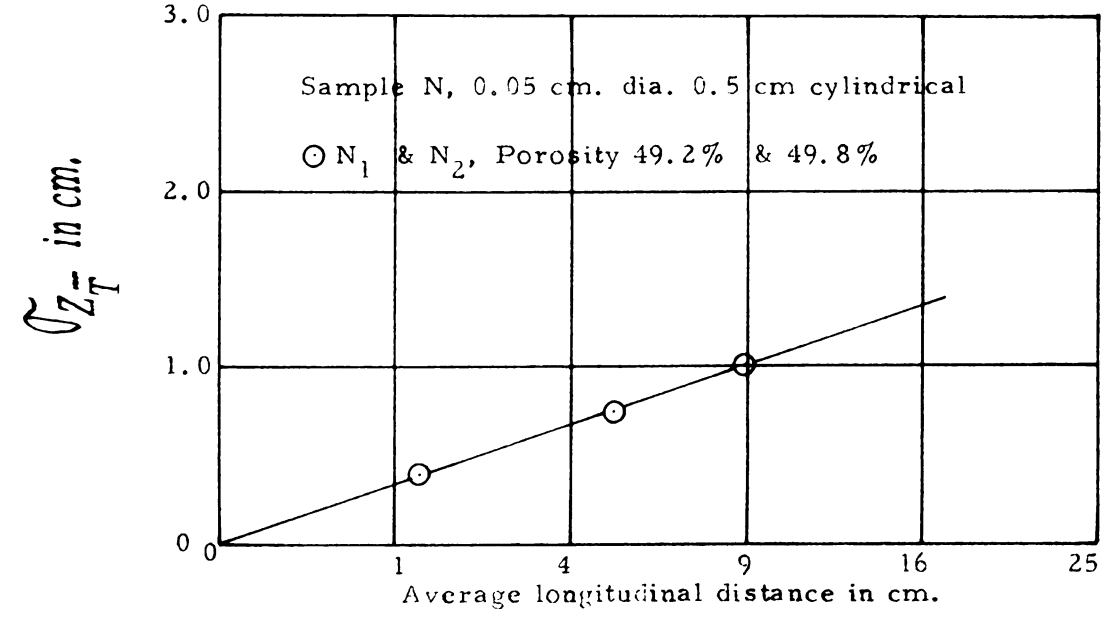

Figure 5-3f. Relation between standard deviation and longitudinal distance, N.

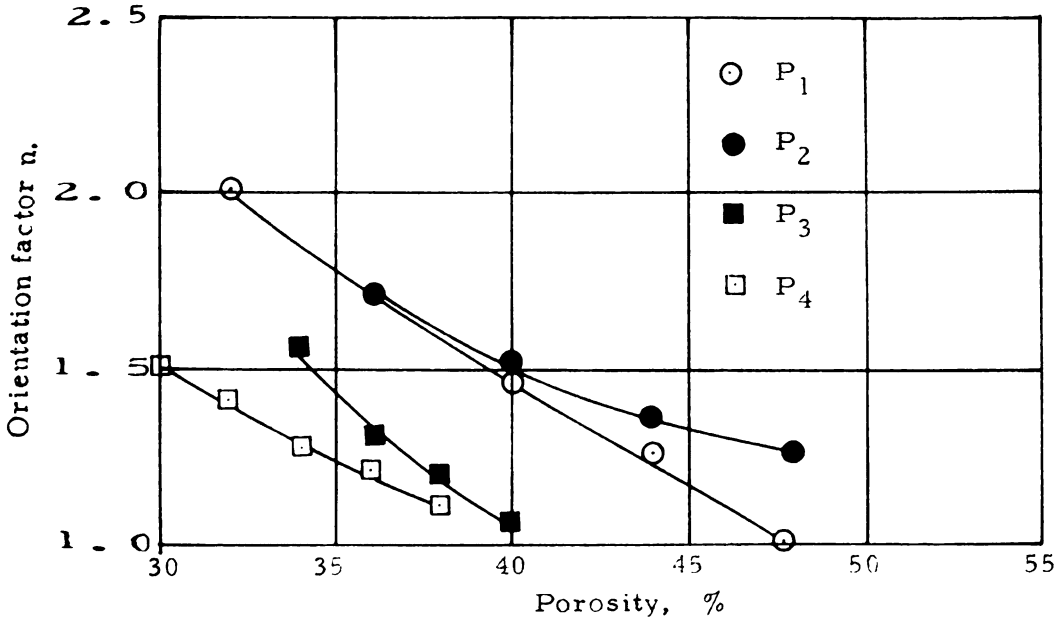

Figure 5-4. Relation between porosity and the orientation factor n obtained from Figure 3-8.

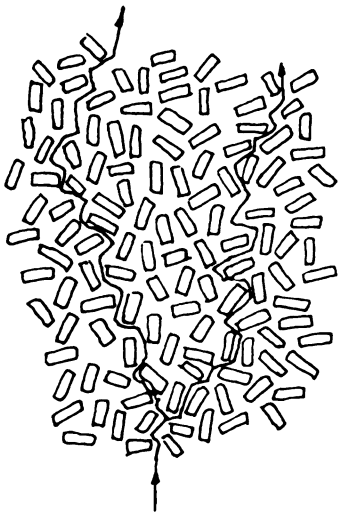

(a) Assumed pattern of flow paths in either loose or dense packing of plates.

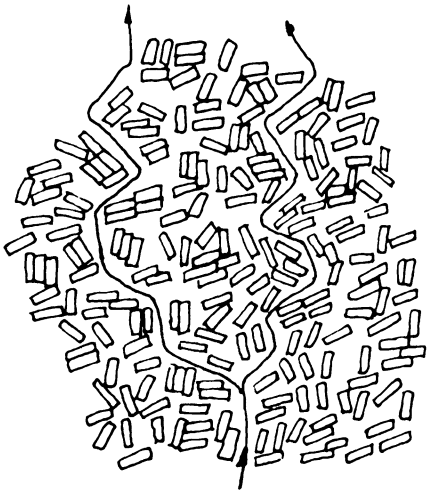

(b) Probable pattern of flow paths in a dense packing through pores between clusters of plates.

Figure 5-5. Schematic sketch of the possible patterns of flow paths in a porous medium consisting of plate shaped particles.

CHAPTER 6

DISCUSSIONS AND CONCLUSIONS

Statistics were applied to study the mechanism of fluid flow in a porous medium. If the medium is such that its pores have different orientations with respect to certain direction and the hydraulic gradient is the sole cause for the fluid particles to move in the pores, then the tortuous paths of the pores will immediately result in a dispersion of fluid flow in the porous medium. It was expected that this treatment would give a functional relationship between the characteristics of the fluid flow and the porous medium. Two sets of equations were derived representing the relationship between the standard deviation of a break through curve, distance, pore dimension and the orientation factor of the pore canals.

In order to simplify the theoretical analysis, a canal network model was used to represent the pore system in a porous medium. A series of assumptions with regard to the orientation of an individual pore and the average orientation of a path were made. These assumptions introduce an inevitable error into the result of the theoretical derivations whose magnitude depends on the particular path.

Since anisotropy is a basic property of a porous medium, the theoretical consideration was based on an assumption that the directions of pores will have a distribution of preferred orientation and that this distribution can be expressed mathematically. Therefore, the degree of dispersion as represented by the standard deviation of the break through curve contains a factor indicative of the orientation of the porous medium. It was also shown that this orientation factor could be related to the ratio of permeability coefficients in two perpen-

dicular directions in the porous medium.

The following conclusions can be drawn from the theoretical considerations of this study:

(1) A mathematical relationship representing the break through curve of a miscible fluid front in a porous medium may be derived from a theoretical consideration of canal network model and an assumption of pore direction distribution functions.

(2) The degree of dispersion as represented by the standard deviation of a break through curve is a function of the longitudinal distance, the length of the pores and the orientation of the porous medium.

(3) According to the functional relationships derived, the standard deviation is directly proportional to the square root of the longitudinal distance for a given porous medium.

(4) The standard deviation for different porous media, other factors being equal, increases with the square root of the length of the unit canals.

(5) The effect of the orientation of the porous medium when other factors being equal, is such that the standard deviation increases with an increase in the orientation factor n, for n smaller than 4, and decreases with increasing n, for n greater than 4.

(6) The magnitude of error introduced in the assumptions of the theoretical considerations depends on the particular path chosen. When the longitudinal distance of travel by a fluid particle is considered, this error may amount to 10% to 20%. An accurate estimate of the error in an actual case is not possible.

The results of the experimental analysis in the laboratory showed that the dispersion phenomenon in a porous medium is a macroscopically measurable quantity. However, the experimental results agree only qualitatively with the basic equations of dispersion derived from a theoretical consideration in this study. The dispersion as represented by the standard deviation of the break through curve was found to be a property of the porous medium. The medium properties that affect the dispersion were found to be the length of the pore canal, the distance of travel by the fluid particles, and the orientation of the pore canals.

Comparisons of the experimental results with the theoretical equations showed that the present theory is consistently underestimating the degree of dispersion by an amount up to approximately 30 %. This may be an indication of the magnitude of error involved in the assumptions made in the theoretical analysis. Since the length of the pores in a porous medium consisting of spherical particles can only be roughly estimated, and an estimate of the length of pores in an anisotropic porous medium consisting of plate shaped particles would be much less accurate, the above mentioned difference between the theoretical and experimental results would prevent a reliable calculation of the medium properties from the experimental data. However, a qualitative deduction of the effects of the factors affecting the dispersion phenomenon in a porous medium is still possible.

The experimental data on the permeability measurements on two perpendicular directions in anisotropic porous media showed that the orientation factors thus obtained seemed to be much less than expected. This suggests that for a dense packing the fluid flow may largely occur in pores between clusters of particles. Therefore,

the length and orientation of the pores in such a porous medium are likely to be greatly influenced by the size of the clusters and also the distribution of the clusters in the porous medium. The evaluation of medium properties in such a case would be very difficult and the deviations from theory would tend to be greater.

The following conclusions may be drawn from the experimental analysis of this study:

(1) The standard deviation of a break through curve is found to increase with square root of the longitudinal distance as predicted by the theoretical analysis.

(2) Generally speaking, the length of pores as evaluated from the experimental data increases with the increase in the size of the grain particles. An actual length of the pores is a function of the packing characteristics and the factors affecting the length are not clearly known. The formation of clusters of particles may be one probable explanation.

(3) The standard deviation increases with increase in the length of the pores as indicated by the theoretical analysis.

(4) The orientation factor of the porous medium is a function of the packing characteristics. It increases with decrease in porosity. The experimental results indicate that for a dense packing, the orientation of pores does not follow closely with the direction of the grain particles.

(5) For the range of the orientation factors used in this investigation, the standard deviation increases with increase in the orientation factor.

(6) Anisotropy is the result of preferred orientation of grain particles or pores. Permeability coefficients in two different

directions in a porous medium may be used to study this anisotropic characteristics.

Based on the above discussions and conclusions, it is possible to assume a statistical model to study the mechanism of dispersion phenomenon in a porous medium. From this result, it should also be possible to investigate the characteristics of the porous medium by observing the dispersion phenomenon of the fluid flow in the medium. Although an assumption of the identical unit canals joined together in a porous medium is an oversimplification, and the assumptions with regard to the orientations of the paths introduce an inevitable error, this type of study provides an understanding of the mechanism of the fluid flow taking place in the porous medium.

The packing characteristics of the porous medium which were not considered in the present theoretical analysis such as porosity, packing uniformity, are found to affect the dispersion. An accurate estimate of the size and shape of the pores was not possible in the present investigation. These are affected also by the packing characteristics. This effect is very complicated and further investigation is recommended along this line.

LITERATURE CITED

(1) Bastow, S. H. and Bowden, F. P.; Physical properties of surfaces. Proceedings, Royal Society of London. A151, 1935, p220.

(2) Blake, F. C.; The resistance of packing to flow. Transactions, American Institute of Chemical Engineers, Vol. 14, 1922, p415.

(3) Carman, P. C.; Permeability of saturated sands, soils and clays. Journal of Agricultural Science. Vol. 29, 1939, p262.

(4) Childs, E. C. and N. Collis-George; The permeability of porous materials. Proceedings, Royal Society of London. Vol. 201A, 1950, p392.

(5) Day, P. R.; Dispersion of a moving salt-water boundary advancing through saturated sand. Transactions, American Geophysical Union, Vol. 37, 1956, p595.

(6) De Josselin de Jong, G.; Longitudinal and transverse diffusion in granular deposits. Transactions, American Geophysical Union, Vol. 39, No. 1, 1958, p67.

(7) Elton, G. A. H.; Electroviscosity, Proceedings, Royal Society of London. Vol. 194A, 1948, p259.

(8) Kendall, M. G.; The Advanced Theory of Statistics, Vol. 1, J. B. Lippincott Company, 1943.

(9) Kozeny, J.; Berin Wien Akad. 1927, 136a, p271.

(10) Lambe, T. W.; The engineering behavior of compacted clays. ASCE Proceedings, Journal of Soil Mechanics. Vol. 84, Paper 1655, 1958.

(11) Marshall, T. J.; A relation between permeability and size distribution of pores. Journal of Soil Science. Vol. 9, p1.

(12) Michaels, A. S. and C. S. Lin; Effect of counterelectro-osmosis and sodium ion exchange on permeability of Kaolinite. Ind. and Eng. Chem. Transactions, Vol. 47, 1955, p1249.

(13) Mitchell, J. K.; The importance of structure to the engineering behavior of clay. MIT Thesis. 1956.

(14) Olsen, H. W.; Hydraulic flow through saturated clays. MIT Thesis. 1961.

(15) Quirk, J. P.; Permeability of porous media. Nature, Vol. 183, 1959, p387.

(16) Saffman, P. G.; A theory of dispersion in a porous medium. Journal of Fluid Mechanics. Vol. 6, 1959, p321.

(17) Scheidegger, A. E.; Statistical hydrodynamics in porous media. Journal of Applied Physics. Vol. 25, 1954, p994.

(18) Scheidegger, A. E.; Statistical approach to miscible displacement in porous media. The Canadian Mining and Metallurgical Bulletin. 1959, p26.

(19) Terzaghi, C.; Determination of permeability of clay. Engineering News Record, Vol. 95, No. 21, 1925, p832.

(20) Zunker, F.; Z. PflErnahr. Dung, A. 25, p1.

APPENDIX I

DERIVATIONS OF THE RELATIONSHIPS

1. Derivation of Eq. (13).

Eq. (12) is the probability distribution function of canal direction at any point in a porous medium. Let P be the toal probability of the choice of directions, then

$$P = \int_0^{2\pi} d\phi \int_0^{\frac{1}{2}\pi} \frac{a}{2\pi} \sin^n\theta d\theta = 1$$

or

$$\int_0^{\frac{1}{2}\pi} a \sin^n\theta \, d\theta = 1$$

The normalization constant a is evaluated as follows:

$$\int_0^{\frac{1}{2}\pi} \sin^n\theta d\theta = \frac{(n-1)(n-3) \ldots 3.1}{n(n-2) \ldots 4.2}\left(\frac{\pi}{2}\right)$$

for n even and

$$\int_0^{\frac{1}{2}\pi} \sin^n\theta d\theta = \frac{(n-1)(n-3) \ldots 4.2}{n(n-2) \ldots 3.1}$$

for n odd. Therefore, the normalization constant a may be expressed as

$$a = \frac{n(n-2) \ldots}{(n-1)(n-3) \ldots}\left(\frac{2}{\pi}\right)^b \quad \ldots\ldots\ldots \quad (13)$$

where b = 1 for n even and b = 0 for n odd.

2. Derivation of Eq. (22).

Since $z = L \cos\theta$, the variance of Z can be expressed as

$$\text{Var}(L\cos\theta) = \int_g L^2\cos^2\theta \; g_{\theta\phi} - E(z)^2.$$

where $g_{\theta\phi}$ is represented by Eq. (17) and E(z) is represented by Eq. (21) in Chapter 3. Now, substituting Eq. (17) into the above equation, it is obtained that

$$\int_g L^2\cos^2\theta \; g_{\theta\phi} = \int_0^{2\pi}\int_0^{\frac{1}{2}\pi} \frac{(n+1)L^2}{2} \sin^n\theta \; \cos^2\theta d\theta$$

$$= \frac{2L^2}{n+3}$$

Therefore

$$\text{Var}(z) = \frac{2L^2}{n+3} - \left(\frac{L(n\ 1)\ (n-1)\ .\ .\ .}{(n+2)\ (n)\ .\ .\ .}\left(\frac{\pi}{2}\right)^b\right)^2 . \quad . \quad . \quad . \quad . \quad (22)$$

3. Derivations of Eq. (79) and Eq. (80).

For the gradient in X-direction, letting ψ be the angle of orientation measured from the X- axis, then the following expression may be written:

$$\cos\psi = \sin\theta\cos\phi$$

and

$$g'_{\theta\phi} = B\frac{(n+1)\ (n-1)\ .\ .}{2n(n-2)\ .\ .\ .} \sin^{n+1}\theta\cos\phi d\theta d\phi$$

where B = $1/\pi$ for n odd and B = $\frac{1}{2}$ for n even. In the above expression, $g'_{\theta\phi}$ is defined as the probability function of the choice of canals based on the discharge and geometric distribution for X-gradient.

Therefore, the quantities $\langle\overline{\cos\psi}\rangle$ and $\langle\overline{1/\cos\psi}\rangle$ may be written as

$$\langle \overline{\cos\psi} \rangle = \int_\theta \int_\phi g'_{\theta\phi} \cos\psi \quad .$$

$$= B \frac{(n+1)(n-1) \ . \ . \ .}{2n(n-2) \ . \ . \ .} \int_{-\frac{1}{2}\pi}^{\frac{1}{2}\pi} \int_0^{\pi} \sin^{n+2}\theta \cos^2\theta \, d\theta \, d\phi \quad . \quad . \quad (79)$$

and

$$\langle \overline{1/\cos\psi} \rangle = \int_\theta \int_\phi g'_{\theta\phi} (1/\cos\psi)$$

$$= B \frac{(n+1)(n-1) \ . \ .}{2n(n-2) \ . \ . \ .} \int_{-\frac{1}{2}\pi}^{\frac{1}{2}\pi} \int_0^{\pi} \sin^{n}\theta \, d\theta \, d\phi \quad . \quad . \quad . \quad . \quad (80)$$

APPENDIX II

AN ESTIMATE OF ERROR IN ASSUMING AN AVERAGE COSINE OF THE ANGLE OF ORIENTATION FOR A GIVEN PATH IN A PORE CANAL NETWORK

The basic relationships between the distance Z, time of travel T, and the number of canals N in terms of canal orientation angle are as follows:

$$Z = L \sum_{j=1}^{N} \cos\theta_j \quad \ldots\ldots\ldots\ldots\ldots\ldots \quad (19)$$

$$T = t_o \sum_{j=1}^{N} \frac{1}{\cos\theta_j} = t_o \sum_{j=1}^{N} \sec\theta_j \quad \ldots\ldots\ldots\ldots \quad (27)$$

Assuming that there exists an average cosine such that

$$N \langle \cos\theta \rangle = \sum_{j=1}^{N} \cos^{\alpha}{}_j \quad \ldots\ldots\ldots\ldots\ldots \quad (82)$$

and

$$N \langle \sec^{\alpha} \rangle = \sum_{j=1}^{N} \sec\theta_j \quad \ldots\ldots\ldots\ldots\ldots \quad (83)$$

For N larger than unity, the above two equations do not lead to a common value of the orientation angle, that is, $\langle\cos\theta\rangle$ is not equal to $1/\langle\sec\theta\rangle$. The factors affecting the average values are, for a given path, the number of unit canals traversed, and the magnitude and combination of the individual canal orientation angles. For N becoming larger, the average cosine value may be evaluated by using the probability distribution function derived in Chapter 3 as follows:

$$\langle\cos\theta\rangle = \int_0^{2\pi} \int_0^{\frac{1}{2}\pi} \cos\theta \, g_{\theta\phi} \quad . \quad . \quad . \quad . \quad . \quad . \quad . \quad . \quad . \quad . \quad . \quad . \quad (84)$$

$$\langle\sec\theta\rangle = \int_0^{2\pi} \int_0^{\frac{1}{2}\pi} \sec\theta \, g_{\theta\phi} \quad . \quad . \quad . \quad . \quad . \quad . \quad . \quad . \quad . \quad . \quad . \quad . \quad (85)$$

where $g_{\theta\phi}$ is represented by Eq. (17) in the following form:

$$g_{\theta\phi} = \frac{n+1}{2\pi} \sin^n\theta\cos\theta d\theta d\phi \quad . \quad . \quad . \quad . \quad . \quad . \quad . \quad . \quad . \quad . \quad . \quad . \quad (17)$$

An evaluation of $\langle\cos\theta\rangle$ value from the above equations results in the following magnitudes of errors for various n values:

n =	1,	4,	7,	10,	13,	16	∞
Value of $\langle\cos\theta\rangle\langle\sec\theta\rangle$	1.33	1.45	1.49	1.51	1.52	1.53	$\frac{\pi}{2}$

Assuming that $\langle\cos\theta\rangle$ is evaluated from Eq. (75) then Eq. (19) may be written as

$$Z = NL \langle\cos\theta\rangle \quad . \quad . \quad . \quad . \quad . \quad . \quad . \quad . \quad . \quad . \quad . \quad . \quad (86)$$

and Eq. (27) may be written by taking into consideration the error involved as

$$T = A \, Nt_o \frac{1}{\langle\cos\theta\rangle} \quad . \quad . \quad . \quad . \quad . \quad . \quad . \quad . \quad . \quad . \quad . \quad . \quad (87)$$

where A is a correction factor. For n = 1, A equals $1/1.33 = 0.75$ and for n = 16, A would equal to $1/1.525 = 0.655$.

As stated previously the error involved would actually depend on the number of canals, paths and combination of the canal orientations. Therefore, in Figure 3-5, path 1 and path 2 in case (b) will not have the same magnitude of error with the same number of

canals $\bar{N}$. Similarly, considering path 1 in case (a) and case (b), the percent error will not be the same because the number of canals and the combinations of the angles are different.

The bracket in Eq. (45) may be written as follows:

$$\left[\frac{\langle\overline{\sec\theta}\rangle_{\bar{N}}\ \langle\overline{\cos\theta}\rangle_{\bar{N}}\ \langle\cos\theta\rangle_{\bar{T}}\ \bar{T}Z_o}{\langle\sec\theta\rangle_{\bar{T}}\ \langle\cos\theta\rangle_{\bar{N}}\ \langle\cos\theta\rangle_{\bar{N}}\ \bar{T}\bar{N}}\right] \quad \ldots\ldots\ (88)$$

The discussions in Chapter 3 showed that the ratios

$$\frac{\langle\cos\theta\rangle_{\bar{T}}}{\langle\cos\theta\rangle_{\bar{N}}}$$

and

$$\frac{\bar{T}Z_o}{\bar{T}\bar{N}}$$

can be considered as approximately equal to unity.

Let $\langle\overline{\sec\theta}\rangle_{\bar{N}} = A_1/\langle\overline{\cos\theta}\rangle_{\bar{N}}$

and $\langle\overline{\sec\theta}\rangle_{\bar{T}} = A_2/\langle\overline{\cos\theta}\rangle_{\bar{N}}$

then, the quantity in the bracket as expressed by Eq. (88) can be represented by A_1/A_2 and, from Eq. (45)

$$Z_{\bar{T}} = \frac{A_1}{A_2}\ \frac{Z_{\bar{N}}^2}{\bar{Z}_{\bar{N}}} \quad \ldots\ldots\ (89)$$

If A_1 is assumed to have the magnitude of error equivalent to that for canal orientation n = 1, and A_2 is assumed to have the magnitude of error for n = 16, then

$$A_1/A_2 = 0.75/0.655 = 1.145$$

Therefore, the error involved in this case will be approximately 15 percent. The above investigation with regard to the assumption of Eq. (88) to be equal to unity can also be analyzed in the following manner. Since $\langle\overline{\cos\theta}\rangle_{\overline{N}}$ is for the average of the total paths, and $\langle\cos\theta\rangle_{\overline{N}}$ is for an arbitrary path, it is obvious that if $\langle\overline{\cos\theta}\rangle_{\overline{N}}$ is larger than $\langle\cos\theta\rangle_{\overline{N}}$, then $\langle\overline{\sec\theta}\rangle_{\overline{N}}$ will be smaller than $\langle\sec\theta\rangle_{\overline{N}}$, and by assuming that $\langle\sec\theta\rangle_{\overline{N}}$ is approximately equal to $\langle\sec\theta\rangle_{\overline{T}}$, the product,

$$\frac{\langle\overline{\sec\theta}\rangle_{\overline{N}}}{\langle\sec\theta\rangle_{\overline{T}}}\;\frac{\langle\overline{\cos\theta}\rangle_{\overline{N}}}{\langle\cos\theta\rangle_{\overline{N}}}$$

will not deviate from unity appreciably.

In Eq. (49), the bracket may be written here as follows:

$$\left[\frac{\langle\overline{\sec\theta}\rangle_{\overline{N}}\;\langle\cos\theta\rangle_{\overline{T}}\;\overline{T}_{Z_o}}{\langle\sec\theta\rangle_{\overline{T}}\;\langle\cos\theta\rangle_{\overline{N}}\;\overline{T}_{\overline{N}}}\right] \quad \ldots\ldots\ldots\ldots \quad (90)$$

Based on the preceding discussions the ratios, $\langle\cos\theta\rangle_{\overline{T}}/\langle\cos\theta\rangle_{\overline{N}}$ and $\overline{T}_{Z_o}/\overline{T}_{\overline{N}}$ will be approximately equal to unity. However, the ratio

$$\frac{\langle\overline{\sec\theta}\rangle_{\overline{N}}}{\langle\sec\theta\rangle_{\overline{T}}}$$

represents the ratio of the average secant of all paths over an arbitrary path and the error in assuming it to be unity will produce an error of magnitude dependent on the average orientation of the individual paths. Since the range of the dispersion in a porous medium is usually small compared to the distance of the journey of individual particles, the assumption of this ratio to be equal to

unity for the purpose of this analysis may not affect the result significantly.

APPENDIX III

THE NUMERICAL COMPARISON OF PRESENT THEORY TO THOSE OF SAFFMAN'S AND DE JOSSELIN DE JONG'S

It is shown in Appendix I that a certain amount of error is introduced by the assumptions made in the derivation of the equations in Chapter 3.

The consequent error can be estimated by a comparison of the present theory with the theories of Saffman and De Josselin de Jong.

The theory presented by Saffman may be summarized as

$$\sigma_z = (TVLS^2)^{1/2} \qquad \ldots\ldots\ldots\ldots\ldots\ldots \quad (7)$$

where the quantity S^2 is represented by the following equations:

$$S^2 = \frac{1}{48}\left(\log \frac{54VT}{L}\right)^2 \qquad \ldots\ldots\ldots\ldots \quad (7a)$$

if $\dfrac{4VT_o/L}{\bar{n}^{1/2}\log \bar{n}^{1/4}} \gg 1$

$$S^2 = \frac{1}{3}\log \frac{3Vt_o}{L} - \frac{1}{12} \qquad \ldots\ldots\ldots\ldots \quad (7b)$$

if $\dfrac{Vt_o/L}{\bar{n}^{1/2}\left(\log \frac{3Vt_o}{L}\right)^{1/2}} \ll 1$

$$S^2 = \frac{1}{6}\log \frac{27VT}{2L} \qquad \ldots\ldots\ldots\ldots \quad (7c)$$

if $\dfrac{3Vt_o/L}{\bar{n}^{1/2}(\log \bar{n}^{1/2})^{1/2}} \gg 1.$

De Josselin de Jong's equation may be written as

$$z = \frac{L}{3}\left(\frac{3Z_o}{L}\left(\lambda + \frac{3}{4} - \log r\right)\right)^{1/2} \quad . \quad . \quad . \quad . \quad . \quad . \quad . \quad (6)$$

In order to apply Saffman's equation it is necessary that certain tests have to be made to determine the applicability of the equations. By taking the velocity range used in the dispersion measurements, a molecular diffusivity of $k = 1.5 \times 10^{-5} cm^2/sec$, and an orientation factor of unity which corresponds an average path of $\langle \cos\theta \rangle = 0.654$, the results of the tests are tabulated in Table III-1. It is seen that both Eq. (7a) and Eq. (7c) apply to the flow condition in the present investigation. From Eq. (7), Eq. (7a) and Eq. (7c), standard deviations are calculated and compared with those obtained from De Josselin de Jong's equation and the present theory in Table III-2. The average values of the corresponding standard deviations obtained in the dispersion measurements are also shown in Table III-2.

Table III-1. Test of applicability of Saffman's equations.

Type of Sample	Assumed L in cm.	$t_o = \frac{L^2}{2k}$ in sec.	Z_o in cm.	$\bar{n} = \frac{Z_o}{L\langle\cos\theta\rangle}$	V cm/sec. (10^{-2})	$\frac{4Vt_o/L}{\bar{n}^{1/2}\ln\bar{n}^{1/2}}$	$\frac{Vt_o/L}{\bar{n}^{1/4}(\ln 3Vt_o/L)^{1/2}}$	$\frac{3Vt_o/L}{n^{1/2}(\ln\bar{n}^{1/2})^{1/2}}$	Eq. Appli.
S	0.07	163	1.25	27	2.38	55	4.8	37	(7a)
			8.85	193	0.57	14	1.5	1.8	(7c)
P_1 & P_3	0.10	333	1.25	19	1.67	82	5.7	48	(7a)
			8.85	135	0.42	2.1	0.7	2.3	(7c)
P_2 & P_4	0.30	3000	1.25	6.4	1.67	550	27	292	(7a)
			8.85	45	0.42	23	2.8	18	(7c)

Table III-2. Comparison of the numerical results of standard deviation for various theories.

Type of Sample	Z_o in cm.	Saffman's Equations (7a)	(7c)	De Josselin de Jong's *	Present Theory Eq. (71)	Present Exp. Result	
S	1.25	0.288	0.271	0.254	0.171	0.270	
(L=0.07cm)	5.05	0.645	0.635	0.510	0.344	0.452	
	8.85	0.915	0.870	0.665	0.447	0.705	
						(P_1)	(P_3)
P_1 & P_3	1.25	0.291	0.322	0.303	0.204	0.307	0.252
(L=0.1cm)	5.05	0.755	0.695	0.610	0.410	0.625	0.540
	8.85	1.035	1.010	0.808	0.545	0.818	0.682
						(P_2)	(P_4)
P_2 & P_4	1.25	0.425	0.427	0.527	0.355	0.350	0.425
(L=0.3cm)	5.05	1.150	1.127	1.051	0.711	0.843	0.763
	8.85	1.713	1.522	1.400	0.943	1.160	1.068

* A value of 2.0 is assumed for γ in De Josselin de Jong's equation.

APPENDIX IV

THE PRESENTATION OF PERMEABILITY MEASUREMENTS

Table IV-1. Permeability test data for sample P_1.

Sample Test No.	Weight of Sample (gms)	Porosity (%)	Head (cm)	Discharge (cm^3/min)	K (cm/min)	Direct. of Flow
P_{11}	130.91	34.50	0.28	5.25	6.45	Transv.
			0.60	11.40		
			0.93	17.80		
P_{12}	127.35	36.10	0.35	7.50	6.95	Transv.
			0.70	14.10		
			1.02	23.40		
P_{13}	106.16	46.80	0.46	12.90	9.60	Transv.
			0.76	21.00		
			1.08	30.50		
P_{11}'	130.91	34.50	0.50	12.80	8.75	Longit.
			0.85	22.00		
			1.20	31.00		
P_{12}'	116.36	41.70	0.50	15.00	9.34	Longit.
			0.95	26.00		
			1.22	33.00		

Table IV-2. Permeability test data for sample P_2.

Sample Test No.	Weight of Sample (gms)	Porosity (%)	Head (cm)	Discharge (cm^3/min)	K (cm/min)	Direct. of Flow
P_{21}	122.70	39.00	0.25	6.50	8.75	Transv.
			0.40	10.50		
			0.70	18.00		
P_{22}	107.75	46.40	0.37	11.50	10.52	Transv.
			0.63	18.20		
			1.08	32.50		

Table IV-2. (continued)

Sample Test No.	Weight of Sample (gms)	Porosity (%)	Head (cm)	Discharge (cm^3/min)	K (cm/min)	Direct. of Flow
P_{21}'	120.05	39.20	0.25	7.50	10.70	Longit.
			0.71	21.00		
			1.03	31.50		
P_{22}'	113.79	43.10	0.20	6.50	11.22	Longit.
			0.61	20.60		
			0.93	31.00		
P_{23}'	112.83	43.50	0.36	11.75	11.28	Longit.
			0.68	22.50		
			1.00	33.00		

Table IV-3. Permeability test data for sample P_3.

Sample Test No.	Weight of Sample (gms)	Porosity (%)	Head (cm)	Discharge (cm^3/min)	K (cm/min)	Direct. of Flow
P_{31}	132.80	34.00	0.20	3.50	8.04	Transv.
			0.50	11.60		
			0.80	20.00		
			1.20	28.00		
P_{32}	123.40	38.60	0.17	5.40	11.00	Transv.
			0.53	17.00		
			0.73	27.00		
P_{31}'	140.08	29.60	0.45	10.90	8.65	Longit.
			0.75	19.50		
			1.15	29.10		
P_{32}'	131.52	34.20	0.22	6.30	10.10	Longit.
			0.61	18.50		
			0.98	29.50		

Table IV-4. Permeability test data for sample P_4.

Sample Test No.	Weight of Sample (gms)	Porosity (%)	Head (cm)	Discharge (cm^3/min)	K (cm/min)	Direct. of Flow
P_{41}'	140.62	29.60	0.45	13.40	10.41	Longit.
			0.67	20.40		
			1.09	33.50		
P_{42}'	129.61	35.20	0.29	9.25	11.17	"
			0.61	20.00		
			0.94	30.90		
P_{41}	140.50	31.00	0.30	8.00	9.05	Transv.
			0.50	13.50		
			0.90	24.00		
P_{42}	131.80	34.40	0.25	8.00	10.24	Transv.
			0.60	18.50		
			1.00	30.50		
P_{43}	129.50	35.60	0.30	9.50	10.24	Transv.
			0.55	17.00		
			1.10	33.50		

Table IV-5. Permeability test data for sample N.

Sample Test No.	Weight of Sample (gms)	Porosity (%)	Head (cm)	Discharge (cm^3/min)	K (cm/min)	of Flow
N_1	101.70	49.20	0.18	6.80	12.75	Transv.
			0.43	16.00		
			0.59	21.80		
			0.79	29.00		
N_1'	101.70	49.20	0.40	12.25	11.00	Longit.
			0.72	22.80		
			1.04	32.80		

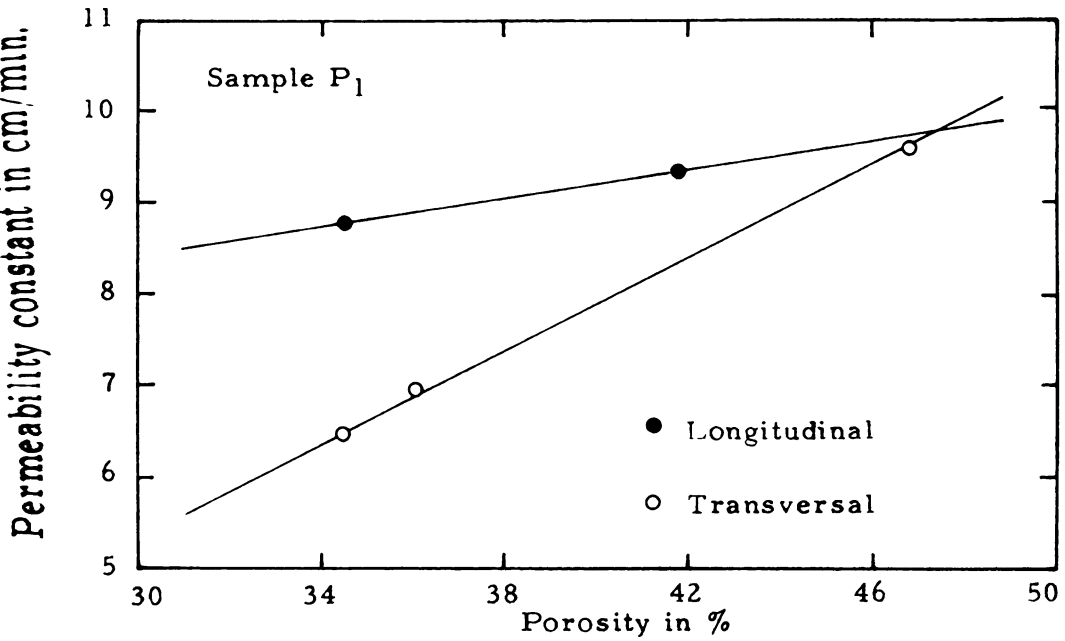

Figure IV-1. Permeability and porosity for sample P_1.

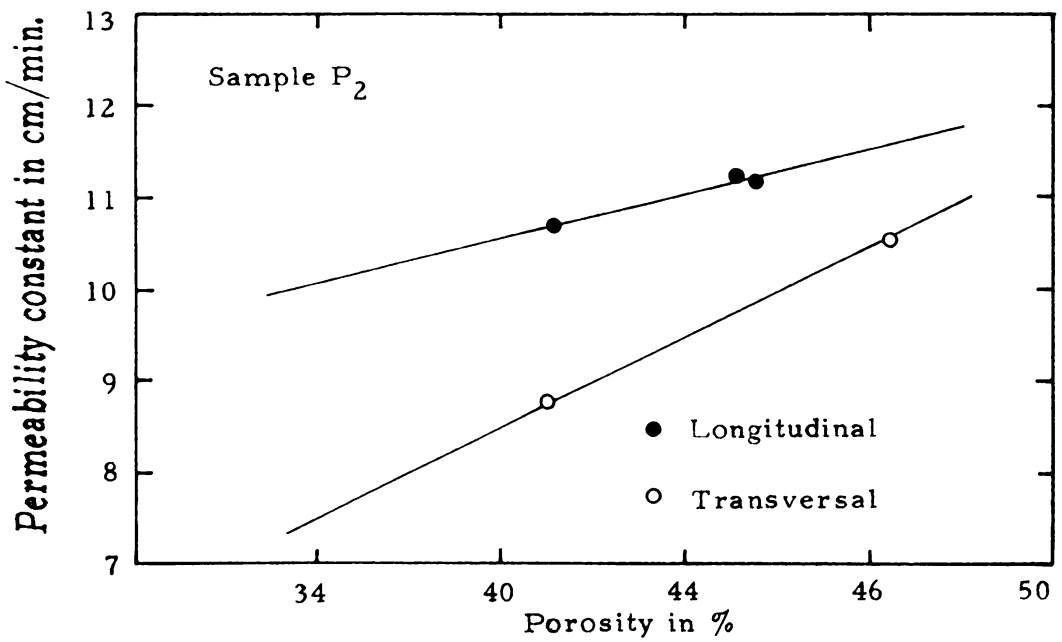

Figure IV-2. Permeability and porosity for sample P_2.

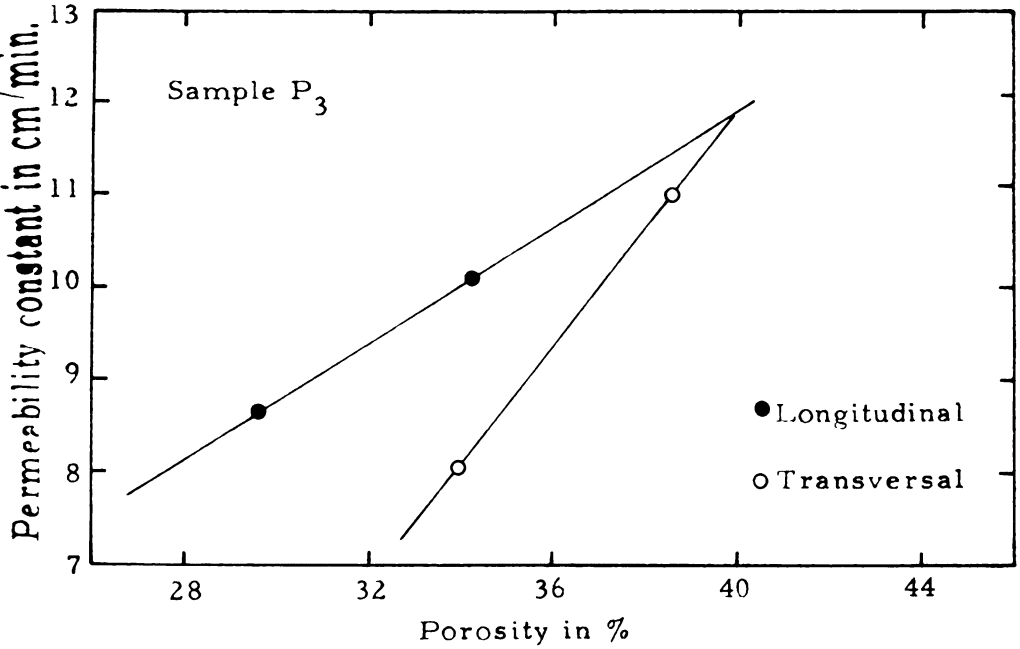

Figure IV-3. Permeability and porosity for sample P_3.

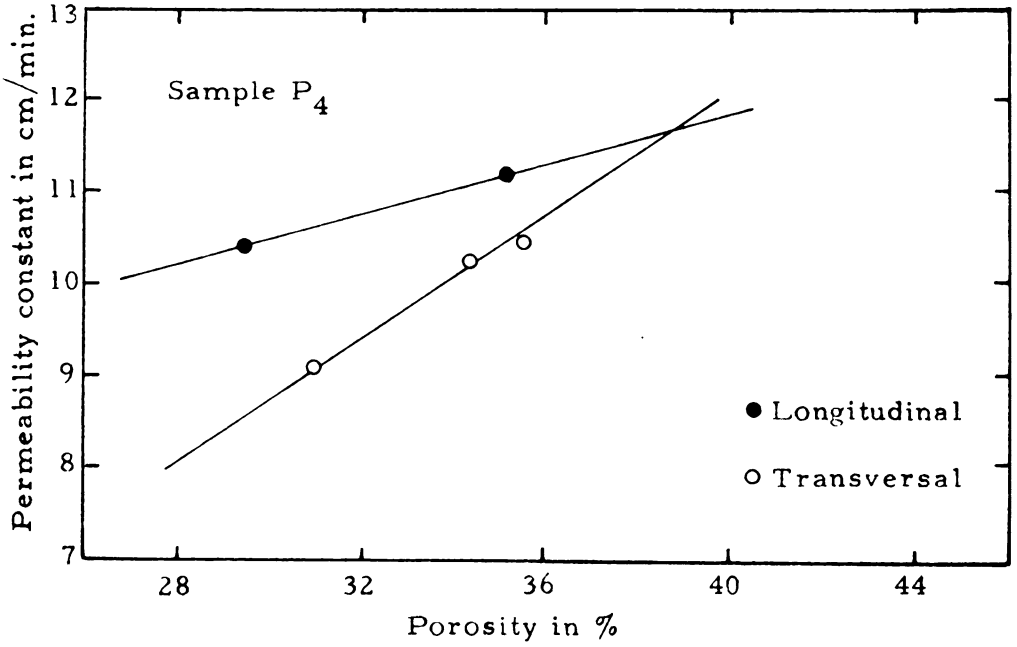

Figure IV-4. Permeability and porosity for sample P_4.

APPENDIX V

THE PRESENTATION OF EXPERIMENTAL DATA ON DISPERSION

Table V-1a. Dispersion measurements, S_{11}, V_m = 0.714 cm/min.

Position 1			Position 2			Position 3		
Time min.	in sec.	Concent. in Normal	Time min.	in sec.	Concent. in Normal	Time min.	in sec.	Concent. in Normal
0	0	.001	0	0	.001	0	0	.001
	15	.0012	5	0	.0021	10	0	.0014
	30	.0014		15	.0024		15	.0016
	45	-		30	.0026		30	.002
1	0	.002		45	.0029		45	.0027
	15	.0025	6	0	.0038	11	0	.0036
	30	.0038		15	.0057		15	.0052
	45	.0082		45	.0078		30	.0075
2	0	.0168	7	0	.0137		45	.0091
	15	.0375		15	.0223	12	0	.012
	30	.058		30	.0325		15	.017
	45	.076		45	.0465		30	.0228
3	0	.085	8	0	.057		45	.0305
	15	.092		15	.069	13	0	.0395
	30	.095		30	.080		15	.047
	45	.098		45	.090		30	.057
			9	0	.096		45	.0625
				15	.098	14	0	.071
							15	.0755
							30	.081
							45	.088
						15	0	.094
							15	.096

Table V-1b. Dispersion measurements, S_{12}, V_m = 0.57 cm/min.

Position 1			Position 2			Position 3		
Time min.	in sec.	Concent. in Normal	Time min.	in sec.	Concent. in Normal	Time min.	in sec.	Concent. in Normal
0	0	.001	0	0	.001	0	0	.001
	30	.0012	5	30	.0016	12	0	.0012
1	0	.0014	6	0	.0019		30	.0015

Table V-1b. (continued)

	30	.0019		15	.0021	13	15	.0021
	45	.0025		30	.0022		30	.0027
2	0	.0038		45	.0024		45	.0033
	15	.008	7	0	.0026	14	0	.0049
	30	.0129		30	.0036		15	.0065
	45	.0255		45	.0053		30	.0074
3	0	.043	8	15	.007		45	.010
	15	.060		30	.010	15	0	.013
	30	.071		45	.0152		15	.0168
	45	.082	9	0	.0225		30	.0223
4	0	.092		15	.0295		45	.027
	15	.094		30	.039	16	0	.0345
	30	.097		45	.051		15	.041
			10	0	.0615	16	30	.048
				15	.071		45	.056
				30	.080	17	0	.062
				45	.089		15	.068
			11	0	.095		45	.075
				15	.098	18	15	.087
							30	.092
							45	.094
						19	0	.098

Table V-1c. Dispersion measurements, S_{13}, V_m = 1.43 cm/min.

Position 1			Position 2			Position 3		
Time min.	in sec.	Concent. in Normal	Time min.	in sec.	Concent. in Normal	Time min.	in sec.	Concent. in Normal
0	0	.001	0	0	.001	0	0	.001
	15	.0012	2	30	.0014	5	45	.0117
	30	.0025		45	.0021	6	0	.020
	45	.0065	3	0	.0040		15	.032
1	0	.0255		15	.0112		30	.045
	15	.053		30	.0205		45	.060
	30	.073		45	.0375	7	0	.0735
	45	.085	4	0	.059		15	.082
2	0	.090		15	.075		30	.089
	15	.095		30	.086	8	0	.0925
				45	.092			
			5	0	.096			

Table V-1d. Dispersion measurements, S_{14}, V_m = 1.065 cm/min.

Position 1			Position 2			Position 3		
Time min.	in sec.	Concent. in Normal	Time min.	in sec.	Concent. in Normal	Time min.	in sec.	Concent. in Normal
0	0	.001	0	0	.001	0	0	.001
	15	.0011	3	30	.0014	7	0	.0016
	30	.0012		45	.0017		15	.0022
	45	.0018	4	0	.0026		30	.0034
1	0	.0036		15	.0044		45	.0062
	15	.0085		30	.0090	8	0	.0090
	30	.0238		45	.0127		15	.0165
	45	.055	5	0	.0275		30	.026
2	0	.077		15	.0355		45	.0372
	15	.092		30	.053	9	0	.051
	30	.097		45	.0705		15	.065
	45	.098	6	0	.088		30	.079
				15	.097		45	.085
						10	0	.090
							15	.095
							30	.097
							45	.098

Table V-1e. Dispersion measurements, S_{21}, V_m = 0.432 cm/min.

Position 1			Position 2			Position 3		
Time min.	in sec.	Concent. in Normal	Time min.	in sec.	Concent. in Normal	Time min.	in sec.	Concent. in Normal
0	0	.001	0	0	.001	0	0	.001
	30	.0013	5	0	.001	15	45	.0011
1	0	.0022	6	0	.0011	15	30	.0013
	30	.0037	7	30	.0013	16	30	.0016
2	0	.0051	8	30	.0018	17	30	.0028
	30	.013	9	30	.0036	18	15	.0047
3	0	.030	10	0	.0063	19	0	.0105
	30	.0535		30	.0115		30	.0145
4	0	.073	11	0	.0195	20	0	.025
	30	.078		30	.036		30	.038
5	0	.083	12	0	.055	21	0	.051
6	0	.089		30	.067		30	.062
7	0	.091	13	0	.076	22	0	.0725
				30	.080		30	.083
			15	0	.092			

Table V-1f. Dispersion measurements, S_{22}, V_m = 0.342 cm/min.

Position 1			Position 2			Position 3		
Time min.	in sec.	Concent. in Normal	Time min.	in sec.	Concent. in Normal	Time min.	in sec.	Concent. in Normal
0	0	.001	0	0	.001	0	0	.001
	30	.0014	8	0	.001	17	30	.001
1	0	.002	9	0	.0011	18	30	.0011
	30	.0029	10	0	.0014	19	0	.0013
2	0	.0037	11	0	.0018	20	0	.0015
	30	.0063		30	.0025	21	0	.0018
3	0	.0147	12	0	.0036	22	0	.0026
	30	.0295		30	.0063	23	0	.0056
4	0	.053	13	0	.0118		30	.0096
	30	.073		30	.0167	24	0	.0102
5	0	.084	14	0	.0282		30	.0197
	30	.088		30	.044	25	0	.029
6	0	.092	15	0	.060		30	.040
				30	.077	26	0	.052
			16	0	.088		30	.063
						27	0	.071
							30	.079
						28	0	.088
							30	.095

Table V-1g. Dispersion measurements, S_{23}, V_m = 0.787 cm/min.

Position 1			Position 2			Position 3		
Time min.	in sec.	Concent. in Normal	Time min.	in sec.	Concent. in Normal	Time min.	in sec.	Concent. in Normal
0	0	.001	0	0	.001	0	0	.001
	15	.0013	2	45	.001	8	0	.001
	30	.002	3	45	.0012	9	0	.0016
	45	.0036	4	30	.0017		15	.002
1	0	.0047	5	0	.0029		30	.0025
	15	.0093		30	.0091		45	.0035
	30	.023	6	0	.0242	10	0	.0051
	45	.051		15	.037		15	.008
2	0	.0725		30	.058		30	.0106
	15	.090		45	.073		45	.0173
			7	0	.081	11	0	.0295
				15	.085		15	.040
				45	.089		30	.055
							45	.067
						12	0	.073
							15	.081
							30	.087
							45	.091
						13	45	.093

Table V-1h. Dispersion measurements, S_{24}, V_m = 0.625 cm/min.

Position 1			Position 2			Position 3		
Time in min.	sec.	Concent. in Normal	Time in min.	sec.	Concent. in Normal	Time in min.	sec.	Concent. in Normal
0	0	.001	0	0	.001	0	0	.001
	30	.0014	4	45	.0011	9	45	.0011
	45	.0021	5	30	.0014	10	30	.0012
1	0	.0031	6	0	.002	11	30	.0017
	15	.0039		30	.0037	12	0	.0025
	30	.0063	7	0	.0083		30	.0043
	45	.015		15	.0165		45	.007
2	0	.0235		30	.0225	13	0	.0103
	15	.046	8	0	.043		15	.0125
	30	.062		15	.053		30	.0175
	45	.078		30	.065		45	.0285
3	30	.092		45	.069	14	0	.035
4	0	.093	9	0	.073		15	.047
			10	0	.091		30	.0555
							45	.062
						15	0	.066
							30	.075
						16	0	.085
							30	.091
						17	0	.0925

Table V-2a. Dispersion measurements, P_{111}, V_m = .575 cm/min.

Position 1			Position 2			Position 3		
Time in min.	sec.	Concent. in Normal	Time in min.	sec.	Concent. in Normal	Time in min.	sec.	Concent. in Normal
0	0	.001	0	0	.001	0	0	.001
	30	.0018	3	30	.0011	9	15	.0021
	45	.0025	4	0	.0015		45	.0028
1	0	.0037		30	.0022	10	15	.0042
	15	.0065	5	0	.0036		45	.0062
	30	.0122		30	.006	11	15	.0088
	45	.0185	6	0	.0103		45	.012
2	0	.031		30	.012	12	30	.015
	15	.0485	7	0	.0183	13	0	.019
	30	.064		30	.0285		30	.024
	45	.078	8	0	.0375	14	0	.0305
3	0	.086		30	.049		30	.0365
	15	.092	9	0	.060	15	0	.0455
				30	.070		30	.052
			10	0	.080	16	0	.062
				30	.088		30	.070
			11	0	.091	17	0	.075
				30	.095		30	.083
						18	0	.089
							30	.095

Table V-2b. Dispersion measurements, P_{112}, V_m = .306 cm/min.

Position 1			Position 2			Position 3		
Time in		Concent. in	Time in		Concent. in	Time in		Concent. in
min.	sec.	Normal	min.	sec.	Normal	min.	sec.	Normal
0	0	.001	0	0	.001	0	0	.001
	30	.0015	5	45	.0011	15	15	.0011
1	0	.0022	7	30	.0015	17	45	.0019
	30	.0028	8	30	.0024	18	45	.0026
2	0	.0044	9	0	.003	19	30	.0035
	30	.010	10	0	.0053	20	30	.005
3	0	.0136	11	0	.0088	21	30	.0073
	30	.0265		30	.012	22	30	.0106
4	0	.046	12	30	.015	24	0	.0137
	30	.063	13	0	.0185		30	.0152
5	0	.079		30	.0237	25	0	.0178
	30	.088	14	0	.0295		30	.0205
				30	.037	26	0	.0245
			15	0	.045		30	.027
				30	.054	27	0	.0305
			16	0	.062		30	.035
				30	.070	28	0	.0395
			17	0	.078		30	.044
				30	.085	29	0	.0495
			18	0	.091		30	.055
				30	.093	30	0	.058
			19	0	.095		30	.065
						31	0	.071
							30	.076
						32	0	.080
							30	.084
						33	0	.089
							30	.092
						34	0	.096

Table V-2c. Dispersion measurements, P_{113}, V_m = 0.44 cm/min.

Position 1			Position 2			Position 3		
Time in		Concent. in	Time in		Concent. in	Time in		Concent. in
min.	sec.	Normal	min.	sec.	Normal	min.	sec.	Normal
0	0	.001	0	0	.001	0	0	.001
	30	.0018	3	45	.001	10	45	.0012
1	0	.002	4	45	.0014	11	45	.0016
	30	.0061	5	30	.002	12	45	.0025
2	15	.0213	6	30	.0042	13	30	.0038
	30	.0315	7	0	.0062	14	30	.0062
3	0	.056	8	0	.0129	16	30	.0155
	30	.076		30	.0137	17	30	.019

Table V-2c. (continued)

4	0	.089	9	0	.0188	18	0	.023
	30	.096		30	.025		30	.0275
5	0	.097	10	0	.033	19	0	.0315
				30	.043		30	.0385
			11	0	.053	20	0	.046
				30	.064		30	.053
			12	0	.073	21	0	.061
				30	.084		30	.0675
			13	0	.088	22	0	.076
			14	0	.090		30	.081
						23	0	.089
							30	.094

Table V-3a. Dispersion measurements, P_{121}, V_m = 1.016 cm/min.

Position 1			Position 2			Position 3		
Time in		Concent. in	Time in		Concent. in	Time in		Concent. in
min.	sec.	Normal	min.	sec.	Normal	min.	sec.	Normal
0	0	.001	0	0	.001	0	0	.001
	15	.0023	2	0	.0011	6	0	.0046
	30	.006		45	.0024		30	.010
	45	.0163	3	15	.0062	7	0	.0168
1	0	.0362		30	.0083		30	.025
	15	.0545		45	.0102	8	15	.042
	30	.0675	4	0	.0187		30	.047
	45	.080		15	.026		45	.054
2	30	.095		30	.033	9	0	.062
				45	.042		15	.068
			5	0	.050		30	.0745
				15	.058	10	0	.082
				30	.0655		15	.089
				45	.074		30	.090
			6	15	.085	11	0	.095
				45	.093			
			7	15	.095			

Table V-3b. Dispersion measurements, P_{122}, V_m = .793 cm/min.

Position 1			Position 2			Position 3		
Time in		Concent. in	Time in		Concent. in	Time in		Concent. in
min.	sec.	Normal	min.	sec.	Normal	min.	sec.	Normal
0	0	.001	0	0	.001	0	0	.001
	15	.0012	3	15	.0012	7	0	.0016
	30	.0016		45	.0032	9	0	.0115
	45	.0036	4	15	.0044		30	.0163

Table V-3b. (continued)

1	0	.0088		45	.0087		45	.020
	15	.0182	5	0	.012	10	0	.0225
	30	.031		15	.0158		15	.0263
	45	.047		30	.020		45	.0365
2	0	.062	5	45	.0255	11	0	.041
	15	.075	6	0	.0315		15	.0465
	30	.085		15	.040		30	.052
	45	.0915		30	.048		45	.059
3	0	.0965		45	.055	12	0	.064
			7	15	.072		15	.068
				30	.078		30	.0725
				45	.081		45	.077
			8	0	.086	13	15	.087
				15	.090		45	.089
				30	.095	14	15	.091
				45	.097	15	30	.094

Table V-3c. Dispersion measurements, P_{123}, V_m = 0.581 cm/min.

Position 1			Position 2			Position 3		
Time in		Concent. in	Time in		Concent. in	Time in		Concent. in
min.	sec.	Normal	min.	sec.	Normal	min.	sec.	Normal
0	0	.001	0	0	.001	0	0	.001
	30	.0016	3	45	.0011	10	30	.0024
	45	.0025	4	45	.0017	11	15	.0043
1	0	.0044	5	30	.0033	12	15	.0097
	15	.0086	6	0	.0056		45	.0135
	30	.013		30	.008	13	30	.020
	45	.0232	7	0	.014	14	0	.026
2	0	.034		30	.0217		45	.037
	15	.045		45	.0262	15	0	.0415
	30	.058	8	0	.032		30	.050
	45	.0685		15	.0365		45	.055
3	0	.075		30	.0405	16	0	.059
	15	.083		45	.0465		15	.063
	30	.089	9	0	.0525		30	.068
4	0	.095		15	.059		45	.0725
	30	.097		30	.065	17	0	.077
				45	.070		15	.081
			10	0	.075		30	.084
				15	.079		45	.087
				45	.089	18	0	.089
			11	0	.092		15	.091
				30	.093		30	.093
			12	0	.0955	19	30	.095
			13	0	.097			

Table V-3d. Dispersion measurements, P_{124}, V_m = .377 cm/min.

Position 1			Position 2			Position 3		
Time in min.	sec.	Concent. in Normal	Time in min.	sec.	Concent. in Normal	Time in min.	sec.	Concent. in Normal
0	0	.001	0	0	.001	0	0	.001
	30	.0015	4	45	.001	14	15	.0013
1	0	.0024	7	30	.0017	15	45	.002
	30	.0037	8	0	.0021	17	15	.0039
2	0	.0097		30	.0029	18	15	.0065
	30	.0172	9	0	.004	19	15	.0095
	45	.024		30	.0057	20	0	.0131
3	0	.0315	10	0	.0067		30	.0162
	15	.0385		30	.0093	21	0	.020
	30	.046	11	0	.013		30	.0245
	45	.0525		30	.0167	22	0	.0285
4	0	.058	12	0	.023		30	.034
	15	.063		30	.0305	23	0	.0395
	30	.067	13	0	.038		30	.0445
5	0	.075		30	.046	24	0	.0505
	30	.079	14	0	.0545		45	.060
6	0	.084		30	.065	25	0	.065
			15	0	.070		30	.070
				30	.078	26	0	.075
			16	0	.084		30	.081
				30	.088	27	0	.0845
			17	0	.091		30	.087
			18	0	.096	28	0	.091
							30	.094
						29	0	.095

Table V-4a. Dispersion measurements, P_{131}, V_m = .476 cm/min.

Position 1			Position 2			Position 3		
Time in min.	sec.	Concent. in Normal	Time in min.	sec.	Concent. in Normal	Time in min.	sec.	Concent. in Normal
0	0	.001	0	0	.001	0	0	.001
	30	.0024	4	45	.0012	12	15	.0016
1	0	.004	5	45	.0014	13	15	.0025
	15	.006	6	30	.0022		45	.0035
	30	.0066	7	0	.0032	14	15	.0046
	45	.0123		30	.0056	15	0	.006
2	0	.0215	8	0	.0072		30	.0078
	15	.036		30	.0122	16	0	.0113
	30	.049	9	0	.020		30	.0152
	45	.062		30	.031	17	0	.018
3	0	.076		45	.0305		30	.0275
	15	.085	10	0	.0435	18	0	.035

Table V-4a. (continued)

	15	.051		15	.040
	30	.059		30	.0445
	45	.065		45	.0495
11	0	.072	19	0	.055
	15	.078		15	.061
	30	.084		30	.065
	45	.088		45	.070
12	0	.0905	20	0	.073
				15	.077
				30	.080
			21	0	.083
				30	.089
			22	0	.094

Table V-4b. Dispersion measurements, P_{132}, V_m = .695 cm/min.

Position 1			Position 2			Position 3		
Time in		Concent. in	Time in		Concent. in	Time in		Concent. in
min.	sec.	Normal	min.	sec.	Normal	min.	sec.	Normal
0	0	.001	0	0	.001	0	0	.001
	30	.0026	3	0	.001	8	15	.0017
1	0	.0068	4	0	.0026	9	15	.0034
	30	.0265	5	0	.005		45	.0054
	45	.047	6	15	.0235	10	30	.0081
2	0	.070		30	.033	11	0	.0125
	15	.085	7	0	.0555		30	.019
				15	.062	12	15	.0335
				30	.0755		30	.041
				45	.082		45	.046
			8	0	.087	13	0	.050
				30	.090		15	.056
			9	0	.0925		30	.062
			10	0	.095		45	.070
						14	0	.075
							30	.086
							45	.090
						15	15	.095

Table V-4c. Dispersion measurements, P_{133}, V_m = .602 cm/min.

Position 1			Position 2			Position 3		
Time in		Concent. in	Time in		Concent. in	Time in		Concent. in
min.	sec.	Normal	min.	sec.	Normal	min.	sec.	Normal
0	0	.001	0	0	.001	0	0	.001
	30	.0025	4	0	.0012	10	15	.0024
1	0	.0052		30	.0015	11	15	.0046
	30	.014	5	0	.0021	12	15	.0105
2	0	.0435		30	.0033	13	0	.014
	15	.061	6	0	.0061		30	.020
	30	.076		30	.008	14	0	.0285
	45	.086	7	0	.0152		30	.0395
				15	.0205		45	.046
				30	.026	15	0	.053
				45	.032		15	.061
			8	0	.041		30	.069
				15	.0485	16	0	.074
				30	.055			
				45	.062			
			9	0	.0675			
				15	.073			
				30	.075			
				45	.079			
			10	0	.080			
				45	.088			
			12		.094			

Table V-5a. Dispersion measurements, P_{211}, V_m = .815 cm/min.

Position 1			Position 2			Position 3		
Time in		Concent. in	Time in		Concent. in	Time in		Concent. in
min.	sec.	Normal	min.	sec.	Normal	min.	sec.	Normal.
0	0	.001	0	0	.001	0	0	.001
	15	.0023	2	15	.0025	7	45	.0174
	30	.0065		45	.0046	8	30	.022
	45	.0146	3	15	.0093	9	0	.0272
1	0	.0205	4	0	.0139		30	.034
	15	.033		30	.0215		45	.0365
	30	.049		45	.0242	10	0	.040
	45	.061	5	0	.0282		15	.044
2	0	.075		15	.033		30	.047
	30	.084		30	.038		45	.0505
3	30	.095		45	.0425	11	0	.054
			6	0	.0475		15	.0575
				15	.0535		30	.060
				30	.058		45	.063
				45	.0625	12	0	.066

Table V-5a. (continued)

7	0	.0675		30	.0725
	30	.077	13	0	.0775
8	15	.083		30	.082
9	15	.090	14	30	.086
			16	0	.092

Table V-5b. Dispersion measurements, P_{212}, V_m = .421 cm/min.

Position 1			Position 2			Position 3		
Time in		Concent. in	Time in		Concent. in	Time in		Concent. in
min.	sec.	Normal	min.	Sec.	Normal	min.	sec.	Normal
0	0	.001	0	0	.001	0	0	.001
	30	.0018	3	45	.0015	8	15	.0017
1	0	.0064	5	15	.0039	9	15	.0023
	30	.0103		45	.0056	10	15	.0033
2	0	.023	6	0	.0065	11	15	.005
	15	.031		30	.007	12	15	.0075
	30	.041	7	0	.009	13	15	.0082
	45	.051		30	.0116	14	15	.0106
3	0	.06	8	0	.0145	15	30	.015
	15	.07		30	.0183	16	30	.0188
	30	.078	9	0	.0222	17	30	.024
4	0	.088		30	.027	18	0	.0275
	30	.0955	10	0	.032		30	.030
			10	30	.0375	19	0	.0345
			11	0	.0435		30	.038
				30	.050	20	0	.043
			12	0	.0565		30	.0475
				30	.063	21	0	.0535
			13	0	.069		30	.058
				30	.076	22	0	.064
			14	0	.0795		30	.0695
				30	.085	23	0	.075
			15	0	.088		30	.080
			16	0	.094	24	0	.083
							30	.088
						25	0	.090
							30	.0925

Table V-5c. Dispersion measurements, P_{213}, V_m = .569 cm/min.

Position 1			Position 2			Position 3		
Time in		Concent. in	Time in		Concent. in	Time in		Concent. in
min.	sec.	Normal	min.	sec.	Normal	min.	sec.	Normal
0	0	.001	0	0	.001	0	0	.001
	30	.0029	3	15	.002	7	15	.0031
	45	.0062	4	15	.0055	8	15	.0052
1	0	.012	5	0	.0085	9	15	.0085
	15	.0156		30	.0121	10	15	.0098
	30	.025	6	0	.016	11	15	.0138
	45	.0355		30	.0208	12	15	.0192
2	0	.0475	7	0	.0264	13	15	.0262
	15	.060		30	.033	14	0	.0325
	30	.068	8	0	.040		30	.0385
	45	.075		30	.048	15	0	.044
3	0	.081	9	0	.056		30	.0505
	30	.085		30	.063	16	0	.057
			10	0	.071		30	.0645
				30	.080	17	0	.0715
			11	0	.084		30	.078
				30	.087	18	0	.0845
			12	0	.089		30	.090
				30	.090	19	0	.095
			13	0	.091			

Table V-6a. Dispersion measurements, P_{221}, V_m = .535 cm/min.

Position 1			Position 2			Position 3		
Time in		Concent. in	Time in		Concent. in	Time in		Concent. in
min.	sec.	Normal	min.	sec.	Normal	min.	sec.	Normal
0	0	.001	0	0	.001	0	0	.001
	30	.0047	2	45	.0013	9	15	.0062
	45	.0091	3	15	.0018	10	15	.007
1	0	.012		45	.0026		45	.0082
	15	.0215	4	15	.0037	11	15	.0093
	30	.0325	5	0	.0063		45	.0108
	45	.0445		30	.0074	12	30	.0136
2	0	.058	6	0	.0103	13	0	.0162
	15	.070		30	.0144		30	.020
	30	.079		45	.0168	14	0	.0248
3	0	.090	7	0	.020		30	.0292
				15	.023	15	0	.0355
				30	.027		30	.0435
				45	.030	16	0	.050
			8	0	.034		30	.057
				15	.0385	17	0	.0635
				30	.044		30	.0675
				45	.050	18	0	.070

Table V-6a. (continued)

9	0	.0545
	30	.060
10	0	.069
	30	.078
11	0	.085
	30	.090

Table V-6b. Dispersion measurements, P_{222}, V_m, = .295 cm/min.

Position 1			Position 2			Position 3		
Time in		Concent. in	Time in		Concent. in	Time in		Concent. in
min.	sec.	Normal	min.	sec.	Normal	min.	sec.	Normal
0	0	.001	0	0	.001	0	0	.001
	30	.0015	4	15	.001	16	45	.003
1	0	.0032	6	30	.0015	18	30	.0042
2	0	.0091	8	30	.0031	19	30	.0052
2	30	.0205	9	30	.0044	23	0	.0069
3	0	.036	11	0	.0066	24	0	.0089
	30	.057	12	0	.0096	25	0	.0121
4	0	.072		30	.0122	26	0	.0167
	30	.087	13	0	.0155	27	0	.0237
7	0	.095		30	.0192		30	.0295
			14	0	.0245	28	0	.035
				30	.0305		30	.0415
			15	0	.036	29	0	.0475
				30	.044		30	.0535
			16	0	.053	30	0	.0595
				30	.061		30	.067
			17	0	.0675	31	0	.0725
				30	.074		30	.077
			18	15	.083	32	0	.078
			20	0	.087	33	0	.081
						34	0	.085
						35	0	.088

Table V-6c. Dispersion measurements, P_{223}, V_m = .366 cm/min.

Position 1			Position 2			Position 3		
Time in		Concent. in	Time in		Concent. in	Time in		Concent. in
min.	sec.	Normal	min.	sec.	Normal	min.	sec.	Normal
			0	0	.001	0	0.	.001
			3	15	.0011	11	45	.0029
			4	0	.0016	12	45	.0035
			5	0	.0021	13	45	.0048
			6	0	.0032	15	45	.0077

Table V-6c. (continued)

	30	.0042	17	30	.0085
7	30	.0047	18	0	.010
8	0	.007		30	.012
	30	.009	19	0	.0147
9	0	.012	19	30	.0183
	30	.0158	20	0	.0225
10	0	.021		30	.0275
	30	.0275	21	0	.033
11	0	.035		30	.0395
	30	.044	22	0	.046
12	0	.050		30	.053
	30	.060	23	0	.060
13	0	.070		30	.065
	30	.075	24	0	.071
14	0	.080		30	.077
15	0	.086	25	0	.081
				30	.085

Table V-7a. Dispersion measurements, P_{311}, V_m = . 0.95 cm/min.

Position 1			Position 2			Position 3		
Time in		Concent. in	Time in		Concent. in	Time in		Concent. in
min.	sec.	Normal	min.	sec.	Normal	min.	sec.	Normal
0	0	.0018	0	0	.001	0	0	.001
	30	.0033	2	15	.0015	5	45	.0021
	45	.0069	3	15	.0045	6	45	.0062
1	0	.015	4	30	.0273	7	15	.0113
	15	.0345		45	.035		45	.014
	30	.050	5	15	.052	8	15	.0218
	45	.066		30	.064		30	.027
2	0	.077	6	0	.079	9	0	.040
	30	.090		30	.090		30	.0515
3	0	.095	7	0	.093		45	.059
						10	0	.066
							15	.0745
							30	.079
							45	.085
						11	0	.090
							30	.095

Table V-7b. Dispersion measurements, P_{312}, V_m = 0.78 cm/min.

Position 1			Position 2			Position 3		
Time in min.	sec.	Concent. in Normal	Time in min.	sec.	Concent. in Normal	Time in min.	sec.	Concent. in Normal
0	0	.002	0	0	.001	0	0	.001
	30	.0028	2	15	.001	8	15	.0029
	45	.0042	3	45	.0022		45	.0043
1	0	.0096	4	15	.004	9	15	.007
	15	.0172		45	.0082		45	.011
	30	.031	5	0	.0093	10	30	.0145
	45	.047		30	.0178	11	0	.0205
2	0	.063	6	0	.030		15	.0247
	30	.080		15	.0375		30	.0285
3	0	.091		30	.047		45	.0335
	30	.096		45	.055	12	0	.038
			7	0	.062		15	.0435
				15	.070		30	.049
				30	.077		45	.0535
				45	.084	13	0	.060
			8	0	.088		15	.0655
				30	.095		30	.071
						14	0	.0775
						15	0	.087
						16	0	.095
						17	0	.097

Table V-7c. Dispersion measurements, P_{313}, V_m = .473 cm/min.

Positon 1			Position 2			Position 3		
Time in min.	sec.	Concent. in Normal	Time in min.	sec.	Concent. in Normal	Time in min.	sec.	Concent. in Normal
0	0	.0017	0	0	.001	0	0	.001
	30	.0027	3	45	.0011	10	45	.0014
	45	.0031	4	45	.0013	11	45	.0017
1	0	.0038	5	45	.0019	12	45	.0023
	15	.0053	6	30	.0029	14	30	.0053
	30	.0088	7	0	.0047	16	0	.0088
	45	.0127		30	.008		30	.0112
2	0	.0195	8	0	.0098	17	0	.014
	15	.0305		15	.0117		30	.018
	30	.0415		30	.0142	18	0	.022
	45	.0555		45	.0178		30	.0275
3	0	.066	9	0	.021	19	0	.0335
	15	.076		15	.0253		30	.041
	30	.082		30	.0297		45	.045
4	0	.093		45	.036	20	0	.049
	30	.095	10	0	.041		30	.0575

Table V-7c. (continued)

	30	.0525	21	0	.064
11	0	.060		30	.070
	30	.068	22	0	.077
12	0	.078		30	.083
	30	.087	23	0	.087
13	0	.0925		30	.094
	30	.095			

Table V-8a. Dispersion measurements, P_{321}, V_m = .396 cm/min.

Position 1			Position 2			Position 3		
Time in		Concent. in	Time in		Concent. in	Time in		Concent. in
min.	sec.	Normal	min.	sec.	Normal	min.	sec.	Normal
0	0	.0018	0	0	.001	0	0	.001
	30	.0037	3	15	.0024	10	45	.0011
1	0	.0041	5	45	.0029	14	15	.0012
	30	.0063	8	30	.0054	16	0	.002
2	0	.0081	9	0	.0068	17	0	.0037
	30	.026	10	0	.0188	18	30	.0075
3	0	.055		30	.0255	19	0	.0113
	30	.080	11	0	.037		30	.016
4	0	.095		30	.0495	20	0	.024
			12	0	.064	20	30	.031
				30	.0755	21	0	.040
			13	0	.081		30	.049
						22	0	.060
							30	.068
						23	0	.077
							30	.0855
						24	0	.094

Table V-8b. Dispersion measurements, P_{322}, V_m = .255 cm/min.

Position 1			Position 2			Positon 3		
Time in		Concent. in	Time in		Concent. in	Time in		Concent. in
min.	sec.	Normal	min.	sec.	Normal	min.	sec.	Normal
0	0	.0034	0	0	.001	0	0	.001
	30	.0038	6	45	.0021	19	45	.001
1	0	.0042	9	0	.0024	23	30	.0012
	30	.0049	11	0	.003	25	0	.0014
2	30	.0068	13	0	.0045	27	0	.0021
3	0	.0129	14	30	.0058	28	0	.0029
	15	.0195	15	0	.0074	29	0	.0046
	30	.029		30	.0103	31	0	.0081
	45	.0405	16	0	.0135	32	0	.0129

Table V-8b. (continued)

4	0	.0525		30	.0178		30	.0162
	15	.065	17	0	.0245	33	0	.020
	30	.076		30	.033		30	.025
	45	.085	18	0	.040	34	0	.030
5	0	.093		30	.0495		30	.036
			19	0	.058	35	0	.0425
				30	.069		30	.0495
			20	0	.079	36	0	.056
				30	.086		30	.064
			21	0	.090	37	0	.071
				30	.095		30	.076
						38	0	.082
						39	0	.0905
						40	0	.095

Table V-8c. Dispersion measurements, P_{323}, V_m = .261 cm/min.

Positon 1			Position 2			Position 3		
Time in		Concent. in	Time in		Concent in	Time in		Concent. in
min.	sec.	Normal	min.	sec.	Normal	min.	sec.	Normal
0	0	.0037	0	0	.001	0	0	.001
	30	.0042	7	30	.0021	21	45	.0011
1	0	.0045	10	0	.0025	25	0	.0015
	30	.0055	12	0	.0033	26	0	.0019
2	30	.0082	14	30	.0065	28	0	.0039
3	0	.0167	15	0	.0087	29	0	.0062
	30	.037		30	.012	30	0	.0077
	45	.047	16	0	.0161		30	.009
4	0	.0575	16	30	.022	31	0	.0112
	30	.078	17	0	.028		30	.014
5	0	.091		30	.035	32	0	.0177
			18	0	.0435		30	.022
				30	.052	33	0	.026
			19	0	.061		30	.032
				30	.071	34	0	.038
			20	0	.081	35	0	.0505
				30	.086	36	0	.063
			21	0	.095		30	.0715
						37	0	.078
							30	.084
						38	0	.088
							30	.091
						39	0	.093

Table V-9a. Dispersion measurements, P_{411}, V_m = cm/min.

Position 1			Position 2			Position 3		
Time in min.	sec.	Concent. in Normal	Time in min.	sec.	Concent in Normal	Time in min.	sec.	Concent. in Normal
0	0	.0029	0	0	.001	0	0	.001
	15	.0036	4	15	.0011	11	15	.0012
	30	.0044	6	30	.0021	13	15	.0018
1	0	.0143	7	30	.0041	15	30	.0034
	30	.0287	8	0	.0062	16	15	.0052
	45	.0042		30	.0094	17	30	.0083
2	0	.0056	9	0	.0107	18	30	.0125
	15	.064		30	.0161	19	0	.0163
	30	.070	10	0	.0243		30	.021
3	0	.082		30	.036	20	0	.028
	30	.090	11	0	.046		30	.034
4	0	.093		30	.057	21	0	.042
	30	.095	12	0	.066		30	.047
5	0	.097		30	.072	22	0	.054
			13	0	.078		30	.060
				30	.081	23	0	.067
			14	0	.085		30	.072
			15	0	.091	24	0	.077
			16	0	.095	25	0	.085
						26	0	.089
						27	0	.096

Table V-9b. Dispersion measurements, P_{412}, V_m = cm/min.

Position 1			Position 2			Position 3		
Time in min.	sec.	Concent. in Normal	Time in min.	sec.	Concent. in Normal	Time in min.	sec.	Concent. in Normal
0	0	.0012	0	0	.001	0	0	.001
1	0	.002	9	0	.001	18	15	.0011
2	0	.0049	12	0	.0018	22	15	.0015
3	0	.0087	13	0	.0028	24	30	.0021
	30	.0142	14	0	.0046	26	30	.0031
4	0	.0223	15	0	.0061	27	30	.0042
	30	.0345	16	0	.010	28	30	.0066
5	0	.0465		30	.013	30	30	.0086
	30	.058	17	0	.0171	31	0	.0103
6	0	.069		30	.0215		30	.0123
	30	.077	18	0	.0272	32	0	.0152
7	0	.085		30	.033		30	.0185
	30	.090	19	0	.040	33	0	.0222
8	30	.095		30	.0465		30	.0263

Table V-9b. (continued)

20	0	.053	34	0	.031
	30	.0595		30	.0355
21	0	.065	35	0	.0405
	30	.070		30	.0475
22	0	.075	36	0	.0515
23	0	.079		30	.0565
24	0	.086	37	0	.060
25	0	.090		30	.063
			38	0	.0675
				30	.070
			39	0	.072
			40	0	.077
			41	0	.080
			42	0	.083
			43	0	.087
			44	0	.089
			45	0	.091

Table V-10a. Dispersion measurements, P_{421}, V_m = cm/min.

Position 1			Position 2			Position 3		
Time in min.	sec.	Concent. in Normal	Time in min.	sec.	Concent. in Normal	Time in min.	sec.	Concent. in Normal
0	0	.001	0	0	.001	0	0	.001
	45	.0087	3	15	.001	13	45	.0037
1	15	.0175	5	30	.0019	15	45	.0075
	30	.0245	6	30	.0032	17	0	.0113
	45	.0325	8	0	.007	18	0	.0125
2	0	.0435	9	0	.0125	19	0	.0165
	15	.053	10	0	.0165	20	0	.0223
	30	.062		30	.0207	21	0	.030
	45	.069	11	0	.0265		30	.034
3	0	.073		30	.0323	22	0	.040
	30	.086	12	0	.040		30	.044
4	0	.094		30	.047	23	0	.050
			13	0	.057		30	.055
				30	.064	24	0	.060
			14	0	.0705		30	.066
				30	.077	25	0	.071
			15	0	.0825	25	30	.076
				30	.0875	26	0	.0795
			16	0	.090	27	0	.088
				30	.093	28	0	.094
			17	30	.096			

Table V-10b. Dispersion measurements, P_{422}, V_m = cm/min.

Position 1			Position 2			Position 3		
Time in min.	sec.	Concent. in Normal	Time in min.	sec.	Concent. in Normal	Time in min.	sec.	Concent. in Normal
0	0	.002	0	0	.001	0	0	.001
	30	.0028	3	15	.0012	9	15	.0019
1	0	.0085	4	15	.0018	10	15	.0029
	30	.0175	5	30	.004	11	15	.0045
2	0	.034	6	30	.0081	12	15	.0069
	15	.044	7	30	.0157	13	15	.0103
	30	.053	8	30	.023	14	30	.0138
3	0	.0675	9	0	.030	15	30	.0195
	30	.079		30	.0385	16	0	.0235
4	0	.085	10	0	.0465		30	.0273
5	0	.095		30	.054	17	0	.0325
			11	0	.062		30	.0375
				30	.069	18	0	.044
			12	0	.076		30	.0495
				30	.081	19	0	.055
			13	0	.086		30	.0605
			14	0	.096	20	0	.067
							30	.072
						21	30	.080
						22	0	.085
						23	0	.091
						24	0	.096

Table V-11a. Dispersion measurements, N_{11}, V_m = 0.40 cm/min.

Position 1			Position 2			Position 3		
Time in min.	sec.	Concent. in Normal	Time in min.	sec.	Concent. in Normal	Time in min.	sec.	Concent. in Normal
0	0	.001	0	0	.001	0	0	.001
	30	.0045	6	30	.0013	14	15	.0011
1	0	.0057	7	30	.002	15	15	.0012
	30	.0085	8	30	.004	16	30	.0016
	45	.0146	9	0	.0055	17	30	.0025
2	0	.0235	10	0	.0079	18	30	.0033
	15	.0355	11	0	.017	19	0	.004
	30	.0445		30	.0245	20	0	.0048
	45	.0505		45	.029		30	.0056
3	0	.054	12	0	.034	21	0	.0071
	30	.063		15	.039		30	.0093
4	0	.068	12	30	.044	22	0	.0118
5	0	.077		45	.049		30	.0158
6	0	.081	13	0	.0535		45	.018
7	0	.083		30	.061	23	0	.0195

Table V-11a. (continued)

14	0	.067		30	.0235
	30	.070	24	0	.0285
15	0	.0725		30	.035
16	0	.074	25	0	.042
				30	.049
			26	0	.056
				30	.066
			27	0	.067
			28	0	.077

Table V-11b. Dispersion measurements, N_{12}, V_m = .472 cm/min.

Position 1			Position 2			Position 3		
Time in min.	sec.	Concent. in Normal	Time in min.	sec.	Concent. in Normal	Time in min.	sec.	Concent. in Normal
0	0	.001	0	0	.001	0	0	.001
	30	.003	4	15	.0011	11	15	.0011
1	0	.0049	5	30	.0016	13	15	.0018
	15	.0082	8	0	.0089	14	30	.003
	30	.0113		30	.013	16	0	.0048
	45	.0195	9	0	.0187		30	.006
2	0	.034		30	.0267	17	0	.0076
	15	.043	10	0	.035		30	.0097
	30	.0565		30	.046	18	0	.0121
3	0	.074	11	0	.054		30	.0151
	30	.082		45	.070	19	0	.019
4	0	.087	12	0	.074		30	.0235
	30	.090		30	.080	20	30	.0375
5	0	.093	13	0	.085	21	0	.041
6	0	.095	14	0	.088		30	.0485
			15	0	.090	22	0	.055
				45	.091		30	.062
						23	0	.067
							30	.071
						24	0	.076
						25	0	.0815
						26	0	.0865
						27	0	.0895

Table V-11c. Dispersion measurements, N_{13}, V_m = .641 cm/min.

Position 1			Position 2			Position 3		
Time in min.	sec.	Concent. in Normal	Time in min.	sec.	Concent. in Normal	Time in min.	sec.	Concent. in Normal
0	0	.001	0	0	.001	0	0	.001
	15	.0021	2	45	.001	8	45	.0012
	30	.0031	4	15	.0016	10	15	.0026
	45	.0042	5	0	.0037		45	.0035
1	0	.0076		30	.0064	11	30	.0057
	15	.0145	6	0	.009	12	30	.0092
	30	.028		30	.0157	13	30	.0182
	45	.045	7	0	.025	14	0	.025
2	0	.062		30	.0375		30	.034
	15	.073	8	0	.052	15	0	.043
	30	.081		30	.064		30	.0535
3	0	.090	9	0	.078	16	0	.0625
				30	.084		30	.071
			10	0	.090	17	0	.077
			11	0	.093	18	0	.085
						19	0	.0895
						20	0	.0905

Table V-11d. Dispersion measurements, N_{21}, V_m = .565 cm/min.

Position 1			Position 2			Position 3		
Time in min.	sec.	Concent. in Normal	Time in min.	sec.	Concent. in Normal	Time in min.	sec.	Concent. in Normal
0	0	.001	0	0	.001	0	0	.001
	15	.0025	3	45	.0012	10	45	.0023
	30	.0028	4	15	.0015	11	30	.0035
	45	.003	5	15	.0021	12	30	.0071
1	0	.0033		45	.0028	13	30	.0107
	30	.0042	6	45	.0055		45	.013
2	0	.0053	7	30	.0135	14	0	.0152
	30	.0163		45	.0178		15	.018
	45	.0265	8	0	.0235		30	.0215
3	0	.041		15	.0295		45	.0253
	15	.057		30	.0365	15	0	.0295
	30	.065		45	.044		15	.034
4	0	.083	9	0	.050		30	.0395
	30	.090		15	.057		45	.045
5	0	.093		30	.065	16	0	.051
	30	.095		45	.070		15	.056
			10	0	.077		30	.061
				30	.083		45	.067
			11	0	.088	17	0	.0715
			12	0	.092		15	.074

Table V-11d. (continued)

	30	.077
18	0	.079
19	0	.0855
20	0	.089
21	0	.093

Table V-11e. Dispersion measurements, N_{22}, V_m = .321 cm/min.

Position 1			Position 2			Position 3		
Time in min.	sec.	Concent. in Normal	Time in min.	sec.	Concent. in Normal	Time in min.	sec.	Concent. in normal
0	0	.0019	0	0	.001	0	0	.001
	30	.0027	6	45	.0011	13	15	.001
1	0	.0032	9	0	.0017	18	30	.0017
	30	.0035	10	0	.0022	19	30	.0022
2	0	.0039		30	.003	20	30	.0031
	30	.0047	11	0	.0043	21	0	.0036
3	30	.0081	12	0	.0068	22	30	.0052
4	0	.0175		30	.0098	23	0	.0064
	15	.026	13	0	.014		30	.008
	30	.035		30	.020	24	0	.010
	45	.0455	14	0	.0263		30	.0127
5	0	.0575		15	.031	25	0	.016
5	15	.066	14	30	.0365	25	30	.020
	30	.072		45	.0415	26	0	.0248
	45	.075	15	0	.047		30	.030
6	0	.077		30	.058	27	0	.037
	30	.080	16	0	.067		30	.0445
				30	.075	28	0	.053
			17	0	.083		30	.060
				30	.089	29	0	.065
			18	0	.092	30	0	.075
						31	0	.083
						32	0	.090
						33	0	.092

Table V-11f. Dispersion measurements, N_{23}, V_m = .49 cm/min.

Position 1			Position 2			Position 3		
Time in min.	sec.	Concent. in Normal	Time in min.	sec.	Concent. in Normal	Time in min.	sec.	Concent. in Normal
0	0	.001	0	0	.001	0	0	.001
	30	.0026	4	15	.0011	11	15	.0011
1	0	.0029	5	0	.0013	13	0	.002
	30	.0036	6	0	.0018	14	0	.0032
2	0	.0055	7	0	.0029		45	.0048
	30	.0073		30	.0043	16	0	.0075
3	0	.019	8	30	.0084		30	.010
	15	.0315	9	0	.0137	17	0	.013
	30	.044		30	.0243		30	.0176
	45	.057	10	15	.039	18	0	.0225
4	0	.065		45	.0505		30	.030
	30	.074	11	0	.059	19	0	.037
5	30	.084		30	.069		30	.046
			12	0	.076	20	0	.054
				45	.088		30	.064
						21	0	.070
							30	.076
						22	0	.082
						23	0	.085

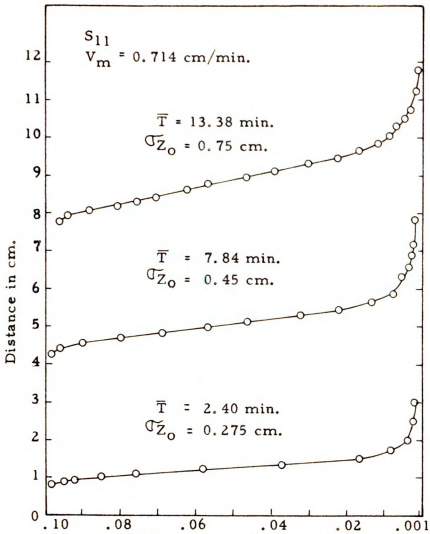

Figure V-1a. Break through curves for S_{11}.

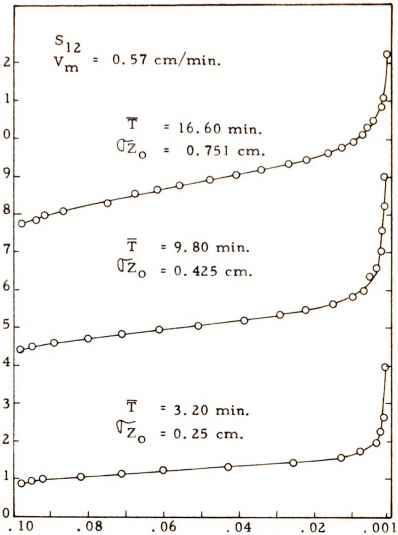

Figure V-1b. Break through curves for S_{12}.

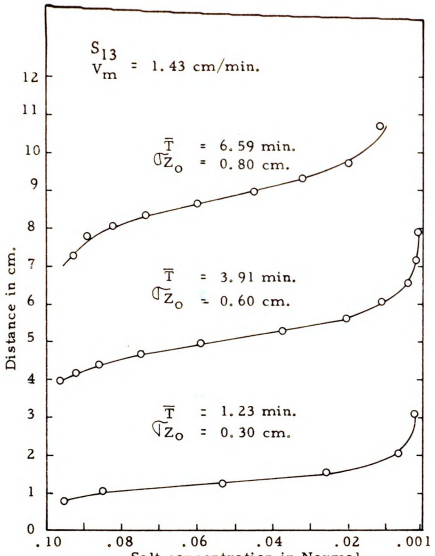

Figure V-1c. Break through curves for S_{13}.

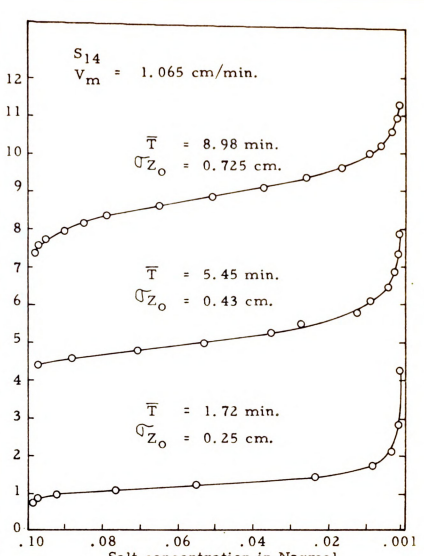

Figure V-1d. Break through curves for S_{14}.

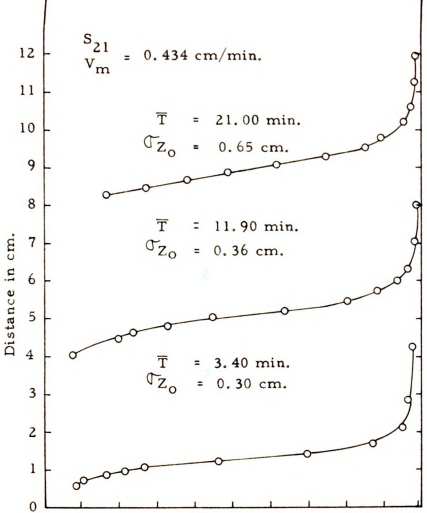

Figure V-1e. Break through curves for S_{21}.

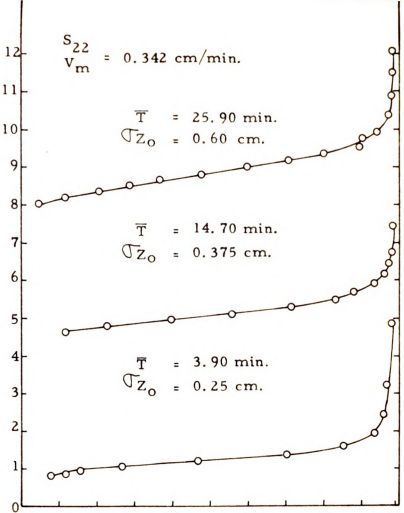

Figure V-1f. Break through curves for S_{22}.

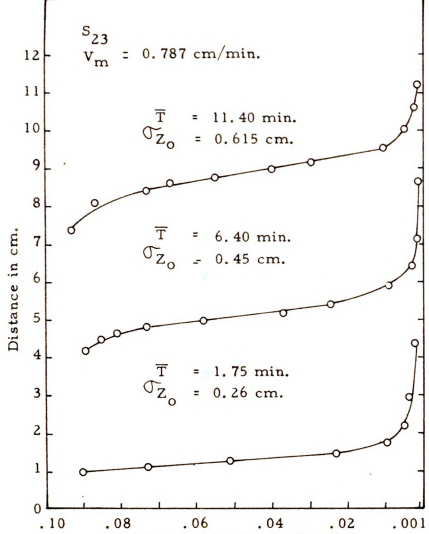

Figure V-1g. Break through curves for S_{23}.

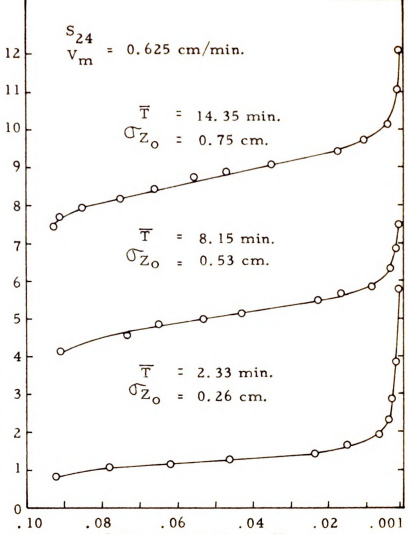

Figure V-1h. Break through curves for S_{24}.

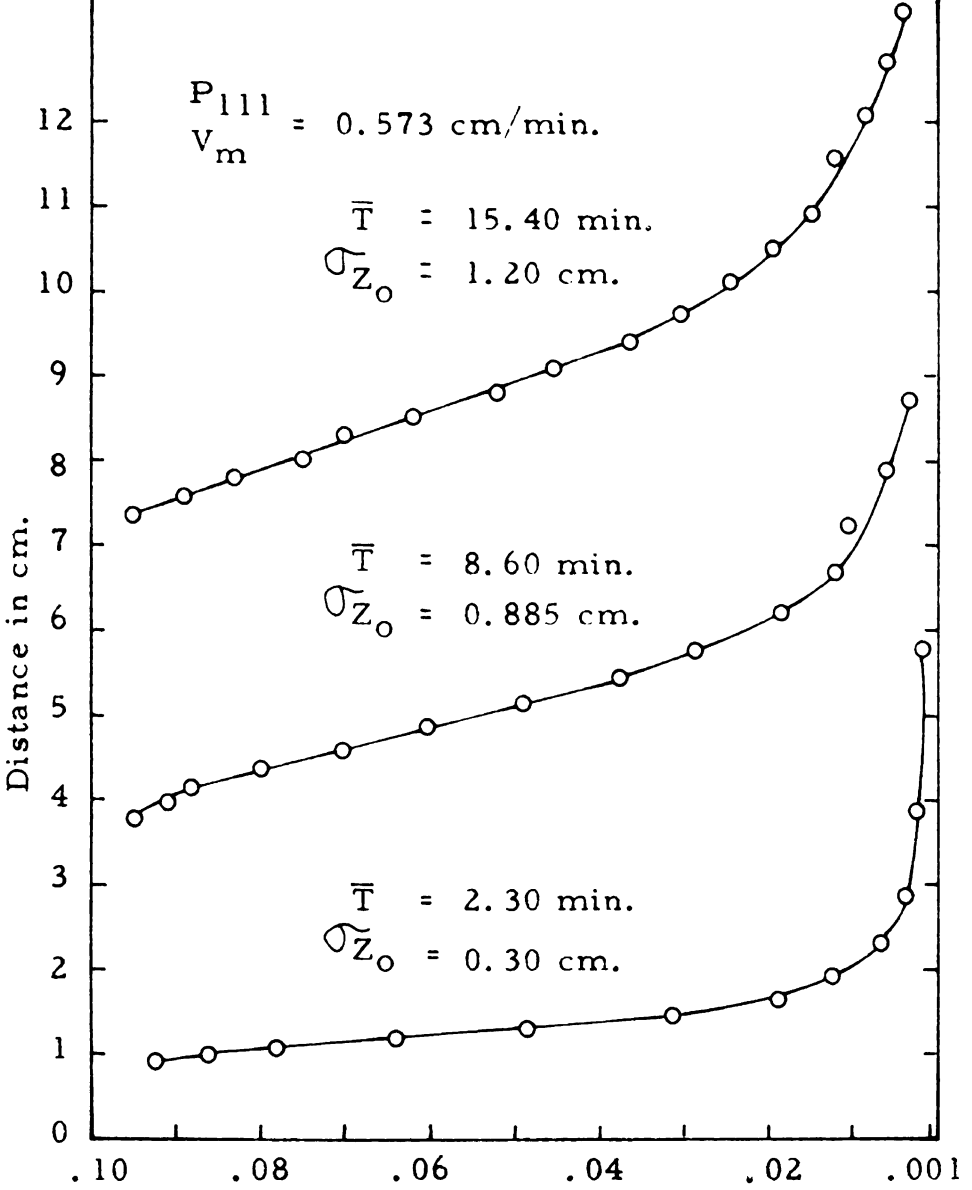

Figure V-2a. Break through curves for P_{111}.

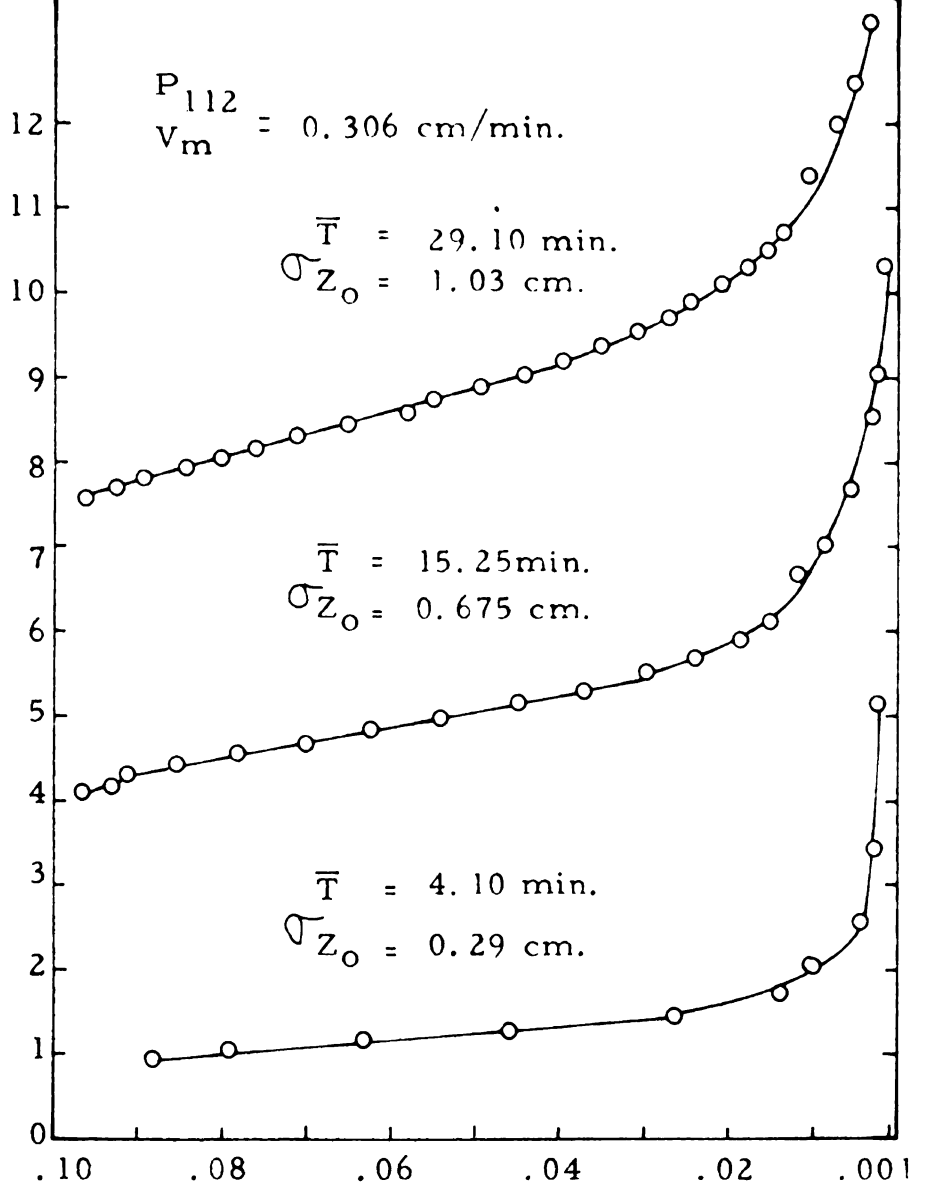

Figure V-2b. Break through curves for P_{112}.

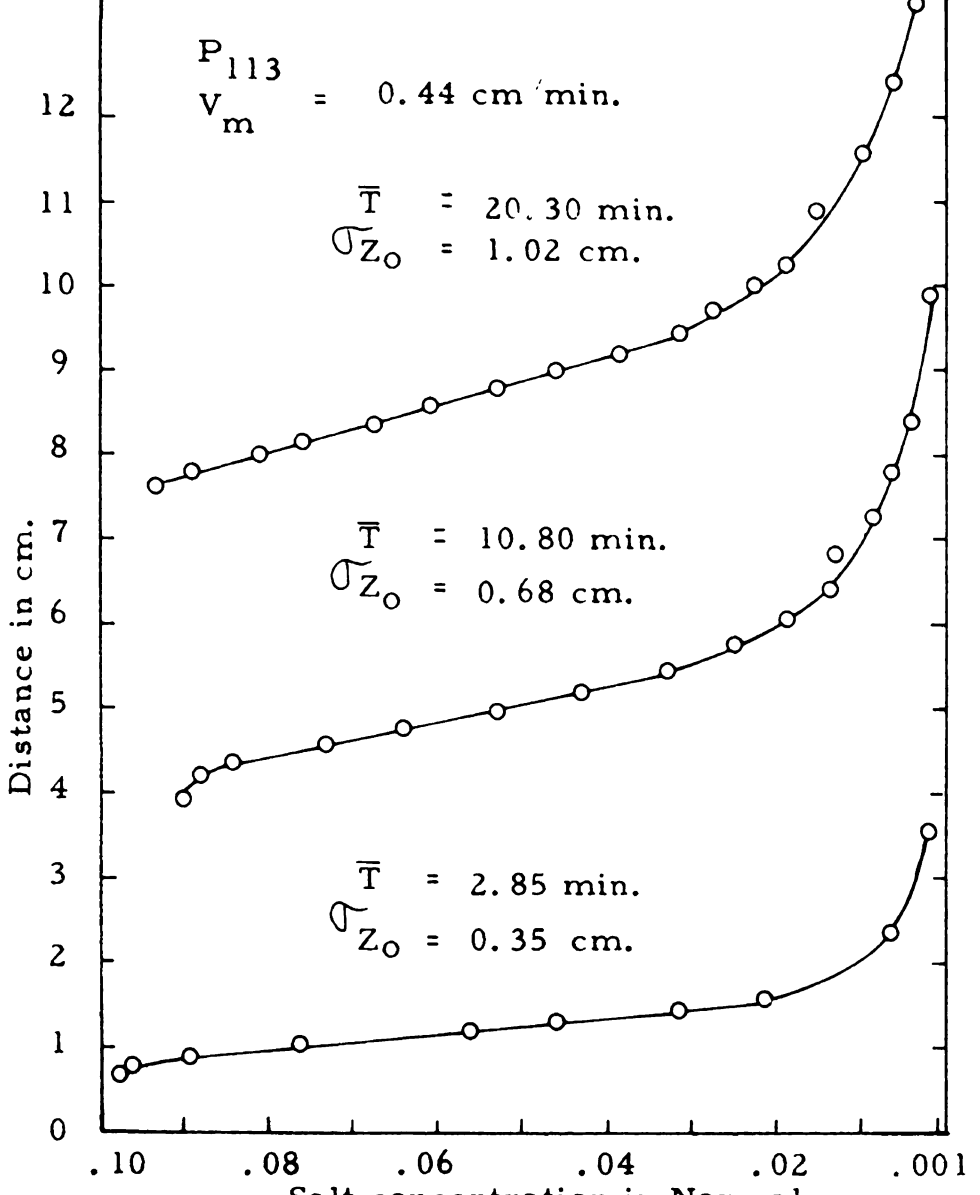

Figure V-2c. Break through curves for P_{113}.

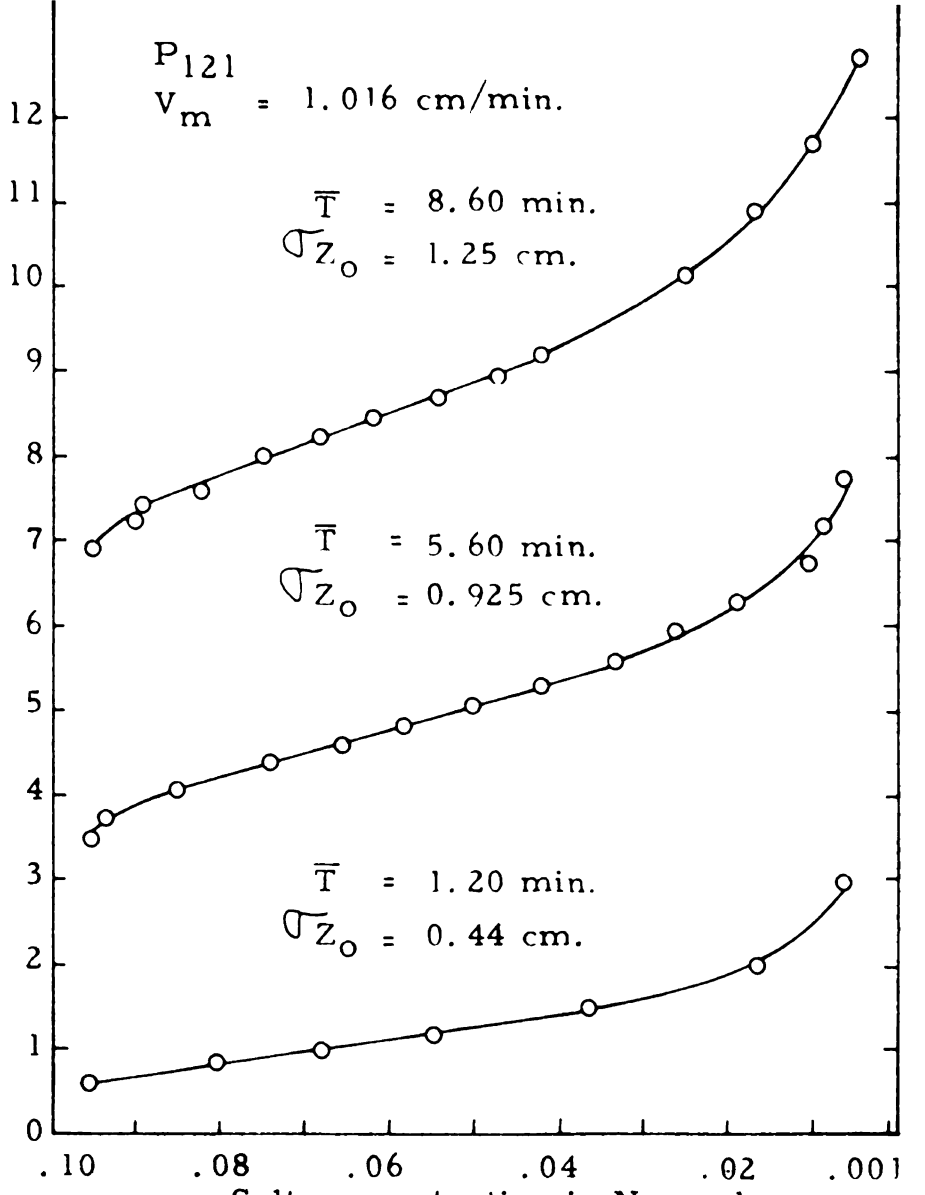

Figure V-3a. Break through curves for P_{121}.

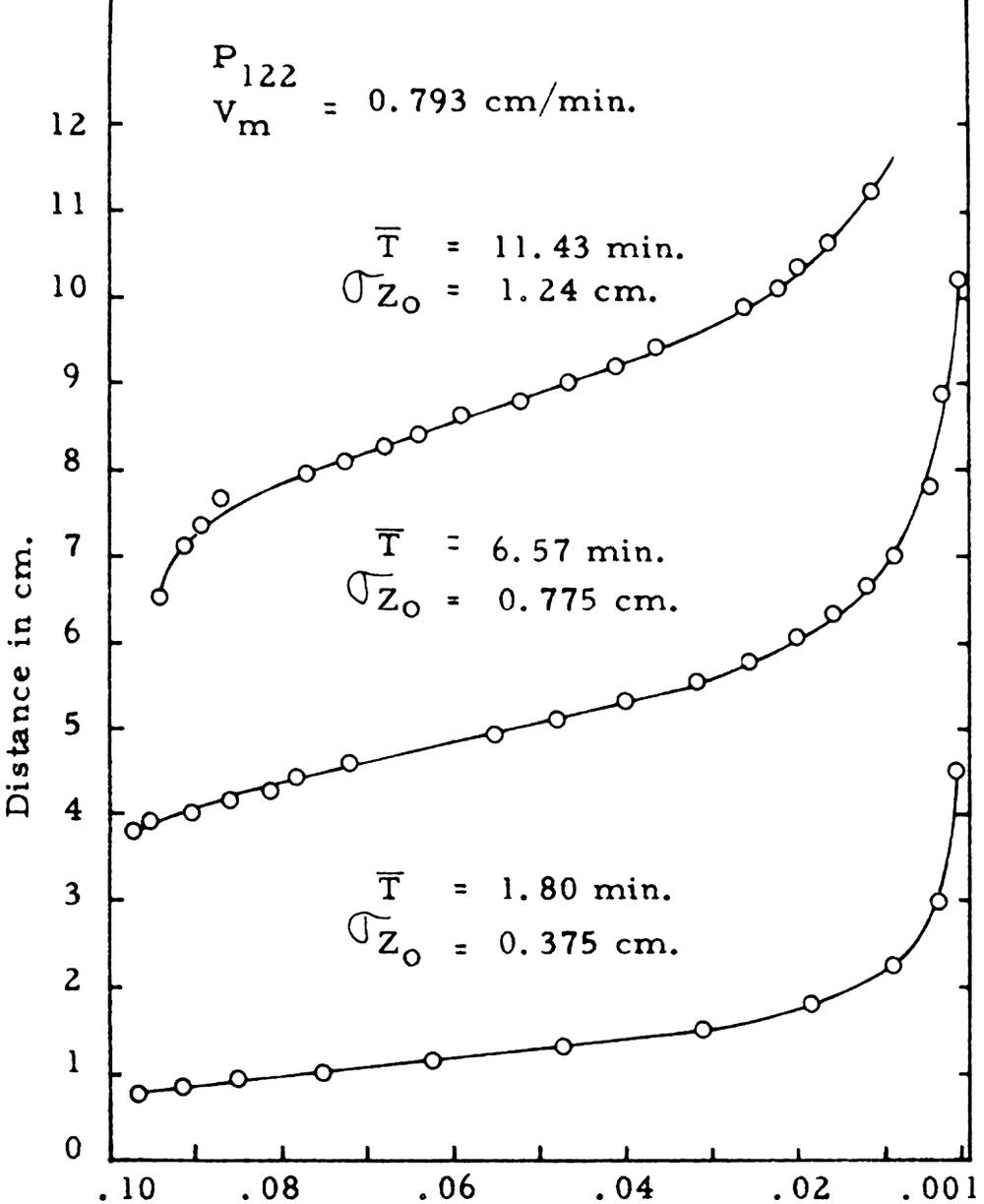

Figure V-3b. Break through curves for P_{122}.

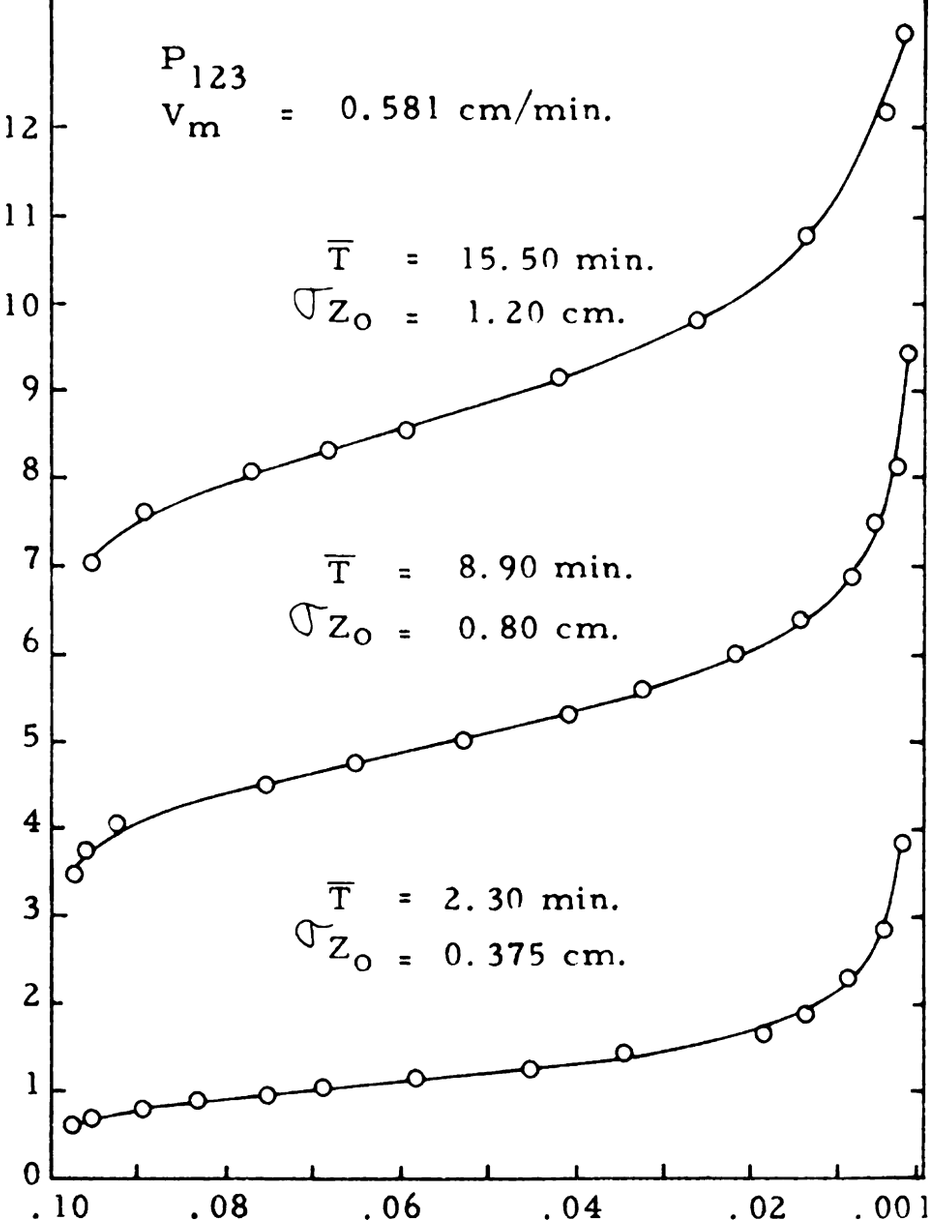

Figure V-3c. Break through curves for P_{123}.

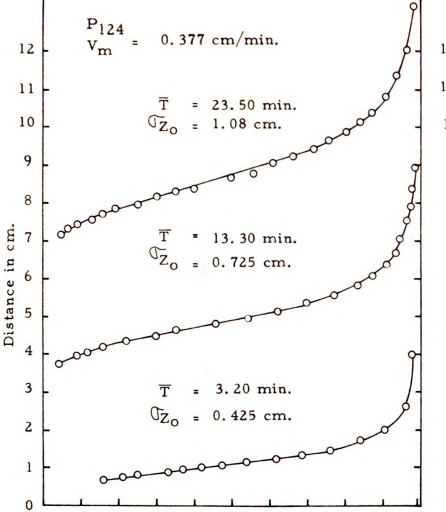

Figure V-3d. Break through curves for P_{124}.

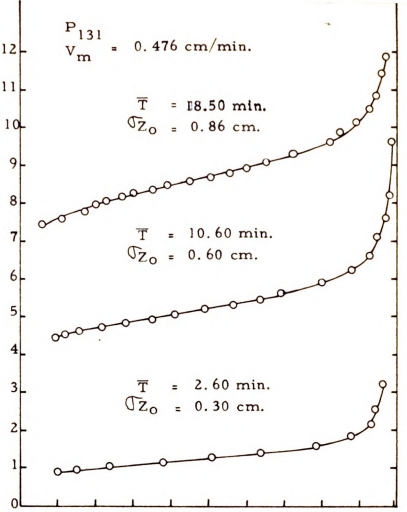

Figure V-4a. Break through curves for P_{131}.

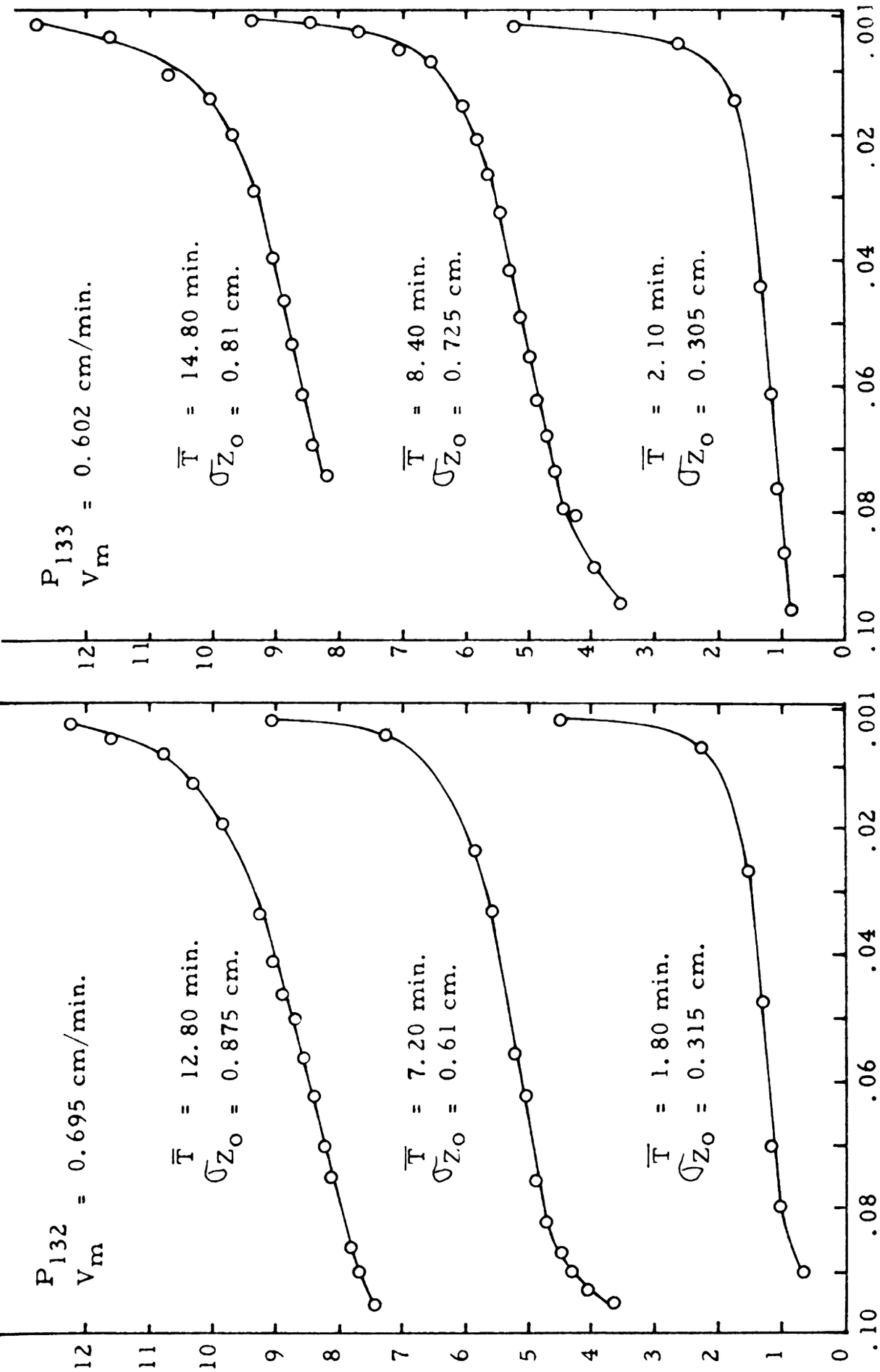

Figure V-4b. Break through curves for P_{132}.

Figure V-4c. Break through curves for P_{133}.

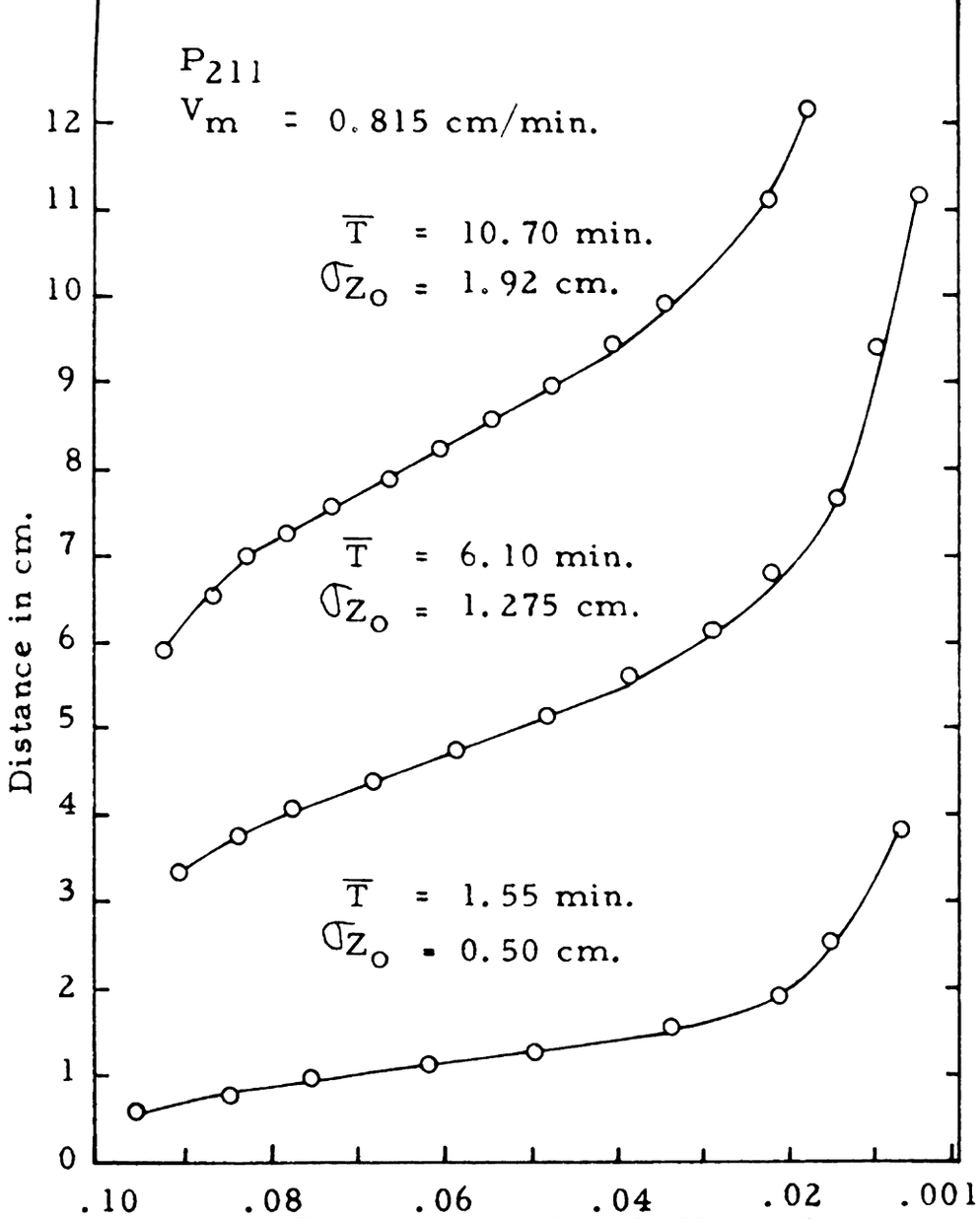

Figure V-5a. Break through curves for P_{211}.

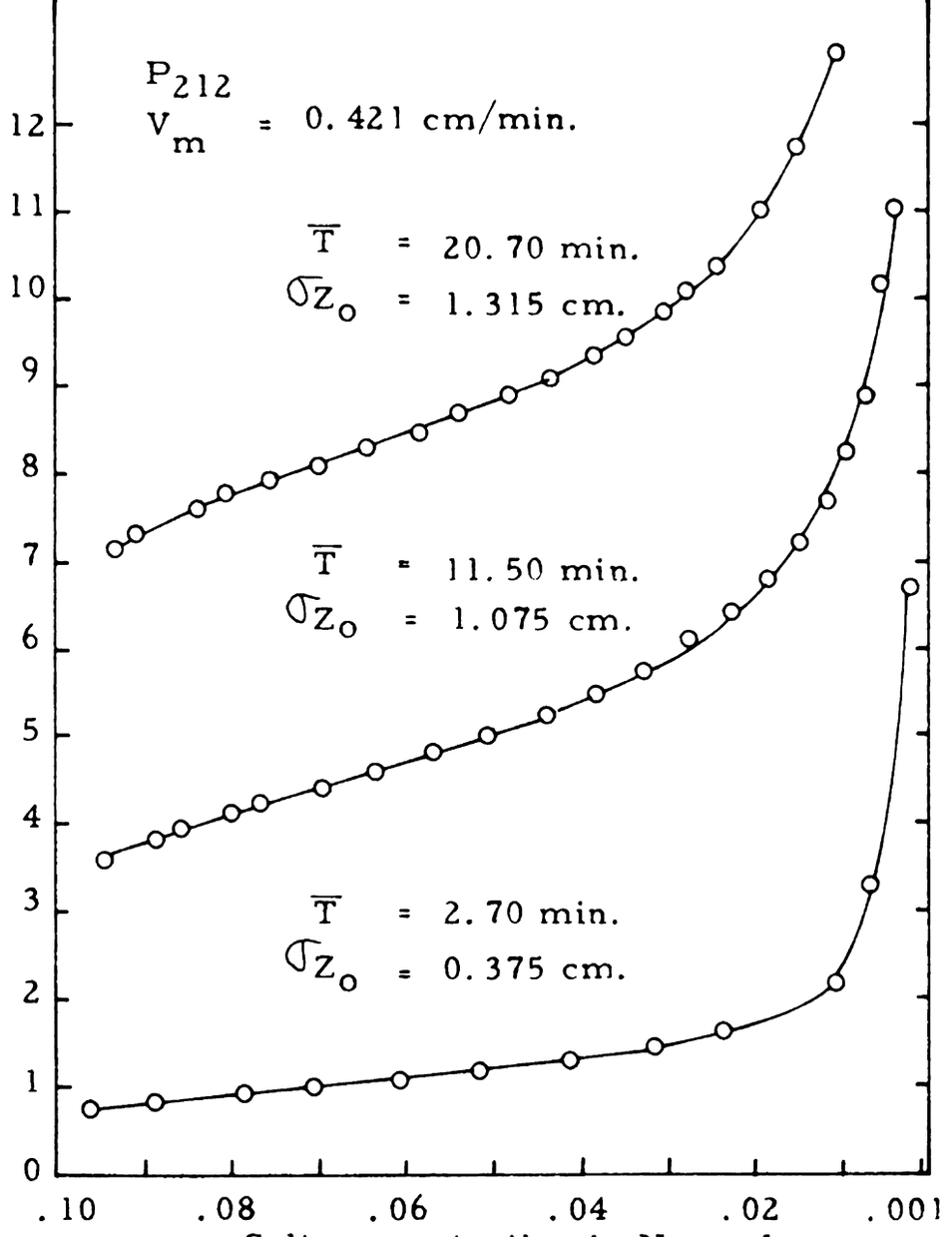

Figure V-5b. Break through curves for P_{212}.

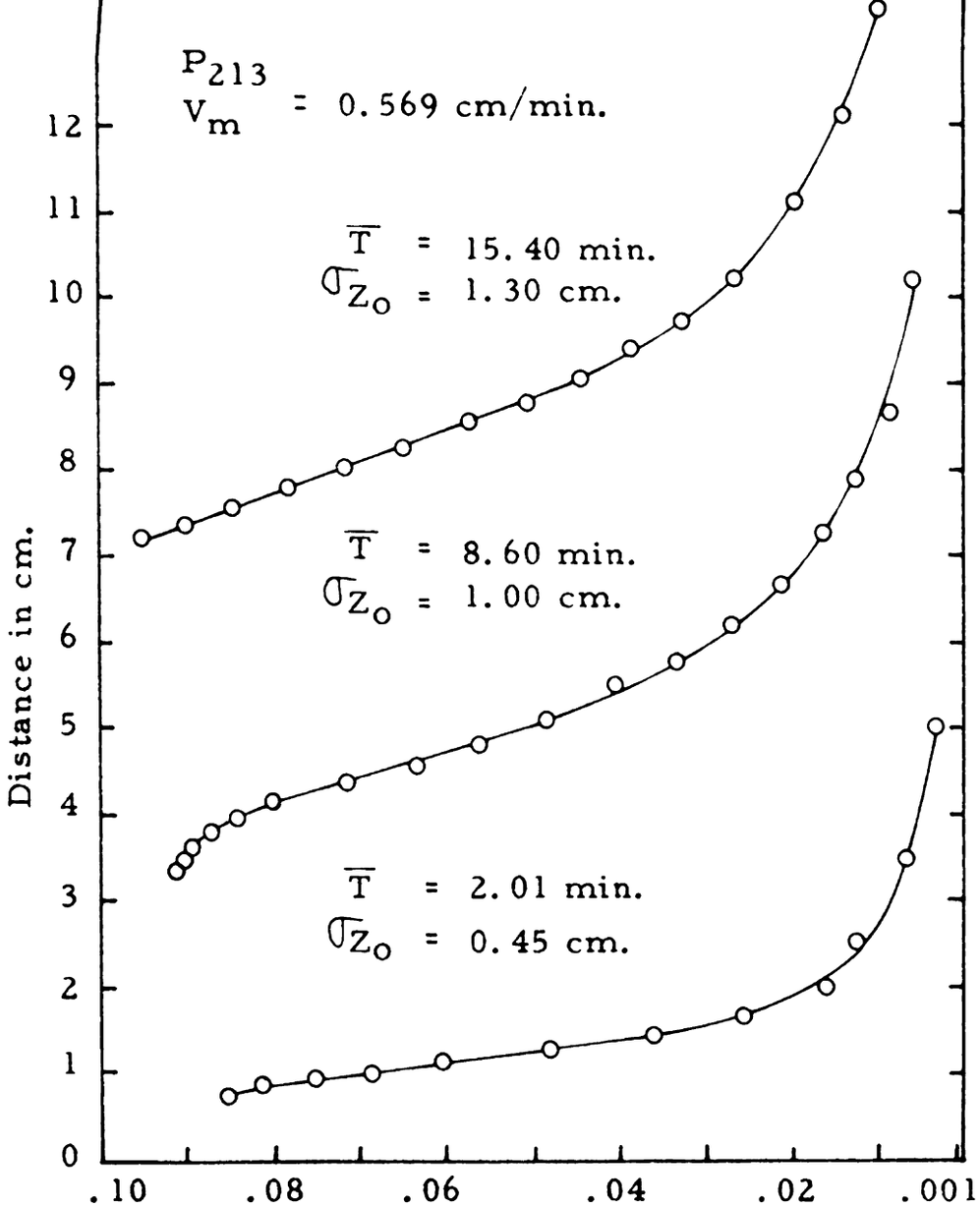

Figure V-5c. Break through curves for P_{213}.

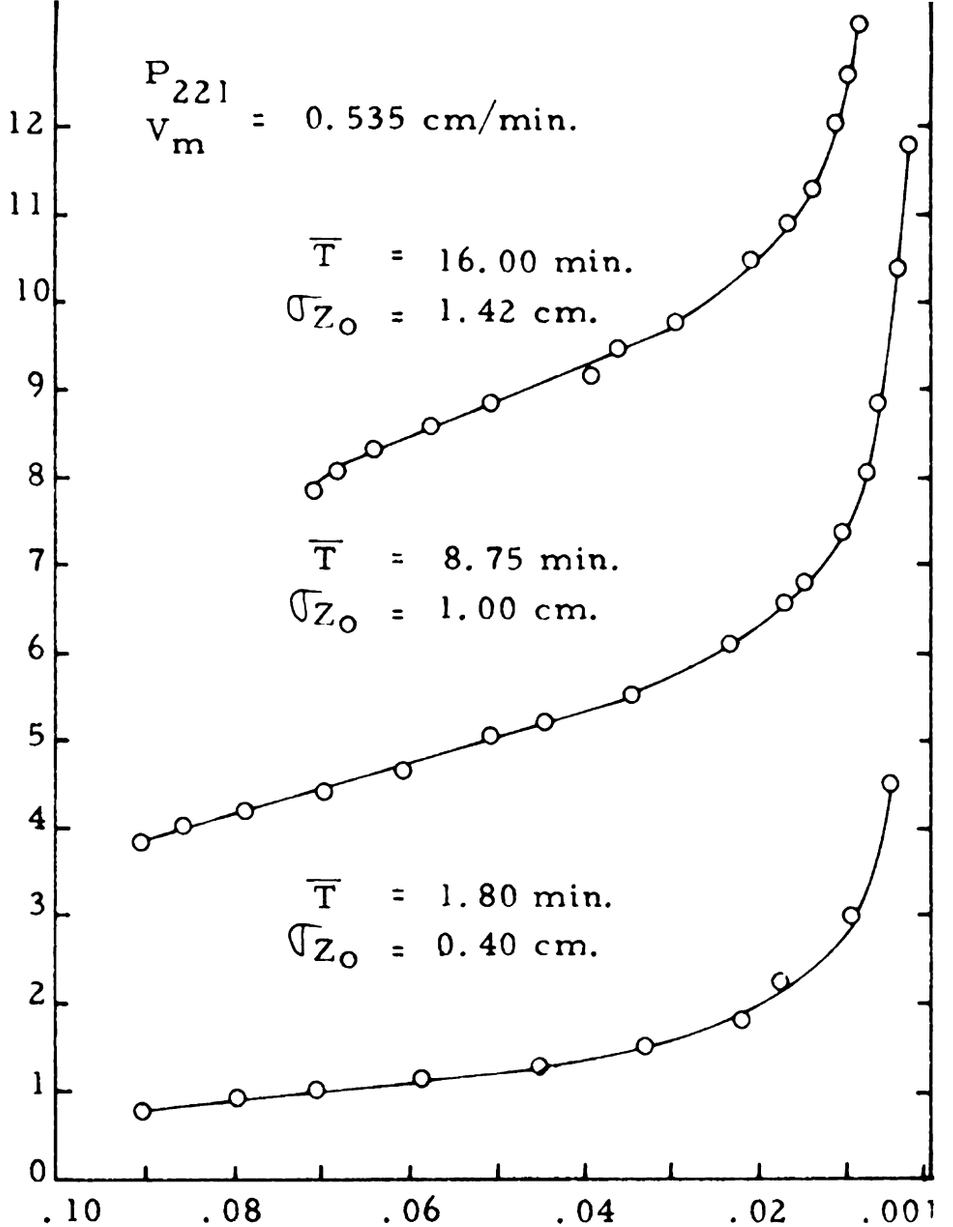

Figure V-6a. Break through curves for P_{221}.

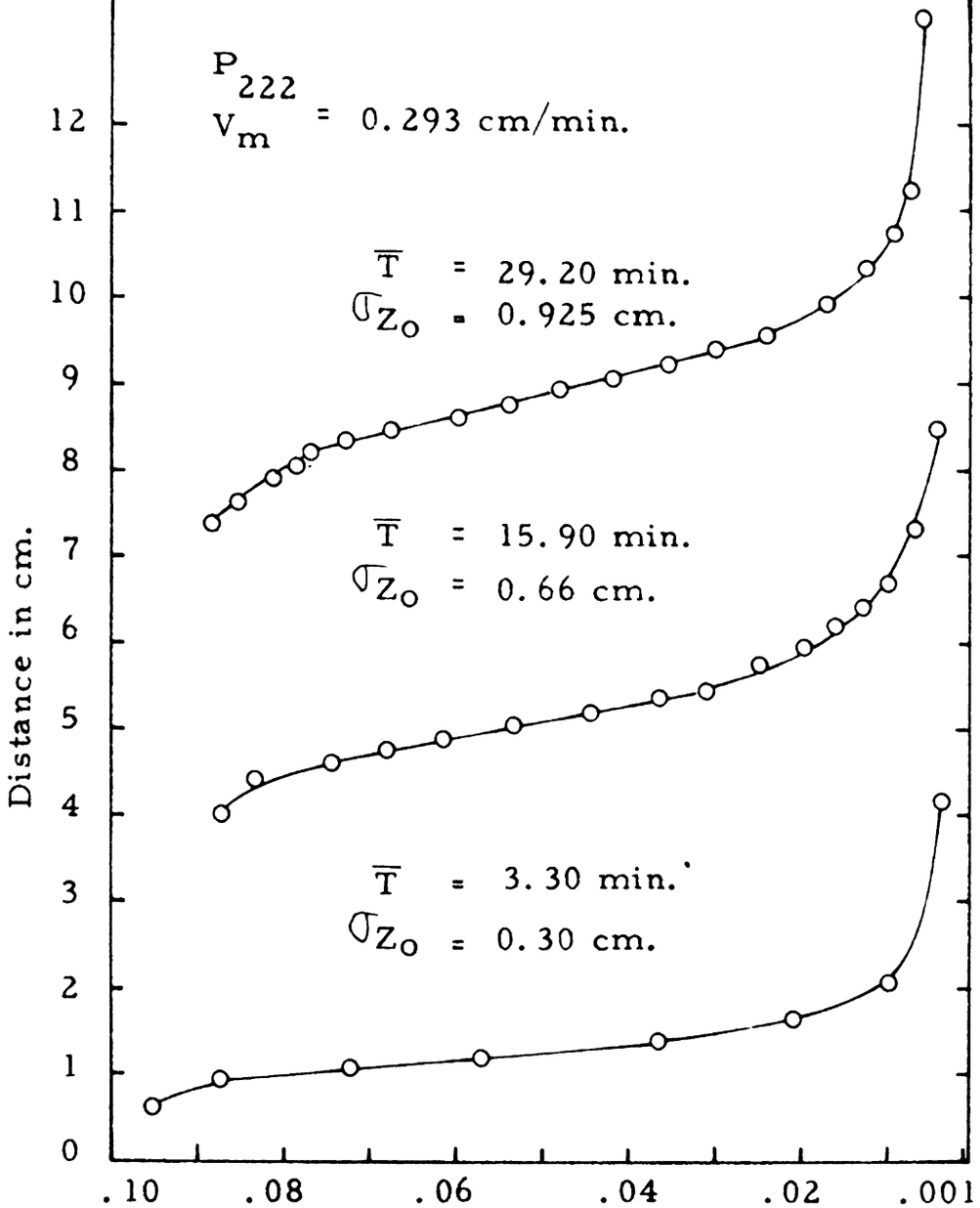

Figure V-6b. Break through curves for P_{222}.

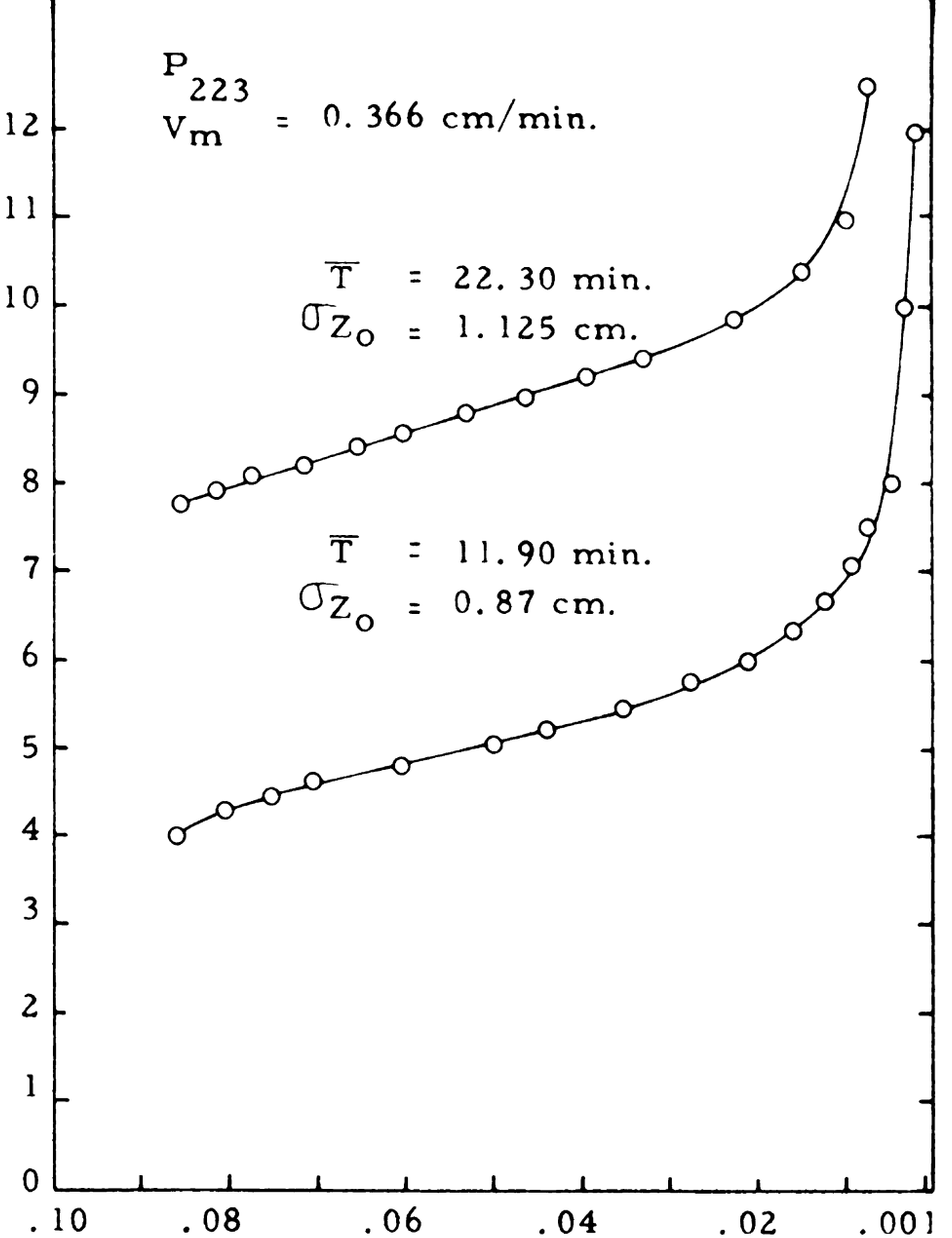

Figure V-6c. Break through curves for P_{223}.

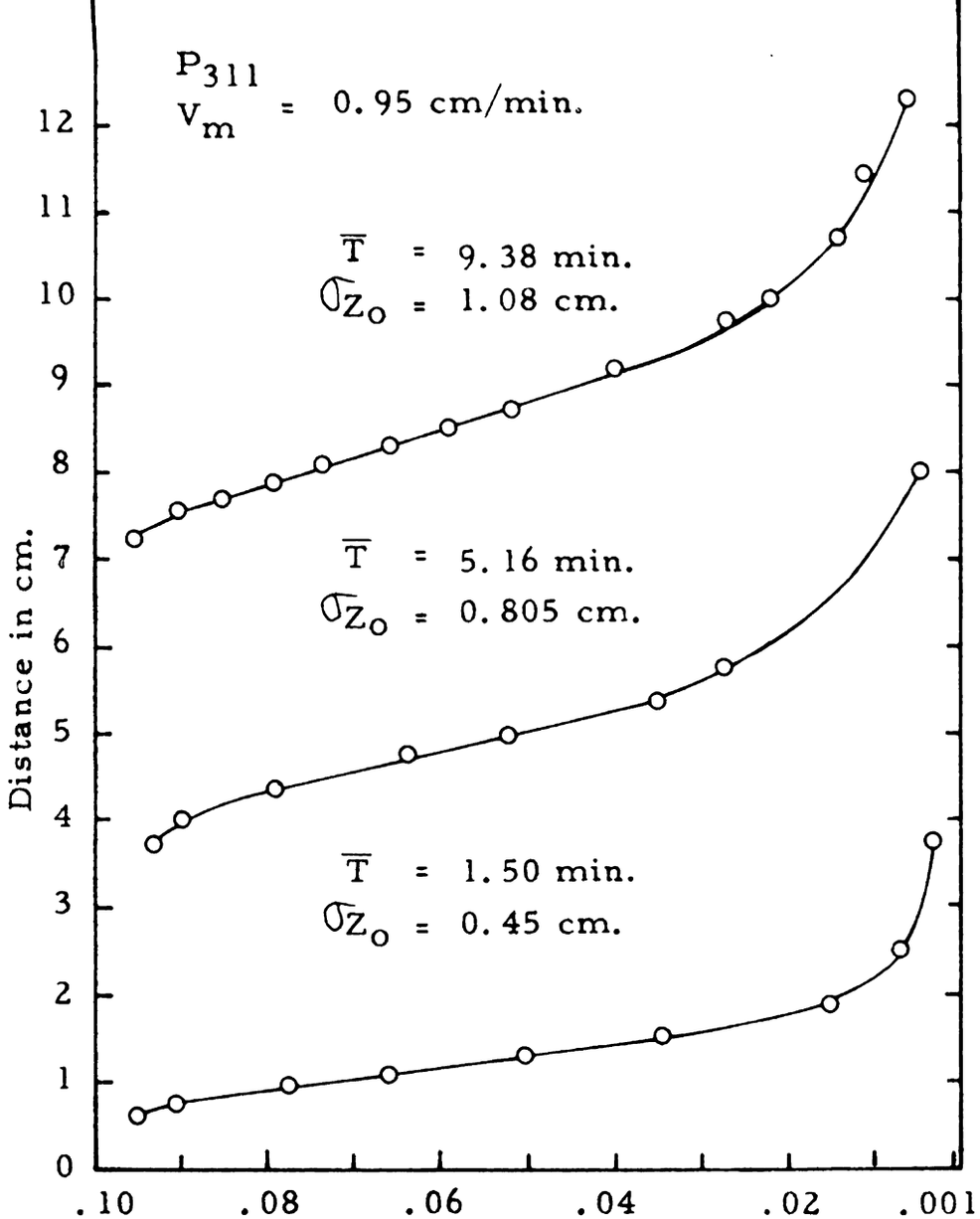

Figure V-7a. Break through curves for P_{311}.

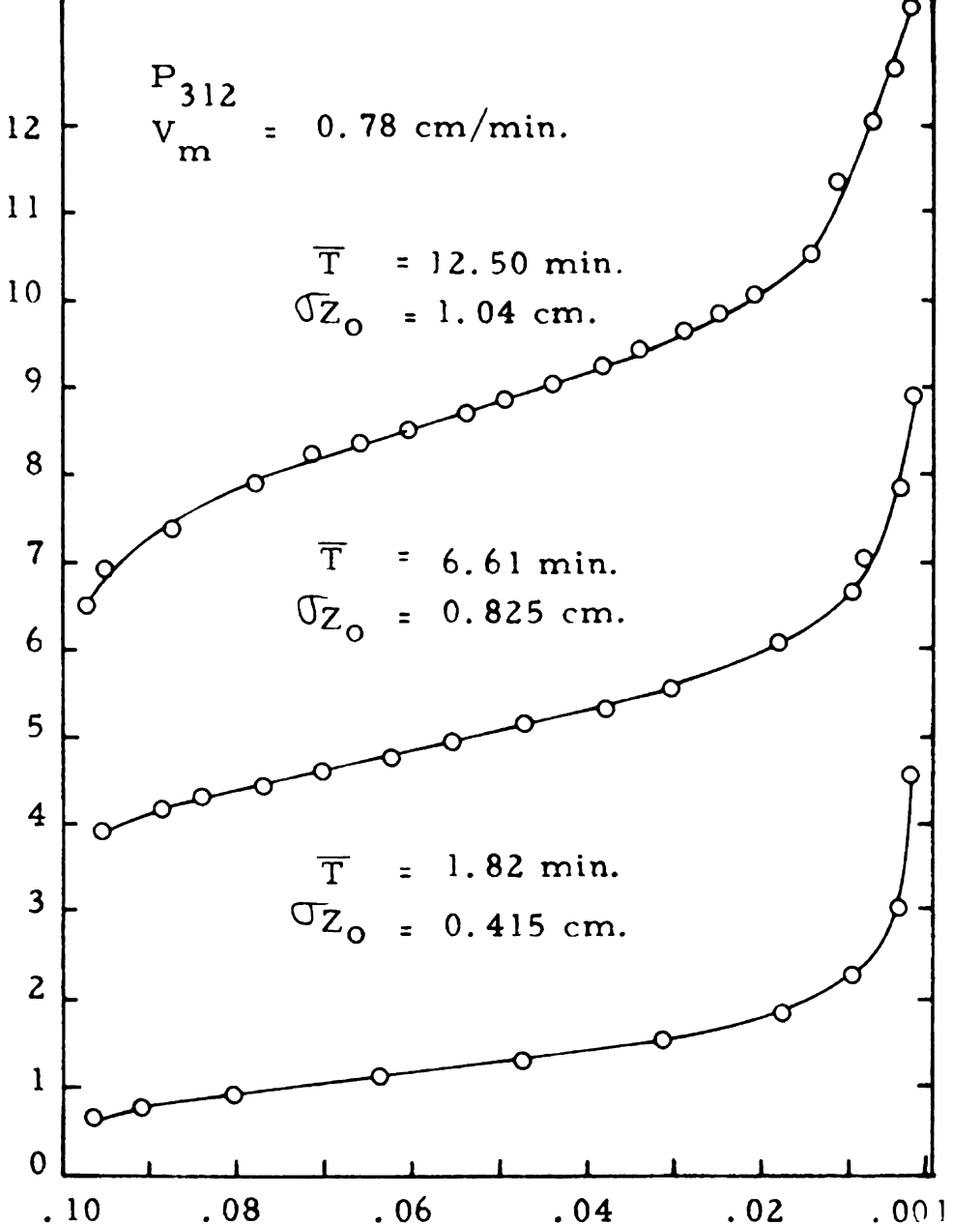

Figure V-7b. Break through curves for P_{312}.

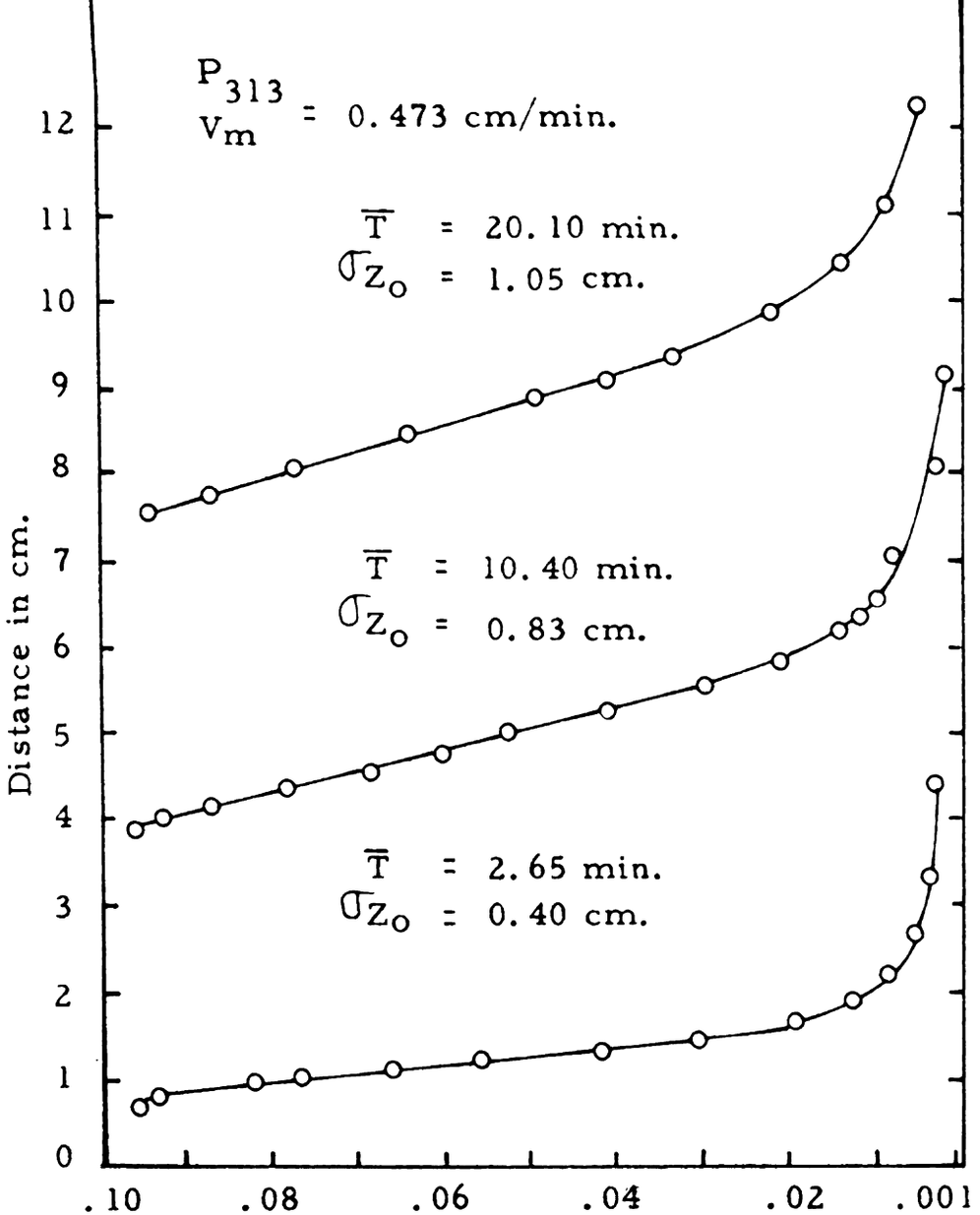

Figure V-7c. Break through curves for P_{313}.

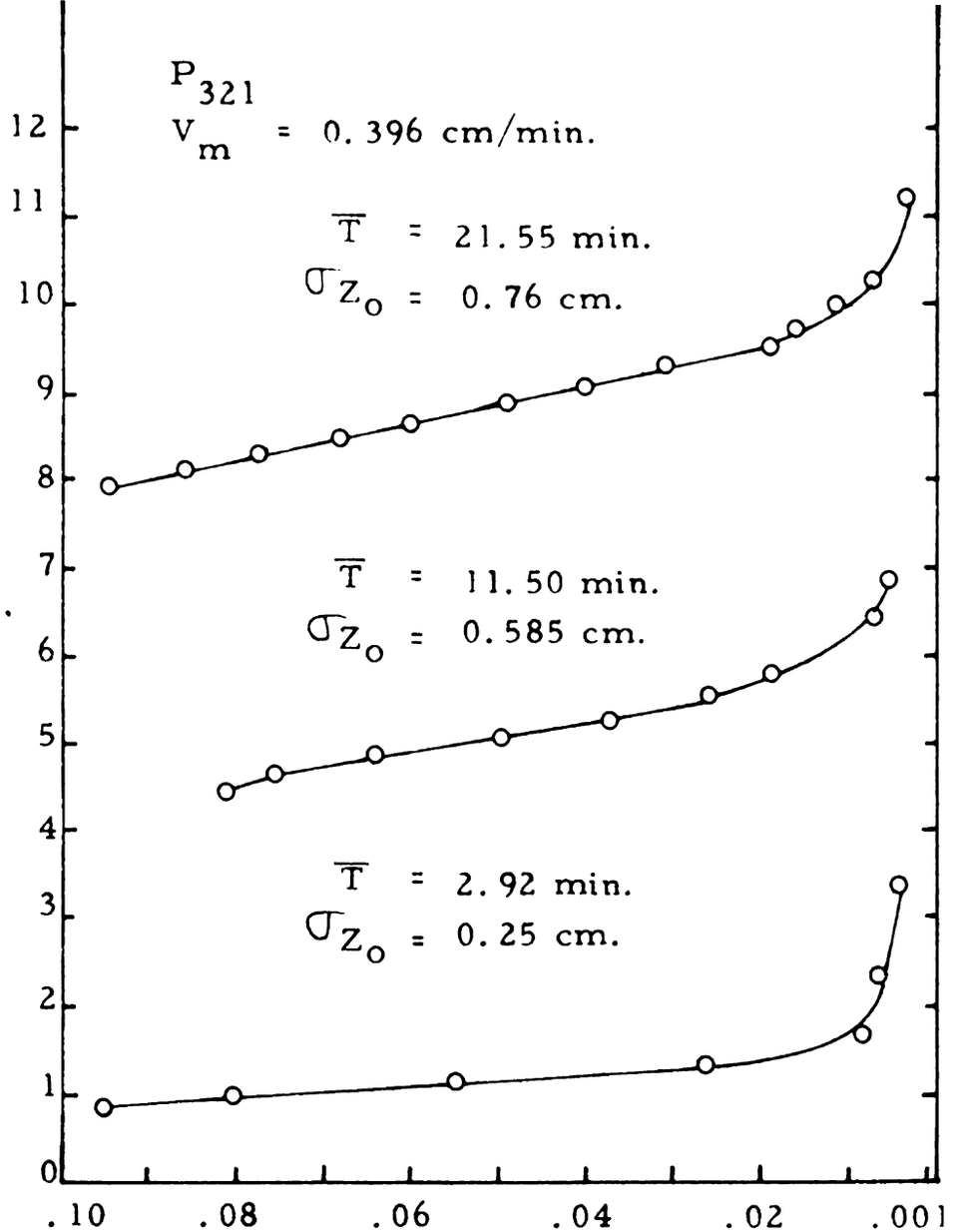

Figure V-8a. Break through curves for P_{321}.

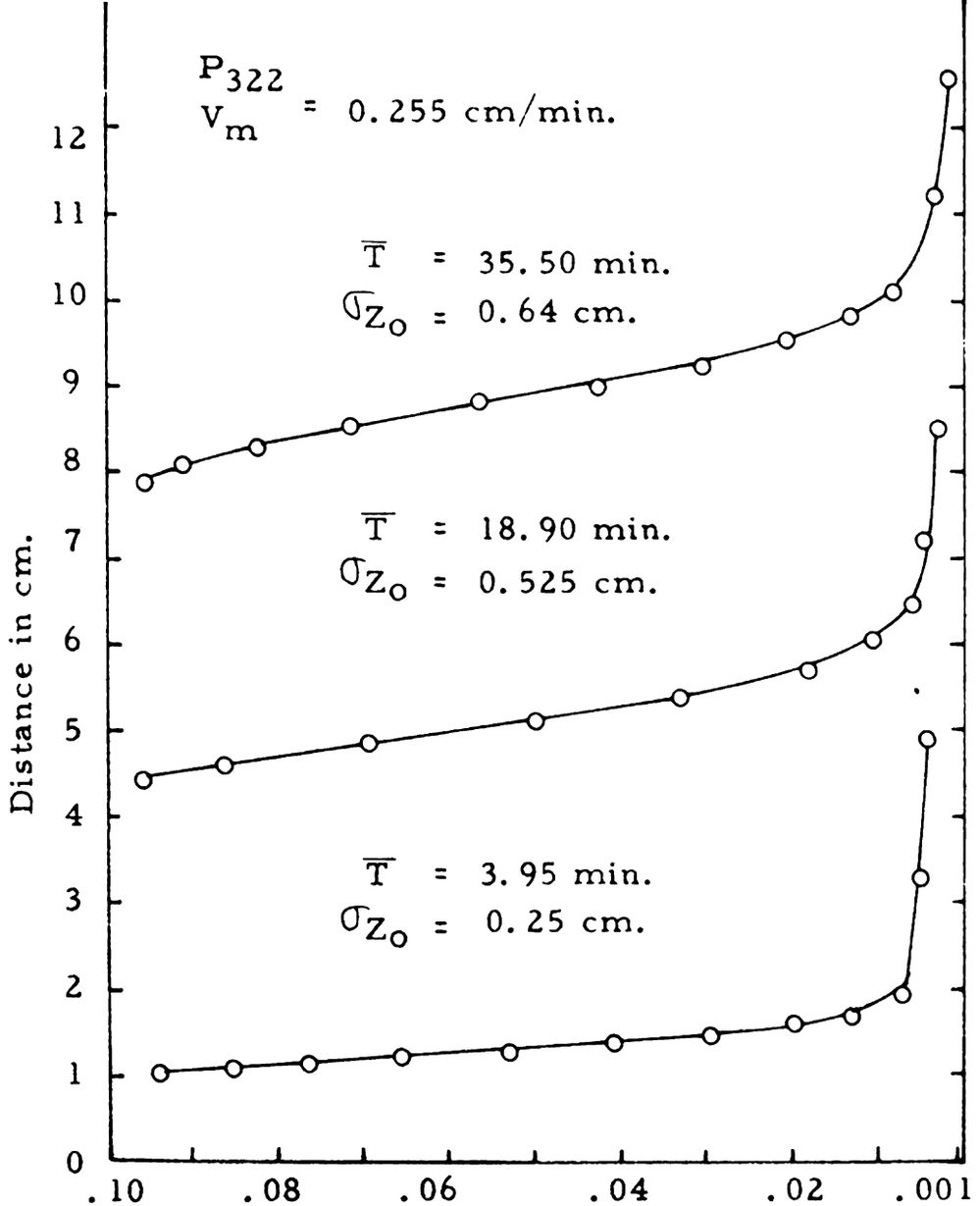

Figure V-8b. Break through curves for P_{322}.

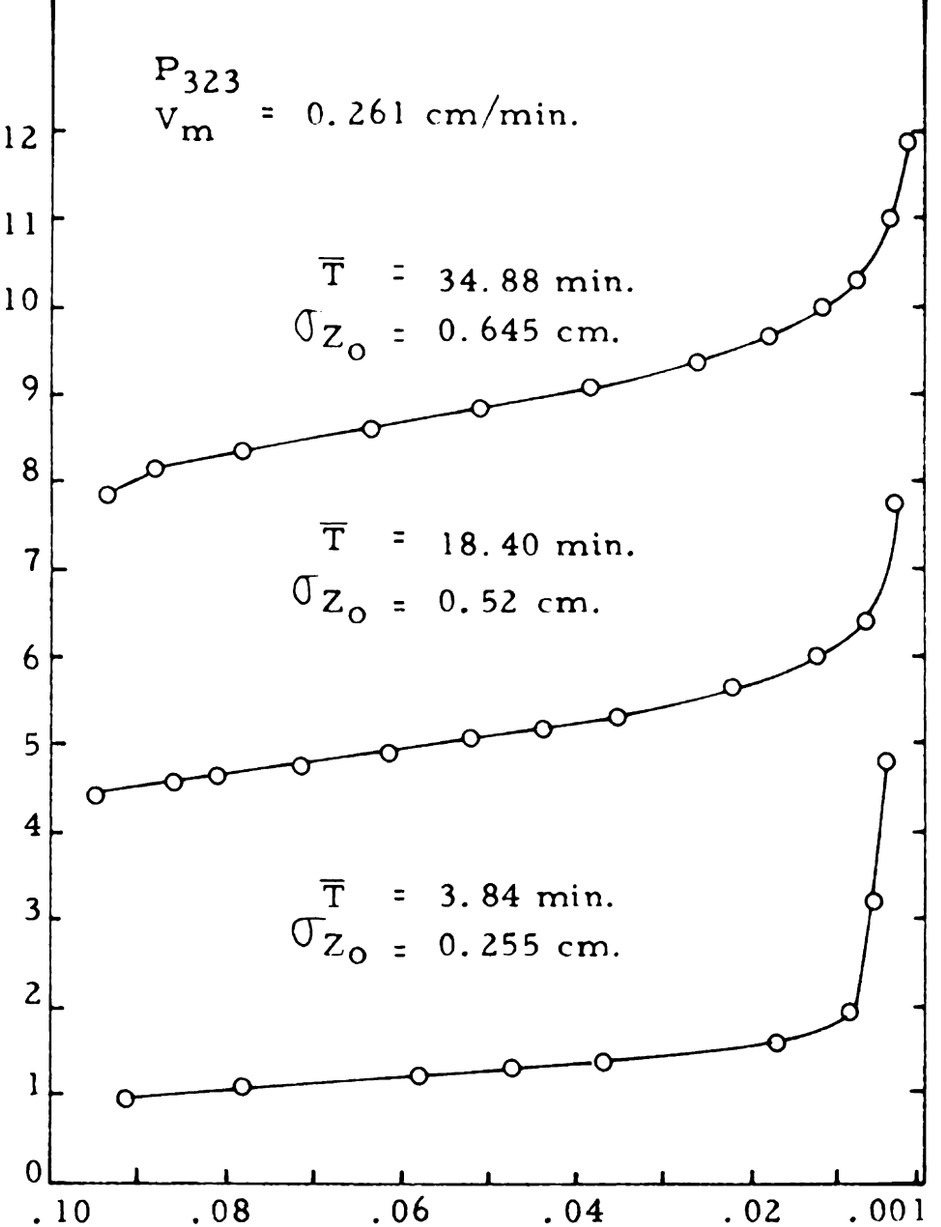

Figure V-8c. Break through curves for P_{323}.

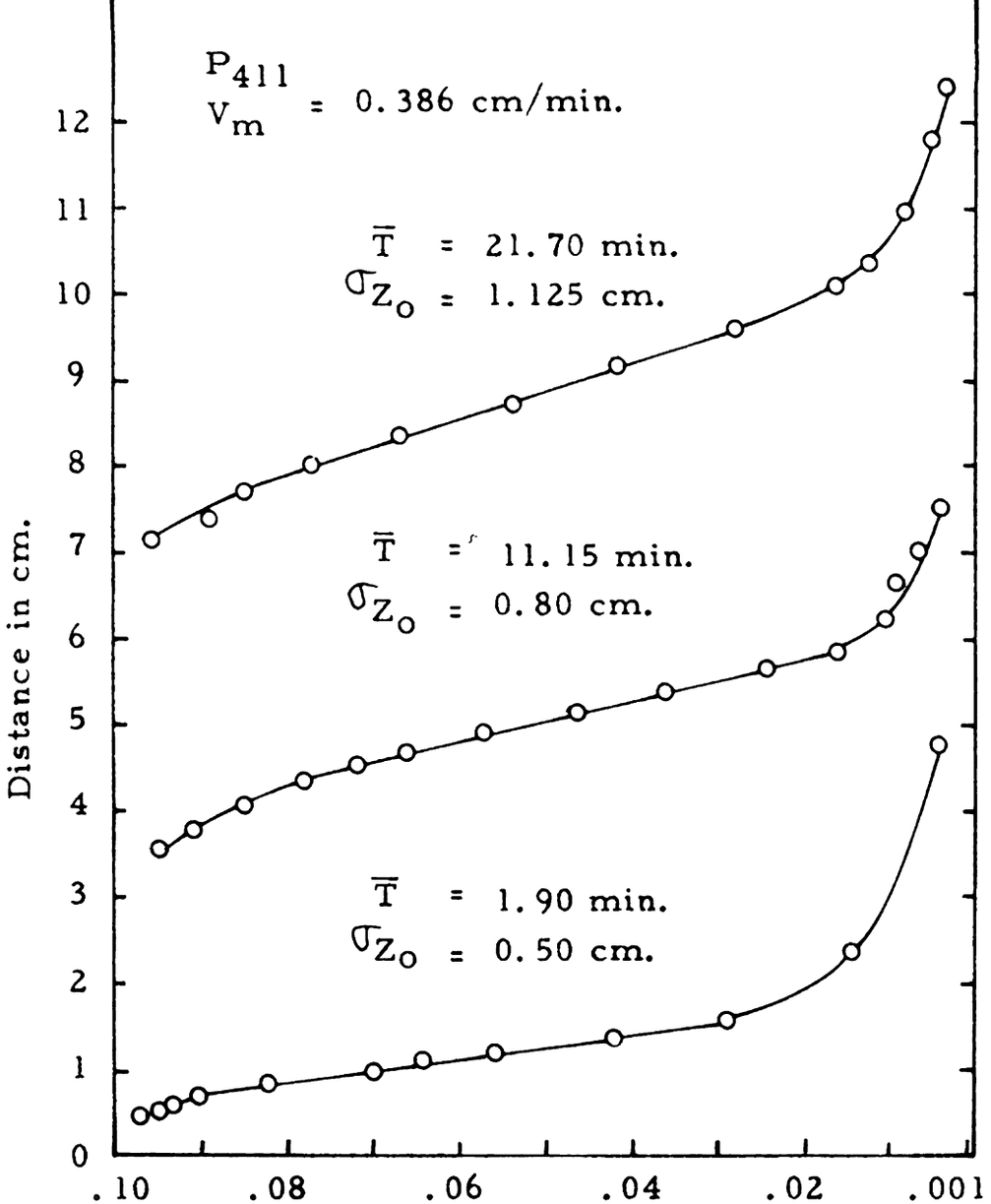

Figure V-9a. Break through curves for P_{411}.

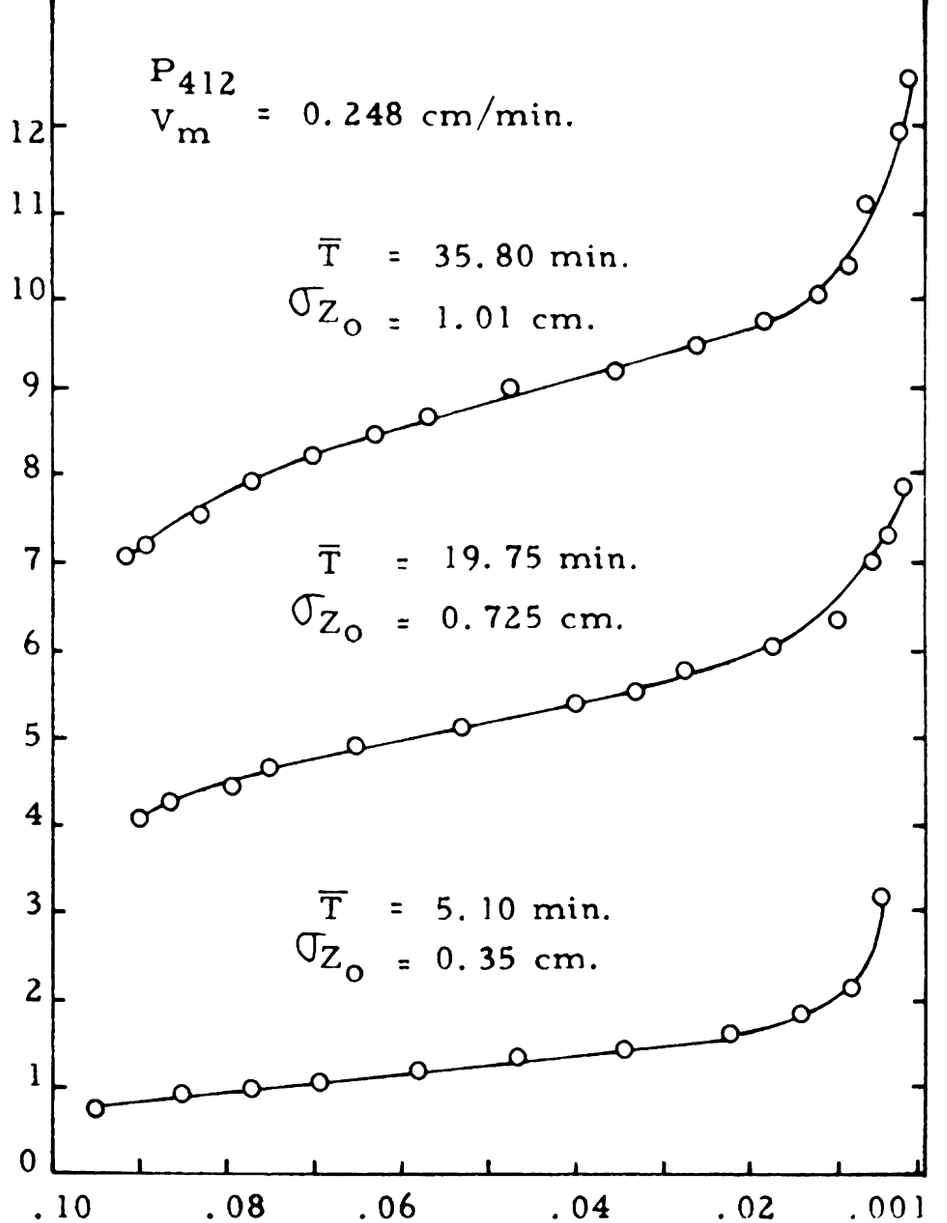

Figure V-9b. Break through curves for P_{412}.

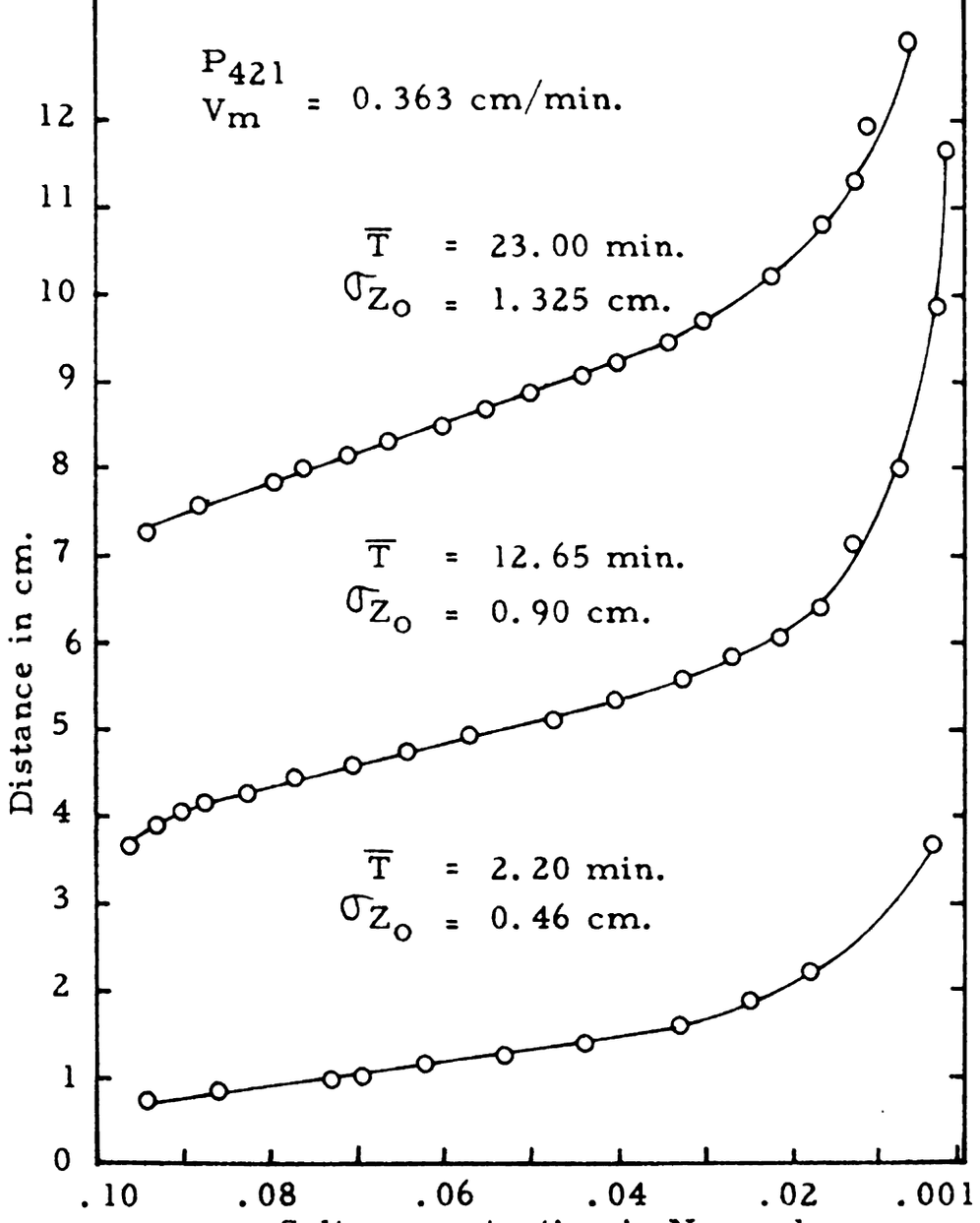

Figure V-10a. Break through curves for P_{421}.

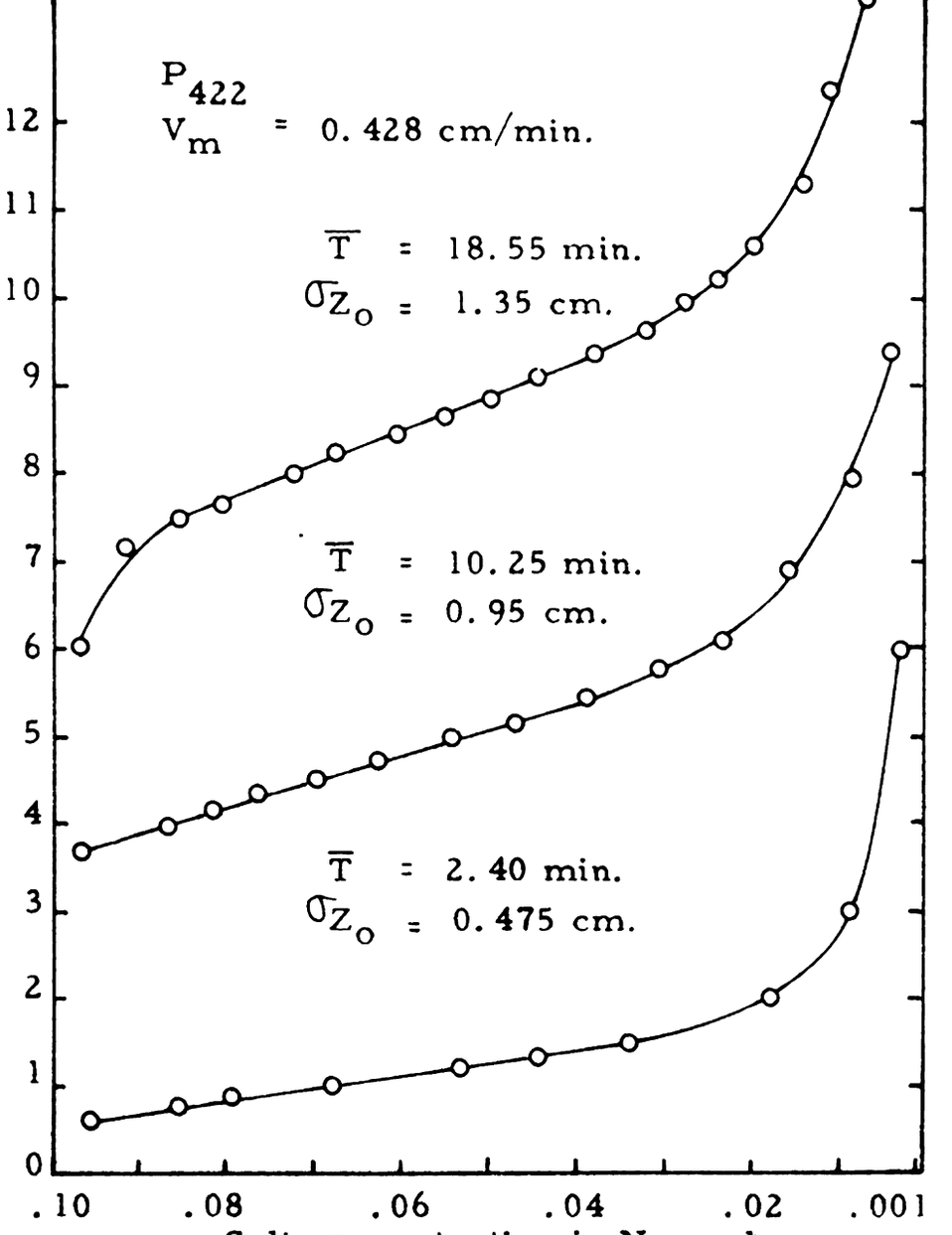

Figure V-10b. Break through curves for P_{422}.

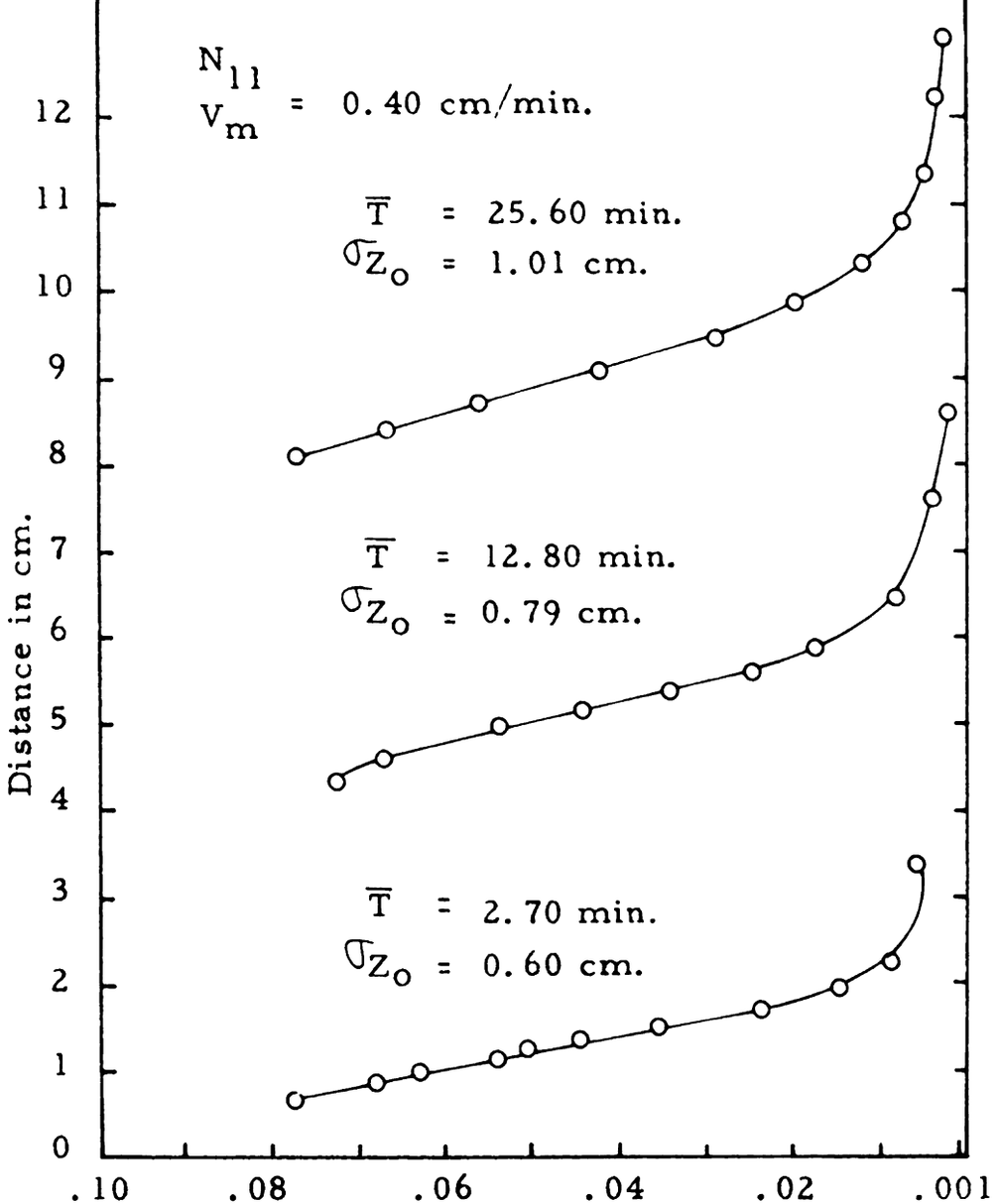

Figure V-11a. Break through curves for N_{11}.

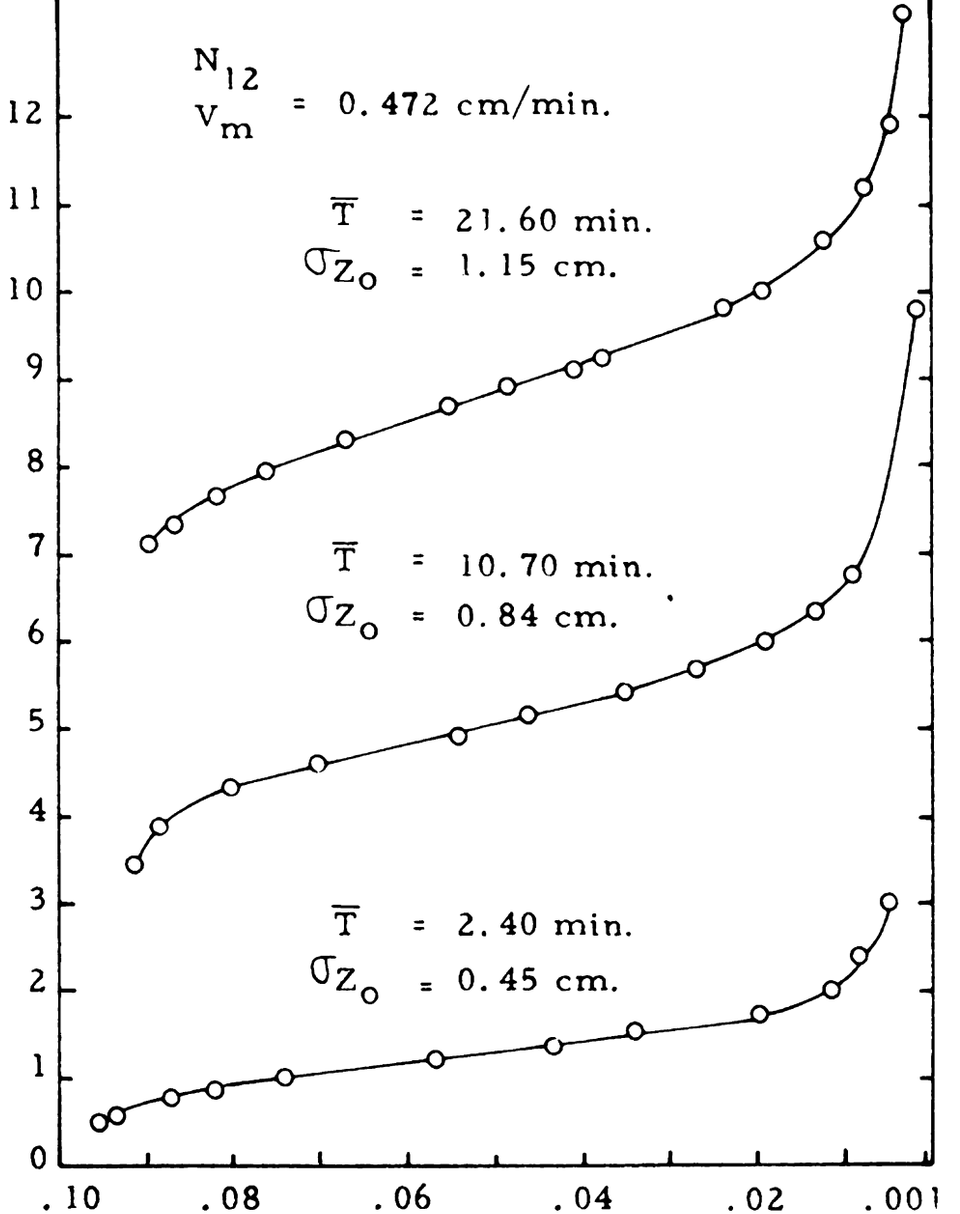

Figure V-11b. Break through curves for N_{12}.

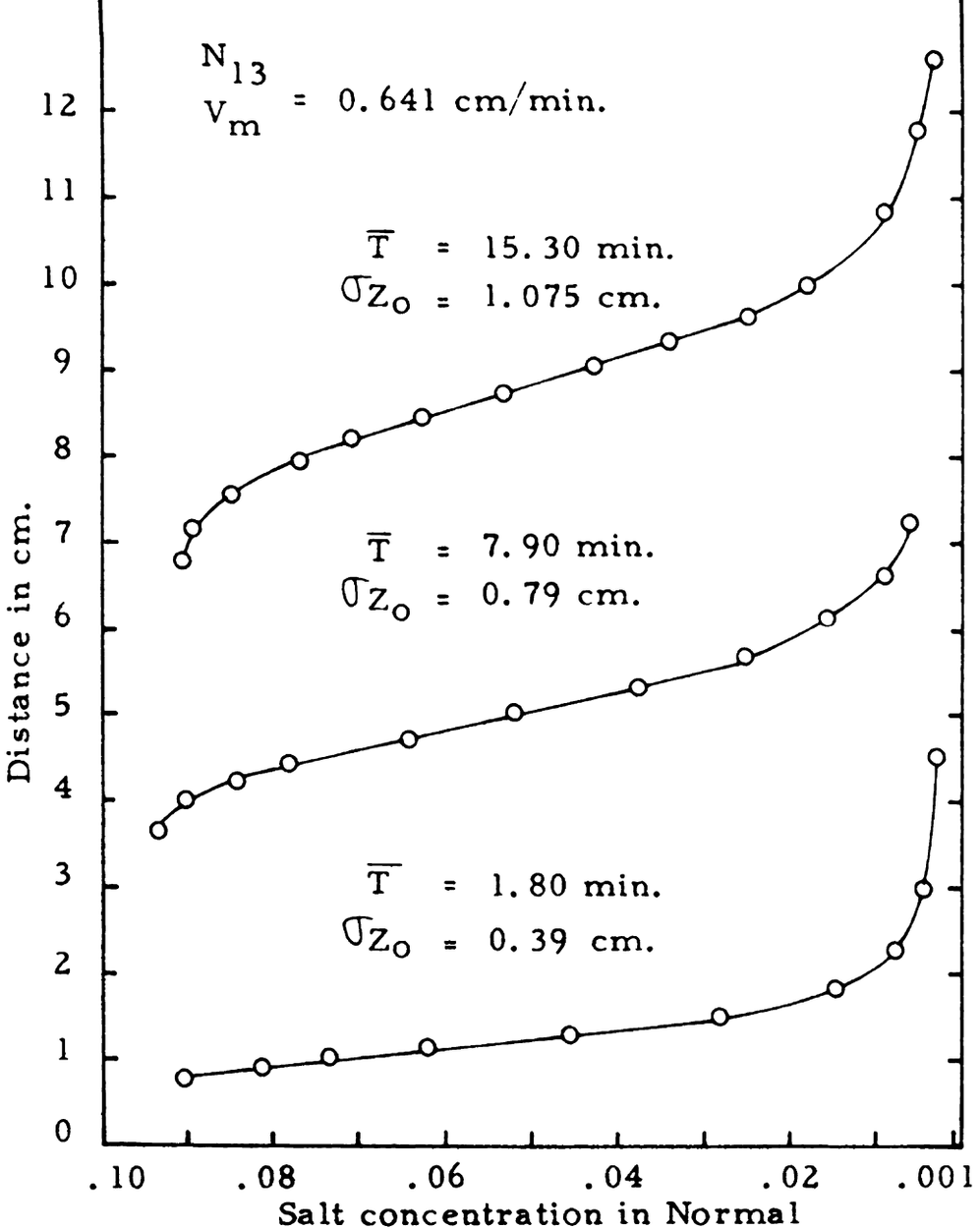

Figure V-11c. Break through curves for N_{13}.

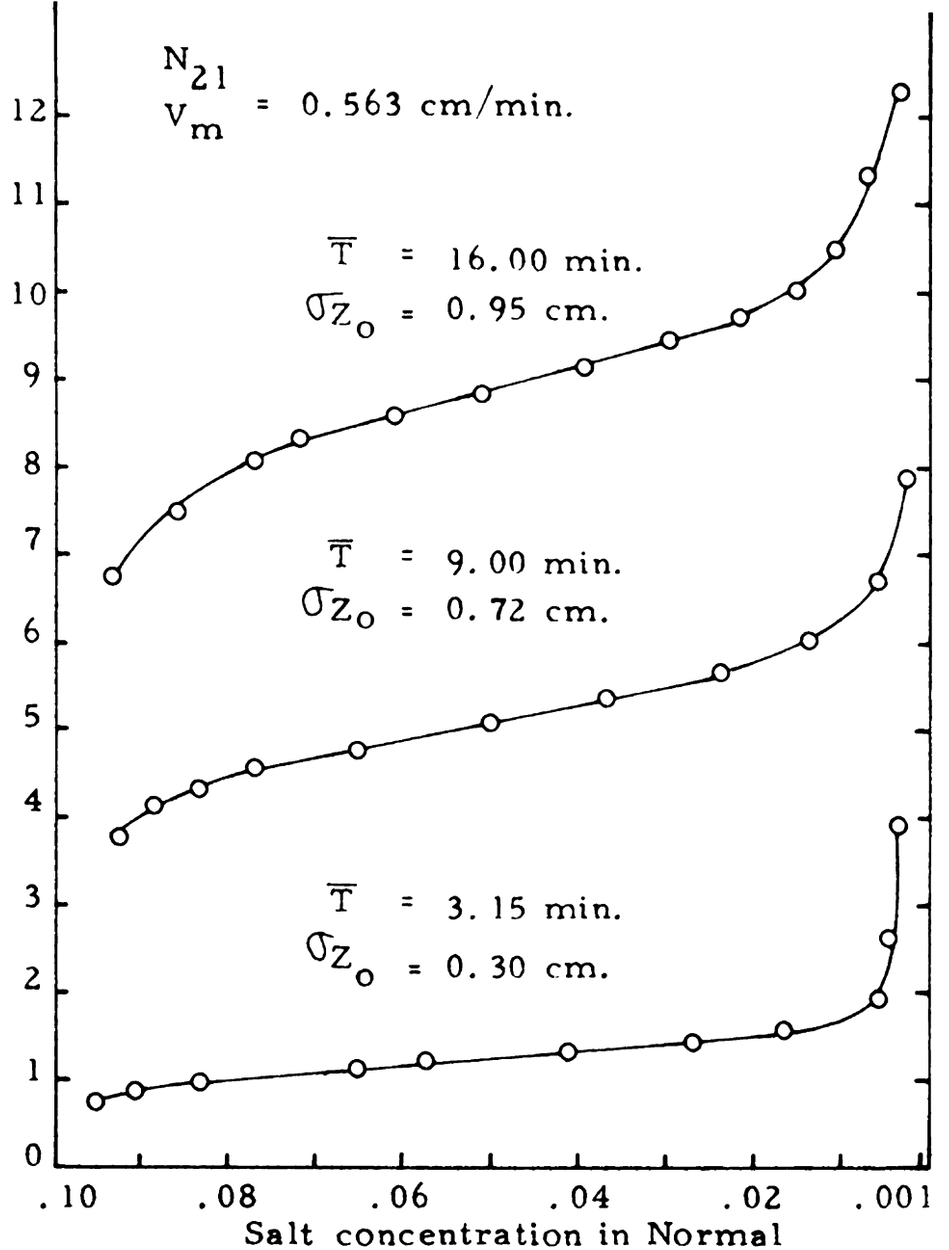

Figure V-11d. Break through curves for N_{21}.

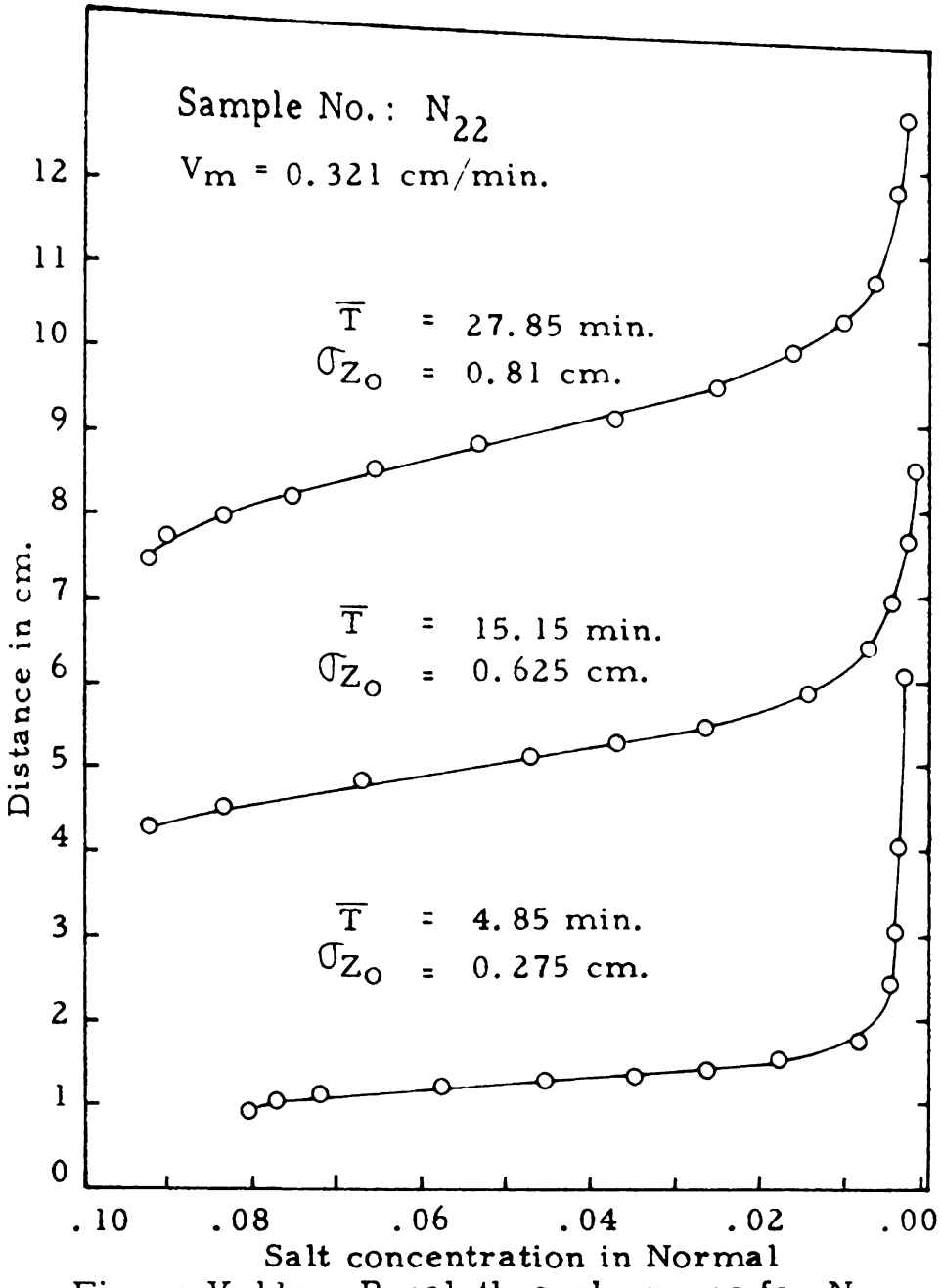

Figure V-11e. Break through curves for N_{22}.

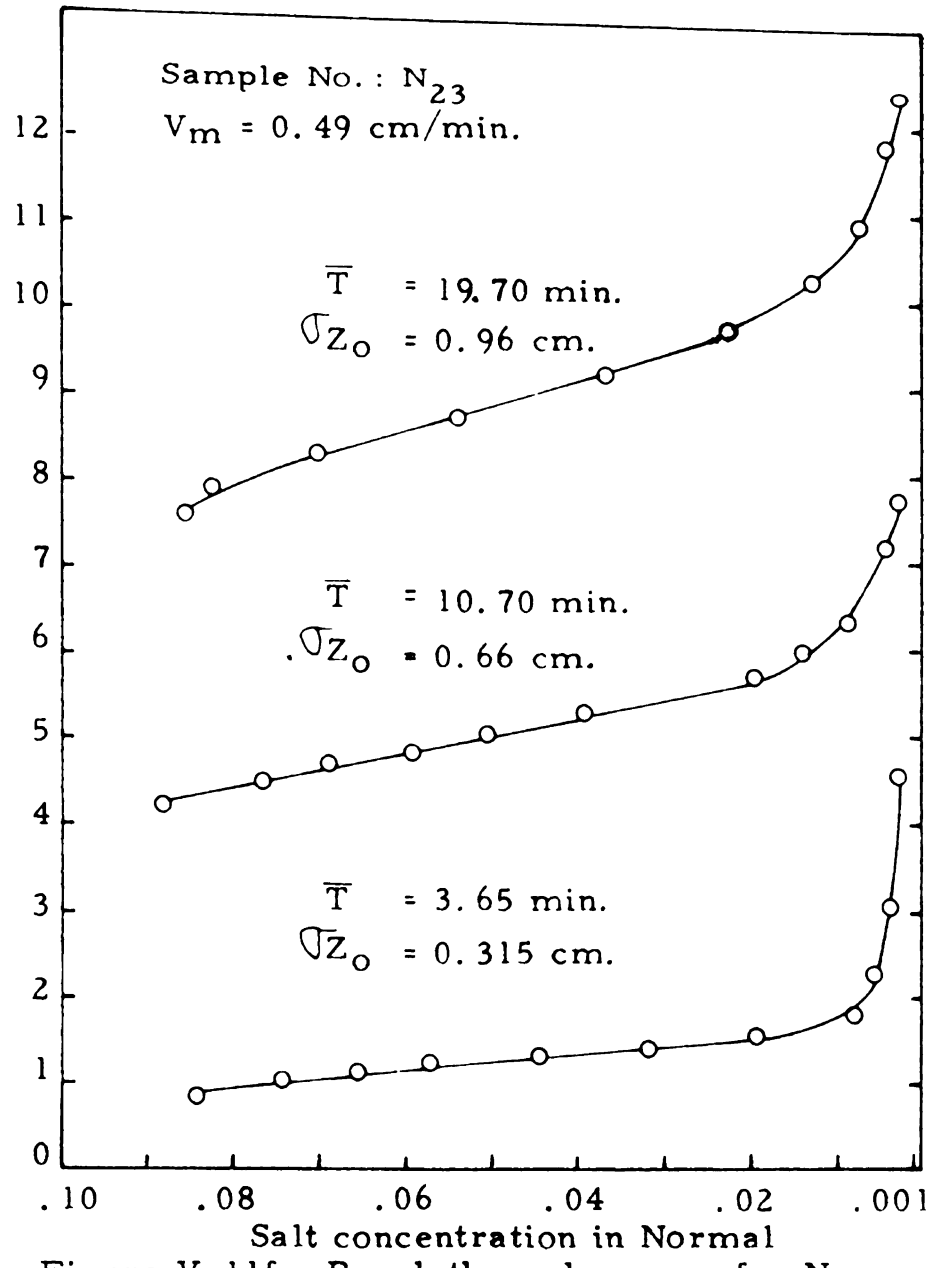

Figure V-11f. Break through curves for N_{23}.